CHAPTER 1

INTRODUCTION

1.1 Description of vapour compression refrigeration cycle

Refrigeration (Is a heat removal process in which we reduce the surrounding temperature), cooling, and heating processes are important in a variety of everyday situations, including the air conditioning and heating of buildings, and in the medical treatment (lowering of a body's temperature for therapeutic purposes), transportation, and preservation of foods and beverages. Refrigeration also finds large-scale industrial application, for example, in the manufacture of ice and the dehydration of gases. Applications in the petroleum industry include lubricating-oil purification, low temperature reactions, and the separation of volatile hydrocarbons.

Refrigeration involves heat transfer from a low-temperature region to a high-temperature region. This process is typically implemented by means of a cycle involving a particular refrigerant (working fluid). There are different types of cycles, but the most commonly used for refrigerators, air-conditioning systems and heat pumps is the vapour compression refrigeration cycle (VCRC). It has been and is the most widely used method for air-conditioning of large public buildings, private residences, hotels, hospitals, theatres, restaurants and automobiles. It is also used in domestic and commercial refrigerators, large-scale warehouses for storage of foods and meats, refrigerated trucks and railroad cars, and a host of other commercial and industrial services.

The design of a VCRC entails the determination of a potential working fluid’s properties at the inlet and exit states of the steps of candidate (working) process

cycles, and the attendant calculation of a measure of the process efficiency for the cycle, called the coefficient of performance (COP). For a given VCRS, the COP is a function of the fluid thermodynamic properties at the states of the cycle, which are typically obtained from an equation of state (EOS) for the refrigerant.

This most common refrigeration cycle uses an electric motor to drive a compressor. In an automobile the compressor is usually driven by a belt connected to a pulley on the engine's crankshaft, with both using electric motors for air circulation. Since evaporation occurs when heat is absorbed, and condensation occurs when heat is released, air conditioners are designed to use a compressor to cause pressure changes between two compartments, and actively pump a refrigerant around. A refrigerant is pumped into the low pressure compartment (the evaporator coil), where, despite the low temperature, the low pressure causes the refrigerant to evaporate into a vapour, taking heat with it as shown in Figure 1.1. In the other compartment (the condenser), the refrigerant vapour is compressed and forced through another heat exchange coil, condensing into a liquid, rejecting the heat previously absorbed from the cooled space. The heat exchanger in the condenser section (the heat sink mentioned above) is often cooled by a fan blowing outside air through it, or in some cases, such as marine applications, by other means such as water.

The thermodynamics of the vapour compression cycle can be analyzed on a temperature versus entropy diagram as depicted in Figure 1.2. At point 3 in the diagram, the circulating refrigerant enters the compressor as a saturated vapour. From point 3 to point 5, the vapour is isentropically compressed (i.e., compressed at constant entropy) and exits the compressor as a superheated vapour.

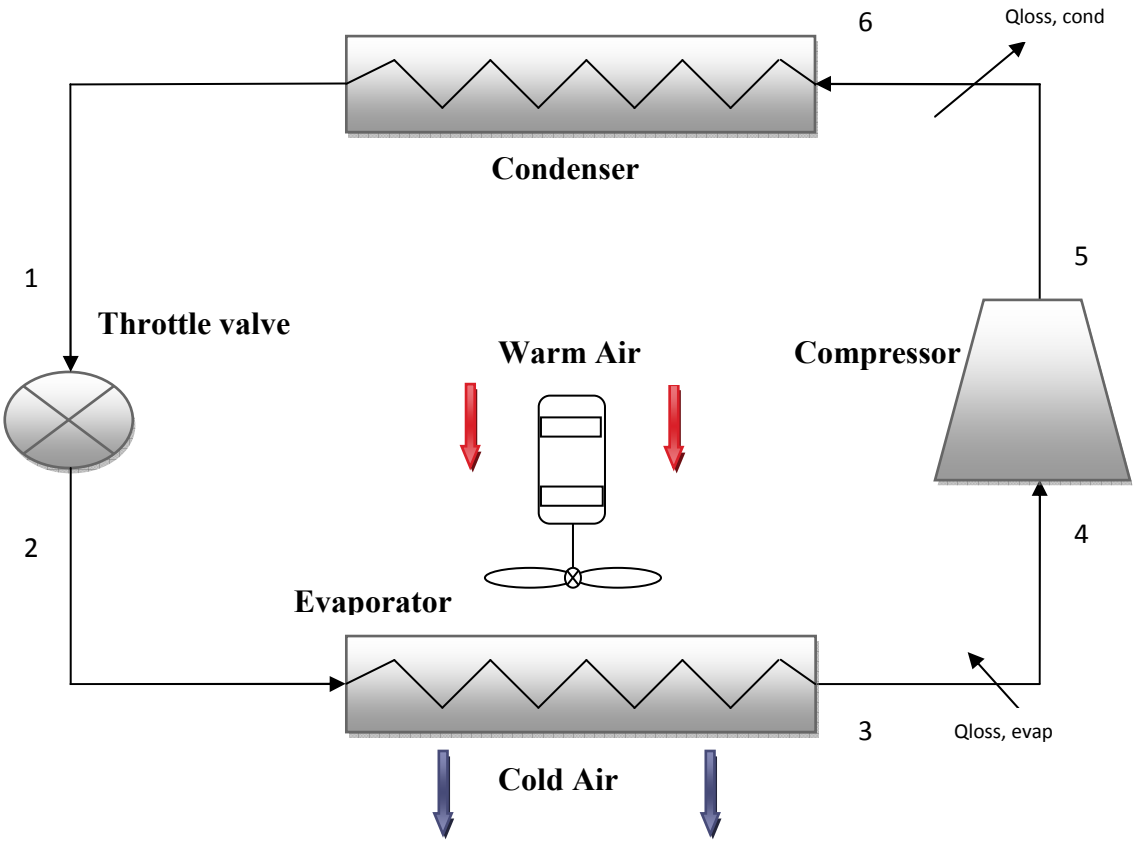

Figure 1.1 Vapour compression cycle

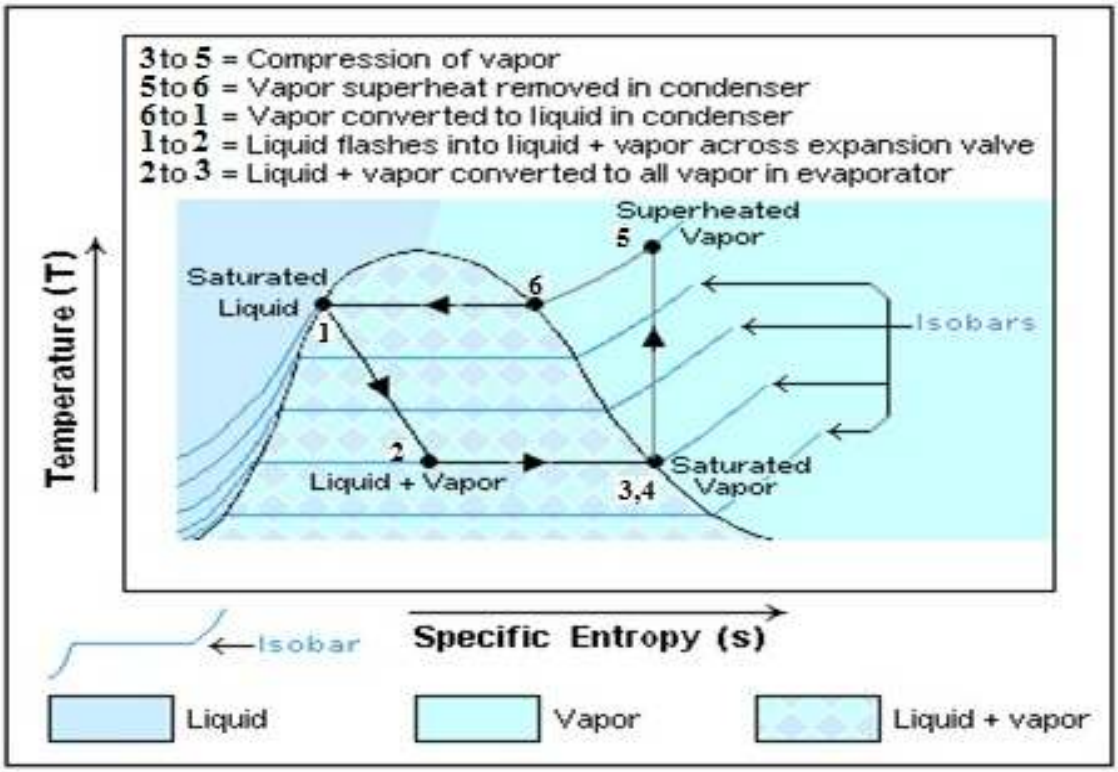

Figure 1.2 Temperature – Entropy diagram of VCRC

From point 5 to point 6, the superheated vapour travels through part of the condenser which removes the superheat by cooling the vapour. Between point 6 and point 1, the vapour travels through the remainder of the condenser and is condensed into a saturated liquid. The condensation process occurs at essentially constant pressure. Between points 1 and 2, the saturated liquid refrigerant passes through the expansion valve and undergoes an abrupt decrease of pressure, that process results in the adiabatic flash evaporation and auto-refrigeration of a portion of the liquid (typically, less than half of the liquid flashes). The adiabatic flash evaporation process is isenthalpic (i.e., occurs at constant enthalpy).

Between points 2 and 3, the cold and partially vaporized refrigerant travels through the coil or tubes in the evaporator where it is totally vaporized by the warm air (from the space being refrigerated) that a fan circulates across the coil or tubes in the evaporator. The evaporator operates at essentially constant pressure. The resulting saturated refrigerant vapour returns to the compressor inlet at point 1 to complete the thermodynamic cycle.

It should be noted that the above discussion is based on the ideal vapour-compression refrigeration cycle which does not take into account real world items like frictional pressure drop in the system, slight internal irreversibility during the compression of the refrigerant vapour, or non-ideal gas behavior.

1.2 Motivation

In a cooling system, evaporation and condensing processes occurring in refrigeration systems are as a result of the heat transfer process occurring by means of refrigerants. The design of a cooling system largely depends on the properties of the refrigerants. Refrigerants have been widely used in several areas in the industry

for a long time. After the discovery of the harmful effects of CFC based refrigerants on the ozone layer, search to finding alternatives to these working fluids gained more interest in the recent few years. Finding drop-in replacements for CFC based working fluids is important due to their harmful effects on the ozone layer and international conventions are requesting to reduce their usage. Due to the reasons listed, the researchers prompted with the alternatives, which can be used instead of CFCs. In finding the alternatives to the CFC based cooling refrigerants often, HCFC, HFO, Mixing two or more refrigerants gives us a chance to obtain the desired thermodynamic properties (i.e. often closing to CFC based ones for current systems) of the refrigerants by changing the mixture ratios.

1.3 Scope

In present work, the effect of fouling on performance of vapour compression refrigeration system has been carried out. The performance has been evaluated by varying condenser coolant inlet temperature (i.e. 35^{o}C, 37.5 ^{o}C and 40 ^{o}C), and also by varying condenser, evaporator conductances individually, and simultaneously (i.e. 0% - 50%), while the evaporator coolant inlet temperature has been kept constant (i.e. 0^{o}C), and with the following set of data: 1) rate of heat absorbed by evaporator, 2) product of condenser effectiveness and capacitance rate of external fluid, 3) product of evaporator effectiveness and capacitance rate of external fluid and 4) efficiency of compressor using refrigerants R134a, R1234yf, and R1234ze for simple vapour compression system.

1.4 Organization of thesis

Chapter 1- gives the overview of simple vapour compression system.

Chapter 2- is about the literature referred in the development of this project.

Chapter 3- deals with the formulation of thermodynamic modelling of simple vapour compression system with solution methodology.

Chapter 4- discusses the results obtained from the thermodynamic analysis.

Chapter 5- gives the conclusion of thermodynamic analysis and scope for the future work.

CHAPTER 2

LITERATURE REVIEW

Declamatory literature is available on refrigerants, thermodynamic modelling and analysis of vapour compression cycle. A brief of literature survey is given below:

2.1 Literature survey on Theoretical & experimental studies of VCRS

Selbas et al. [1] did the exergy based thermo economic optimization of sub cooled and superheated vapour compression refrigeration cycle. The advantage of using the exergy method of thermo economic optimization is that various elements of the system—i.e., condenser, evaporator, sub cooling and superheating heat exchangers—can be optimized on their own. The application consists of determining the optimum heat exchanger areas with the corresponding optimum sub cooling and superheating temperatures. A cost function is specified for the optimum conditions. All calculations are made for three refrigerants: R22, R134a, and R407c. Thermodynamic properties of refrigerants are formulated using the artificial neural network methodology.

Wang et al. [2] investigated the potential benefits of compressor cooling. The compressor is certainly the largest power consumer in a vapour compression system. To reduce the power consumption of the compressors two performance improving options are investigated theoretically for refrigerants R22, R134a, R410A and R744 as working fluids. The first option is cooling the motor by external means other than using the suction gas. Analysis results for this option show that R22, R410A and R744 have larger potential benefits than R134a. In low temperature refrigeration applications larger improvements are achievable than in air conditioning

applications for all four refrigerants. The second option is to make the compression process isothermal by transferring heat from the compression chamber. To approach the isothermal compression process while avoiding wet compression, two cases of combining isothermal and isentropic compression processes are analyzed. The analysis results show that this strategy can reduce the compression work up to 14% as compared to the isentropic compression process for the R22 refrigeration system. The second analysis on the ideal vapour compression cycles using such compressor cooling strategy show that the compression power of the system can be reduced by up to about 16% depending on operating conditions and fluid choice.

Arora and Kaushik [3] did the theoretical analysis of a vapour compression refrigeration system with R502, R404A and R507A. Their work presents a detailed exergy analysis of an actual vapour compression refrigeration (VCR) cycle. A computational model has been developed for computing coefficient of performance (COP), exergy destruction, exergetic efficiency and efficiency defects for R502, R404A and R507A. This research study has been done for evaporator and condenser temperatures in the range of 50°C to 0°C and 40°C to 55°C, respectively. The results indicate that R507A is a better substitute to R502 than R404A. The efficiency defect in condenser is highest, and lowest in liquid vapour heat exchanger for the refrigerants considered.

Khan and Zubair [4] evaluated the performance of vapour compression system. The characteristic performance curves of vapour compression refrigeration systems are defined as a plot between the inverse coefficient of performance (1/COP) and inverse cooling capacity ($1/Q_{evap}$) of the system. A finite- time thermodynamic model which simulates the working of an actual vapour-compression system has been developed. Using the actual data of a simple vapour compression system,

performance curves of the system can be obtained. The curves are linear and this linear relation between 1/COP and $1/Q_{evap}$ can be explained in the light of various losses of the system, resulting from the irreversibility's losses due to finite rate of heat transfer in the heat exchangers, non-isentropic compression and expansion in the compressor and expansion valve of the system, respectively. The model can be used to study the performance of a variable-speed refrigeration system in which the evaporator capacity is varied by changing the mass-flow rate of the refrigerant, while keeping the inlet chilled-water temperature as constant. The model can be also used for predicting an optimum distribution of heat-exchanger areas between the evaporator and condenser for a given total heat exchanger area. In addition, the effect of sub cooling and superheating on the system performance is also investigated.

Winkler et al. [5] did the comprehensive investigation of numerical methods in simulating a steady-state vapour compression system. The purpose of his work was to describe and investigate the robustness and efficiency of three unique algorithms used to simulate a modular/component-based vapour compression system. The three algorithms for the steady-state solution of vapour compression have been formulated and tested. Each algorithm has been formulated to simulate multi-evaporator systems. The three solvers were tested by simulating test cycles operating at off-design conditions. The robustness and computational efficiency of each solver were analyzed and the enthalpy marching solver was superior in both of these categories solving 97% of the test cases. Two methods to determine guess values were used and it was shown that the computational effort required determining more accurate guess values paid off in terms of both robustness and total computational effort required. Two closure equations were discussed and the

effect of the type of closure equation was analyzed. The test matrix was run for three different equation solvers and the numerical performance of each equation solver was discussed.

Cabello et al. [6] made a simplified steady-state modeling of a single stage vapour compression plant. In this work a simplified steady-state model to predict the energy performance of a single stage vapour compression plant was proposed. The model input variables are the total superheating degree, evaporating and condensing temperatures (easily available in an industrial facility), and the main model outputs are refrigerant mass flow rate, cooling capacity, compressor power consumption and COP.

Aprea and Greco [7] evaluated the problem of R22 phase-out in refrigeration plants is addressed. A comparison is performed between R22 and R407C. The latter seems to be a promising drop-in substitute for the former. Experimental tests are performed in a vapour compression plant with a reciprocating compressor. The objective of this paper is to evaluate the compressor performance using R407C in comparison to R22. The plant overall energetic performance is also evaluated. R22 performance is consistently better than that of its candidate substitute. The difference stems from the different irreversibilities of the plan components arising when using R22 and R407C, respectively. Specific attention is devoted to compressor irreversibilities. Performance indices related to the semi-hermetic compressor are evaluated when using either refrigerant fluid. The investigation has revealed that R22 performs better than R407C mainly because of a better compression process due to a number of factors, including the facts that the isentropic and volumetric efficiencies of the semi-hermetic compressor are better than that of R407C.

Ding [8] did the Simulation that has been widely used for performance prediction and optimum design of refrigeration systems. A brief review on history of simulation for vapour compression refrigeration systems is done. The models for evaporator, condenser, compressor, capillary tube and envelop structure are summarized. Some developing simulation techniques, including implicit regression and explicit calculation method for refrigerant thermodynamic properties, model-based intelligent simulation methodology and graph-theory based simulation method, are presented. Prospective methods for future simulation of refrigeration systems, such as noise-field simulation, simulation with knowledge engineering methodology and calculation methods for nanofluid properties are introduced briefly.

2.2 Literature survey on thermodynamic properties

Monte [9, 10] calculated thermodynamic properties of R407C and R410A. A theoretical development of the thermodynamic properties of two mixtures of hydro fluorocarbon (HFC) refrigerants, i.e. R407C and R410A (in the superheated vapour state), is carried out. The modeling is based on the Martin-Hou equation of state, which has long been used for pure hydro fluorocarbons (e.g. R134a) with good results. Since R407C and R410A are very well investigated refrigerants, the analytical procedure here derived concerns with those thermodynamic properties of R407C and R410A (in the superheated state) that are not published in the current specialized literature. They are: compressibility factor, isentropic and isothermal compressibility, volume expansivity, isentropic and isothermal exponent, speed of sound and Joule–Thomson coefficient. These properties may be used as a theoretical basis for research into the optimal HFC-mixture for compressor efficiency

and for performing cycle calculations in the vapour-phase region for systems working with R407C and R410A.

Ecir et al. [11] used ten modeling techniques within data mining process for the prediction of thermo physical properties of refrigerants (R134a, R404A, R407A and R410A). These are linear regression (LR),multi layer perception (MLP), pace regression (PR), simple linear regression (SLR), sequential minimal optimization (SMO), KStar, additive regression (AR), M5 model tree, decision table (DT), M5'Rules models. Relations depending on temperature and pressure were carried out for the determination of thermo physical properties as the specific heat capacity, viscosity, heat conduction coefficient, density of the refrigerants. Obtained model results for every refrigerant were compared and the best model was investigated. Results indicate that use of derived formulations from these techniques will facilitate design and optimization of heat exchangers which is component of especially vapour compression refrigeration system. Selbas et al. [1] formulated thermodynamic properties of refrigerants using the artificial neural network methodology. Arora and Kaushik [3] obtained the thermodynamic properties of refrigerants by using engineering equation solver (EES) software. Khan and Zubair [4] obtained the thermodynamic properties of refrigerant by using SATPRP software.

Ahamed et al. [12] analysed thermodynamically a cascade refrigeration system that uses CO_2 and NH_3 as refrigerants, to determine the optimal condensing temperature of the cascade-condenser given various design parameters, to maximize the COP and minimize the exergy destruction of the system. The design parameter include: the evaporating temperature, the condensing temperature and the temperature difference in the cascade-condenser. The results agreed closely with the reported experimental data. The optimal condensing temperature of the cascade-condenser

increases with Tc, Te and ΔT. The maximum COP increases with Te, but decreases as Tc or ΔT increases. Two useful correlations that yield the optimal condensing temperature of the cascade-condenser and the corresponding maximum COP are presented.

Lee et al. [13] reviewed the possibilities of researches in the field of exergy analysis in various usable sectors where vapour compression refrigeration systems are used. Here, it is found that exergy depends on evaporating temperature, condensing temperature, sub-cooling and compressor pressure. It also depends on environmental temperature. Nowadays, hydrocarbons are considered as refrigerant having, low ODP and GWP, and these are considerable in the aspect of exergy analysis. Refrigerants are R407a, R600a, R410a and R134a are considered and analysed with respect to analyzed with respect to exergy efficiency. Mixtures of hydrocarbons with R134a also show better performance with respect to other refrigerants. Among the components of the vapour compression system, much research showed that measure part of exergy losses is occurred in the compressor. Nanofluid and nanolubricant cause to reduce the exergy losses in the compressor indirectly.

2.3 Literature survey on refrigerants

Calm [14] reviewed the progression of refrigerants, from early uses to the present, and then addresses future directions and candidates. The article breaks the history into four refrigerant generations based on defining selection criteria. It discusses displacement of earlier working fluids, with successive criteria, and how interest in some early refrigerants re-emerged, for example renewed interest in those now identified as ‘‘natural refrigerants.’’ The paper examines the outlook for current

options in the contexts of existing international agreements, including the Montreal and Kyoto Protocols to avert stratospheric ozone depletion and global climate change, respectively. It also examines other environmental concerns and further international and local control measures. The discussion illustrates how isolated attention to individual environmental issues or regulatory requirements, in contrast to coordinated responses to the several issues together, can result in unintended environmental harm that almost certainly will require future reversals. It identifies pending policy and regulatory changes that may impact the next generation of refrigerants significantly.

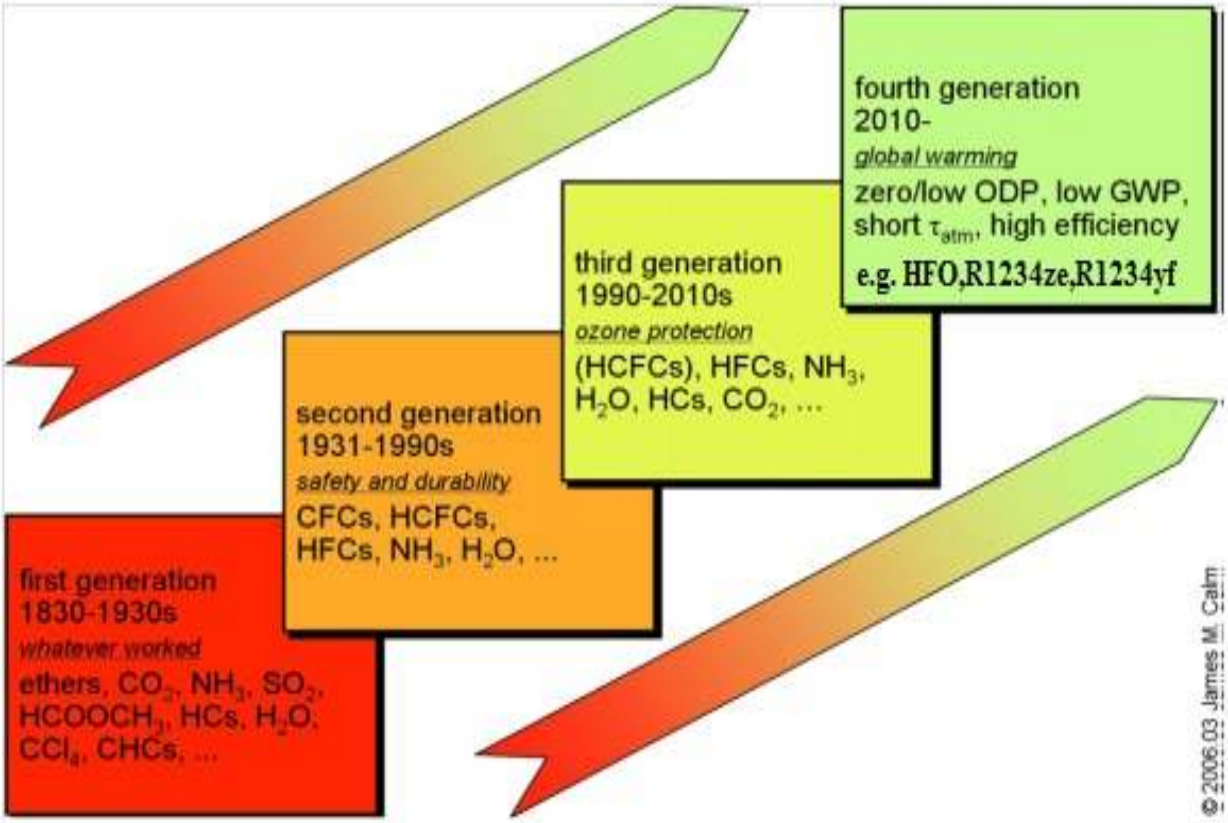

Figure 2.1 Refrigerant progression

McLinden et al. [15] presented the thermodynamic properties of a hydrofluoro-olefin (HFO) refrigerant. The *p*-ρ-*T* behavior of high purity (99.993 %) R1234ze (E) was measured from 240 K to 420 K with pressures to 15 MPa by use of a two-sinker densimeter. The measurements extend from low-density vapour to compressed-liquid states. Vapour pressures were measured in the densimeter from 261 K to 380 K. The equation of state (EOS) for R1234ze (E) is expressed in terms of the Helmholtz energy as a function of temperature and density, and it is valid over the entire fluid surface. The formulation can be used for the calculation of all thermodynamic properties. Comparisons to experimental data are given to establish the accuracy of the EOS.

Reasor et al. [16] studied that due to environmental concerns, refrigerants with a low global warming impact are gaining importance in the refrigeration industry. Refrigerant R1234yf has a low GWP of 4, compare to 1430 for R134a, and has thermodynamic properties similar to R134a, making it a desirable choice for future automotive refrigerants. R1234yf has a significant potential to be a drop-in replacement for R134a in the near future. Additionally, R410A is another commonly used refrigerant, and comparisons can be made between R1234yf and R410A to determine whether R1234yf has any drop in potential for systems designed for R410A. Compressions are made between R1234yf, R134a and R410A, and simulations are conducted to determine the feasibility of using R1234yf as a replacement for R134a or R410A. This paper will present a comparison between the thermo physical properties of R1234yf and R134a and R410A and will present the results of simulation using the three refrigerants in tube-fin and micro channel heat exchangers.

Pearson [17] traced the development of the old carbon dioxide systems, considered the technical, commercial and social reasons for their slow development and subsequent decline and examined the recent renaissance across a surprisingly broad range of applications, from trans-critical car air conditioners to low temperature industrial freezer plants.

Raj and Lal [18] experimental investigation on the performance of a window air-conditioner operated with R22 and M20 refrigerant mixture tested at different refrigerant charge levels. It was concluded that among the mixtures considered M20 (R407C 80% & HC blend 20%) had the optimal composition in respect of better COP and per day energy consumption. R407C is one of the most likely potential substitutes for R22, which is an “ozone-friendly" HFC refrigerant mixture.

2.4 Literature survey on fouling in VCRS

Qureshi and Zubair [19] investigated performance degradation due to fouling in a vapour compression cycle for various applications. Considering the first set of refrigerants i.e. R134a, R410A and R407C, from a first law standpoint, the COP indicates that R134a always performs better unless only the evaporator is being fouled. In contrast to this, the second-law efficiency indicates that R134a performs the best in all cases. Considering the second set of refrigerants i.e. R717, R404A and R290, from a first law standpoint, the COP indicates that R717 always performs better unless only the evaporator is being fouled. In contrast to this, the second-law efficiency indicates that R717 performs the best in all cases. Under the respective conditions volumetric efficiency of R410A and R717 remained the highest. In this performance degradation of the evaporator often has a larger effect on compressor power requirement while that of the condenser has an overall larger effect on the

COP. It also indicates a new performance degradation law in light of the data generated, which can reduce the amount of experimentation and help predict relevant quantities of the refrigeration system.

Qureshi and Zubair [20] investigated performance characteristics due to fouling in a vapour compression cycle with integrated mechanical sub cooling are investigated for various applications. Considering the first set of refrigerants i.e. R134a, R410A and R407C, from a first law standpoint, the COP indicates that R134a always performs better unless only the evaporator is being fouled. From a second law standpoint, the second-law efficiency indicates that R134a performs the best in all cases. Considering the second set of refrigerants i.e. R717, R404A and R290, the COP indicates that R717 always performs better unless only the evaporator is being fouled; however, the second-law efficiency indicates that R717 performs the best in all cases. Furthermore, the performance degradation due to fouling of the evaporator always has a larger effect on cooling load capacity while the performance degradation of the condenser always has an overall larger effect on the sub-cooler compressor power requirement as well as the COP of the system. The data generated indicates a new performance degradation law which is applicable for this system as well that can reduce the amount of experimentation and help predict relevant quantities of the refrigeration system.

2.5 Conclusions of literature survey

- An ample literature is available on vapour compression refrigeration system. There are so many thermodynamic models which are available for their analysis and used by researchers to measure the performance of vapour compression with different refrigerants.

- Different refrigerants have different effect on the performance of vapour compression and are having different physical and thermodynamic properties.
- There is a copious literature on various techniques for measuring the thermodynamic properties of different refrigerants.

2.6 Gaps in Literature survey

Qureshi and Zubair [19] discussed about the effect of fouling on the performance of VCRS, however the results have been calculated for a particular set of data assuming $T_{in,cond}$ (T_9) = 40^{o}C, $T_{in,evap}$ (T_7) = 0^{o}C and $\eta_{cp,isn}$ = 65%.where as in a real practical system condenser temperature depends upon ambient conditions which keeps on varying throughout the day. Similarly evaporator temperature also depends upon application and $\eta_{cp,\ isn}$ depends upon pressure ratio. Further heat losses in various components have been neglected. Thus, the results presented in this paper are of limited use.

2.7 Objective of present work

Based on the gaps discussed above in the work of Qureshi and Zubair [19], the following objectives are set for this particular study.

1) To study the effect of fouling on refrigeration system using energy and exergy analysis technique for refrigerants R134a, R1234yf and R1234ze.
2) To find out percentage change in COP of the system, cooling capacity, compressor work, and effectiveness. The parameters varied are condenser, evaporator conductances individually and simultaneously, and condenser coolant inlet temperatures.

3) Qureshi and Zubair [19] performed the analysis for refrigerant R134a, R407C, R410A, R404A, R717, and R290. All the above refrigerants have high GWP except R290. Hence in the present work R134a has been taken as a reference & two new refrigerants R1234yf and R1234ze which are low GWP alternatives for R134a have been taken into consideration for analysis.

CHAPTER 3

THERMODYNAMIC MODELLING

The development of refrigeration system models which simulates the actual working of a reciprocating chiller has been the goal of many researchers. In this project a property dependent thermodynamic model of a simple reciprocating system given by Khan and Zubair [4], which can simulate the performance of actual system as closely as possible, is developed.

3.1 Thermodynamic model of simple vapour compression refrigeration system

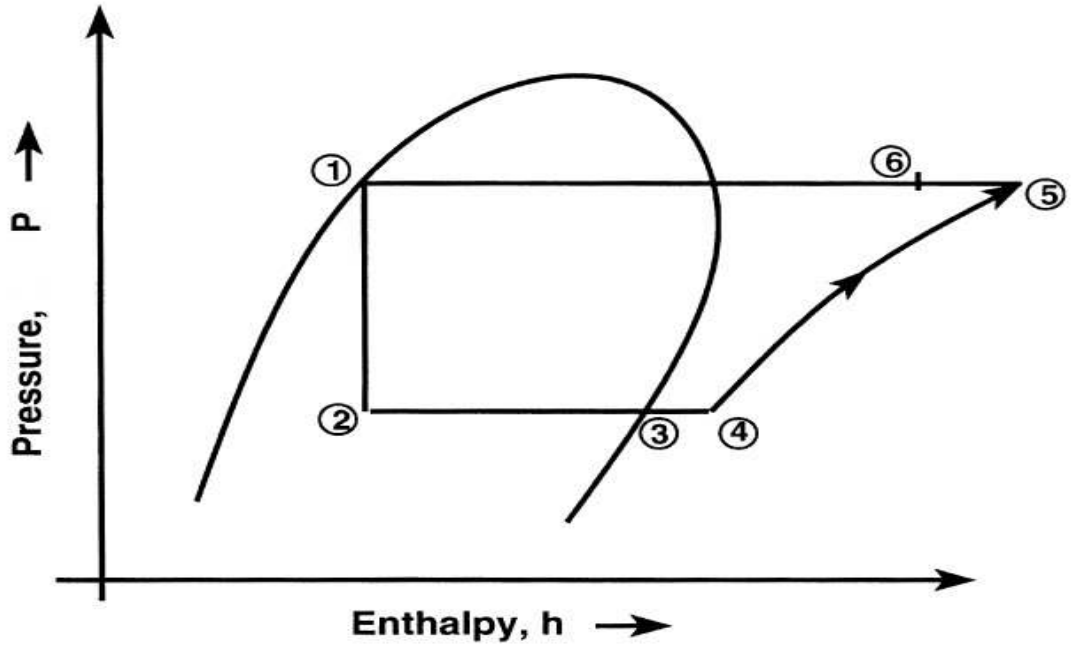

Figure 3.1 Pressure-Enthalpy diagram for simple VCRS

Considering the steady-state cyclic operation of the system as shown in figures 3.1 and 3.2, saturated refrigerant vapour enters the compressor at state 4 and saturated liquid exits the condenser at state 1.The refrigerant then flows through the expansion valve to the evaporator. Referring to figure 3.2, using the first law of

thermodynamics and the fact that change in internal energy is zero for a cyclic process, we get

$$Q_{cond} + Q_{loss,cond} - (Q_{evap} + Q_{loss,evap}) - W_{cp} = 0 \quad \text{.....(1)}$$

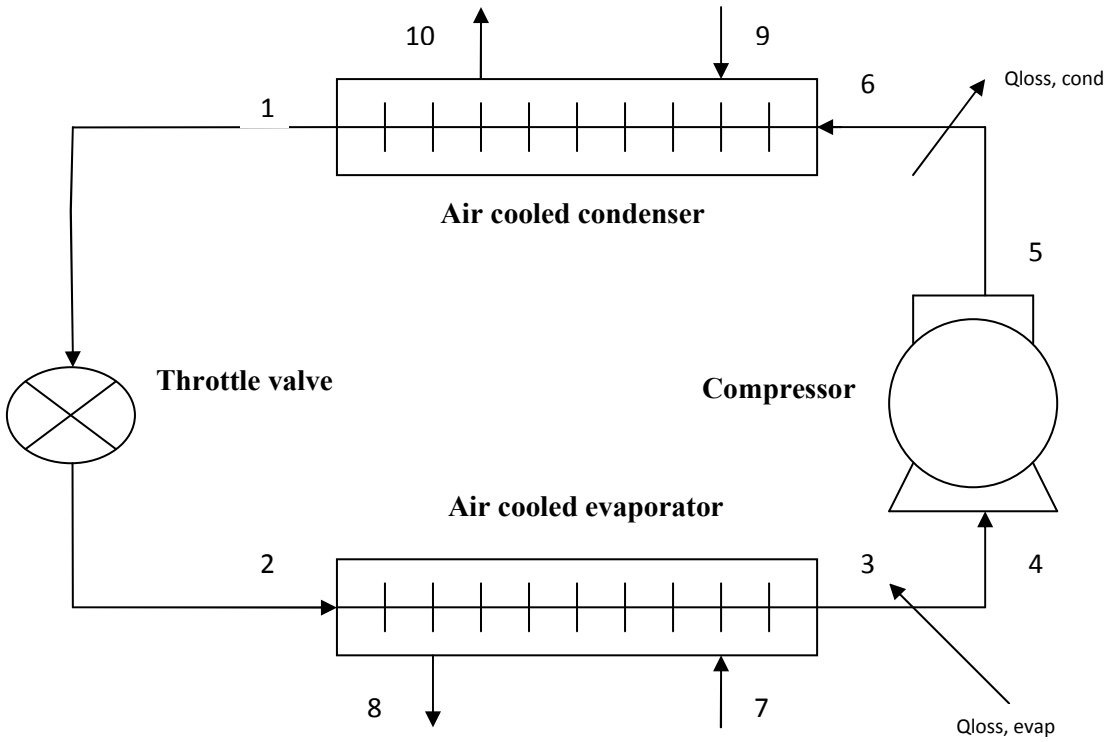

Figure 3.2 Schematic diagram of a simple VCRS

Heat transfer to and from the cycle occurs by convection to flowing fluid streams with finite mass-flow rates and specific heats. Therefore, the heat-transfer rate to the cycle in the evaporator becomes

$$Q_{evap} = (\epsilon C_{min})_{evap} (T_7 - T_2) = m_{ref} (h_3 - h_2) \quad \text{.....(2)}$$

Similarly, the heat-transfer rate between the refrigeration cycle and the sink in the condenser is

$$Q_{cond} = (\epsilon C_{min})_{cond} (T_1 - T_9) = m_{ref} (h_6 - h_1) \quad \text{.....(3)}$$

The power required by the compressor is described in terms of an isentropic efficiency, given by

$$W_{cp} = m_{ref} (h_5 - h_4) = \frac{W_{cp,isn}}{\eta_{cp,isn}} \quad \text{.....(4)}$$

By applying the first law of thermodynamics, work input to the compressor can also be expressed as

$$Q_w - W_{cp} = m_{ref} (h_5 - h_4) \quad \text{.....(5)}$$

We assume that the heat leaking into the suction line is

$$Q_{sl} = m_{ref} (h_4 - h_3) \quad \text{.....(6)}$$

Similarly, the heat leakage from the discharge line can be expressed as

$$Q_{dl} = m_{ref} (h_6 - h_5) \quad \text{.....(7)}$$

The COP is defined as the refrigerating effect over the net compressor work input, i.e.

$$COP = \frac{Q_{evap}}{W_{cp}} \qquad \text{.....(8)}$$

The first law efficiency alone is not a realistic measure of performance of engineering device. To overcome this deficiency, we define second law efficiency, η_{II} as the ratio of the actual thermal efficiency (η_{th}) to the maximum possible (reversible) thermal efficiency ($\eta_{th,rev}$) and the ratio of actual coefficient of performance (COP) to the maximum possible coefficient of performance (COP_{rev}) under the same condition.

The deviation of an actual refrigeration system from a reversible one can be written in the form of second law efficiency as

$$\eta_{II} = \frac{COP}{COP_{rev}} = \frac{\eta_I}{\eta\ \mathrm{th,rev}} \qquad \text{..... (9)}$$

$$\text{Where, } COP_{rev} = \left(\frac{T_7}{T_9 - T_7}\right) \qquad \text{..... (9a)}$$

The exit temperature of external fluid at evaporator can be found from the following equation,

$$\epsilon_{evap} = \frac{T_7 - T_8}{T_7 - T_2} \qquad \text{..... (10)}$$

The exit temperature of external fluid at condenser can be found from the following equation,

$$\epsilon_{cond} = \frac{T_{10} - T_9}{T_6 - T_9} \qquad \text{..... (11)}$$

The overall conductance, we can write from the heat exchanger theory (Incropera et al. [23])

$$UA=C_{min}*ln\left(\frac{1}{1-Є}\right) \quad \text{..... (12)}$$

The reduction in UA value is due to the increase in fouling on the air-side and can be represented as a percentage, UA%, in the following manner

$$UA\%=\left(1-\frac{UA}{UA_{cl}}\right)*100 \quad \text{..... (13)}$$

In the current work, the percentage decrease in the UA% value due to fouling has been varied from 0% to 50% for each heat exchanger where a zero value refers to clean conditions. Furthermore, heat leakages ($Q_{sl,}$ Q_{dl}) in the lines and pressure drop in the heat exchangers are considered as negligible in all the calculation. A computer program is written in Engineering Equation Solver (EES) for solving the above set of equations. In this program, thermo physical properties of the refrigerants are needed at each step of the calculation, which are obtained from the built in functions provided by EES.

CHAPTER 4

RESULTS AND DISCUSSION

This chapter deals with the results and discussion for simple VCRS under fouled condition. Methodology and formulation for these systems are given in chapter 3.

4.1 Model validation

Stoecker and Jones [22] have presented the performance data of each of the components of a vapor compression refrigeration system in which the details of the equations used are also given for York hermetic reciprocating compressor (H62SP-22E,R22,1750rpm). The condenser performance, assuming constant heat exchanger parameters for Bohn heat transfer division air-cooled condenser, refrigerant 22, model number 36 was represented by (Stoecker and Jones [22]):

$$Q_{cond} = 9.39(T_1 - T_{in,cond}) \quad \text{---------- (14)}$$

Where the number 9.39 represents the value of $(\varepsilon C_{min})_{cond}$ in kWK^{-1}

The cooling capacity for a Dunham-Bush, Refrigerant 22, direct-expansion, inner-fin liquid chiller (CH660B) was given by (Stoecker and Jones [22]):

$$Q_{evap} = 6[1+0.046(T_{in,evap} - T_2)]\,(T_{in,evap} - T_2) \quad \text{---------- (15)}$$

It should be noted that in Eq. (14), the term $6[1+0.046(T_{in,evap} - T_2)]$ represents $(\varepsilon C_{min})_{evap}$. Considering the above model of Stoecker and Jones [22], the following data set was used to generate results for comparison purpose: $T_{in,cond} = 40^oC$, $(\varepsilon C_{min})_{cond} = 9.39\ kWK^{-1}$, $\eta_{cp,isn} = 0.65$ wherein $T_{in,evap}$ was varied from 0 to 15 ^oC. It should be noted that, in this range, the cooling capacity varied from 57.24 - 90.56kW and

$(\varepsilon C_{min})_{evap}$ from 7.98 to 8.83 kWK^{-1} in the model of Stoecker and Jones [22]. These values of the cooling capacity and $(\varepsilon C_{min})_{evap}$ were then used in our property based model to compare the prediction of the heat rejected, compressor power and COP along with the condenser and evaporator temperatures (see Table 4.0). It shows that all relevant quantities can be predicted by the property based model accurately wherein the maximum error encountered was 2.84.

Table 4.0 Comparison of performance data from Stoecker and Jones [22] and current model.

$T_{in,evap}$ (^oC)	Q^*_{cond} (kW)	$Q_{cond,mod}$ (kW)	error (%)	W^*_{cp} (kW)	$W_{cp,mod}$ (kW)	error (%)	T^*_1 (^oC)	$T_{1,mod}$ (^oC)	error (%)	COP^* (kW)	COP_{mod} (kW)	error (%)
0	82.16	**82.40**	**0.29**	24.92	**25.19**	**1.07**	48.75	**48.77**	**0.04**	2.30	**2.27**	**-1.32**
15	122.00	**122.93**	**0.57**	31.45	**32.37**	**2.84**	52.99	**53.09**	**0.18**	2.88	**2.80**	**-2.77**

*From the performance data of Stoecker and Jones [22].

4.2 Results of a single stage VCRS

The thermodynamic model given in chapter 3 is used to evaluate the performance of vapour compression system. The performance is evaluated with three refrigerants (R134a, R1234yf, and R1234ze). The results obtained are discussed below. It should be noted that for an actual system, as the refrigeration capacity of the system varies, the performance of the compressor and heat exchangers represented by compressor efficiency and effectiveness respectively, will not be constant. However for the present investigation, we have considered these parameters constant.

4.2.1 Input conditions

The input to the thermodynamic model are evaporator coolant inlet temperature ($T_{in,evap}$ in K), Condenser coolant inlet temperature ($T_{in,cond}$ in K), rate of heat absorbed by evaporator (Q_{evap} in kW), product of condenser effectiveness and capacitance rate of external fluid [$(\epsilon C_{min})_{cond}$, kW/K], product of evaporator effectiveness and capacitance rate of external fluid [$(\epsilon C_{min})_{evap}$, kW/K] and isentropic efficiency of compressor ($\eta_{cp,isn}$). The values of [$(\epsilon C_{min})_{evap}$] has been taken constant for analysis purpose but for actual system it will vary with the refrigeration capacity. The thermodynamic properties of various refrigerants at various state points are calculated using a program developed in EES. The values of inputs at design point are given in Table 4.1, and these are referred from the work of Qureshi and Zubair [19] & Khan and Zubair [4].

Table 4.1 Values of inputs at design point

Parameters	Values
Evaporator coolant inlet temperature ($T_{in,evap}$ in K)	273
Condenser coolant inlet temperature ($T_{in,cond}$ in K)	308-313
Rate of heat absorbed by evaporator (Q_{evap} in kW)	100
Product of condenser effectiveness and capacitance rate of external fluid [$(\epsilon C_{min})_{cond}$, kW/K]	9.39
Product of evaporator effectiveness and capacitance rate of external fluid [$(\epsilon C_{min})_{evap}$, kW/K]	8.2
Isentropic efficiency of compressor ($\eta_{cp,isn}$)	0.65
Effectiveness (Є)	0.80
Refrigerants	R134a, R1234yf, R1234ze

4.2.2 Results

The values of performance parameters (COP_f, $Wact_f$, COP%, W_{cp}%, Qevap%, Є%, $Qevap_f$, T_{1f}, T_{2f}, P_{1f}, P_{2f}, $m_{ref,f}$, η_{II}) obtained for condenser, evaporator fouling individually and simultaneously for different refrigerants are given in tables 4.2-4.10.

Table 4.2

a) Results of performance parameter for R134a on condenser fouling at $T_{in,cond} = 40^o$ C.

UA_{cond} (%)	COP_f	$Wact_f$ (kW)	COP (%)	W_{cp} (%)	Qevap (%)	Є (%)	$Qevap_f$ (kW)
0	1.664	60.11	0	0	0	0	100
10	1.637	60.54	-1.609	0.714	-0.907	-4.365	99.09
20	1.603	61.11	-3.659	1.650	-2.070	-9.493	97.93
30	1.559	61.84	-6.303	2.873	-3.611	-15.52	96.39
40	1.501	62.79	-9.761	4.447	-5.748	-22.59	94.25
50	1.423	64.14	-14.49	6.690	-8.767	-30.90	91.23

UA_{cond} (%)	T_{1f} (^{o}C)	T_{2f} (^{o}C)	P_{1f} (MPa)	P_{2f} (MPa)	$m_{ref,f}$ (kg s^{-1})	η_{II} (%)
0	56.68	-10.42	1.554	0.1975	0.9068	24.37
10	57.38	-10.32	1.581	0.1982	0.9075	23.98
20	58.30	-10.20	1.616	0.1992	0.9085	23.48
30	59.50	-10.04	1.663	0.2004	0.9098	22.80
40	61.13	-9.81	1.728	0.2022	0.9113	21.99
50	63.42	-9.50	1.823	0.2047	0.9138	20.84

b) Results of performance parameter for R134a on condenser fouling at $T_{in,cond}$ = 37.5^{o} C.

UA_{cond} (%)	COP_f	$Wact_f$ (kW)	COP (%)	W_{cp} (%)	Qevap (%)	Є (%)	$Qevap_f$ (kW)
0	1.798	55.63	0	0	0	0	100
10	1.769	56.05	-1.582	0.762	-0.832	-4.365	99.17
20	1.732	56.64	-3.622	1.819	-1.868	-9.493	98.13
30	1.686	57.38	-6.229	3.154	-3.272	-15.52	96.73
40	1.624	58.34	-9.631	4.867	-5.233	-22.59	94.77
50	1.543	59.57	-14.18	7.085	-8.099	-30.90	91.90

UA_{cond} (%)	T_{1f} (^{o}C)	T_{2f} (^{o}C)	P_{1f} (MPa)	P_{2f} (MPa)	$m_{ref,f}$ (kg s^{-1})	η_{II} (%)
0	53.71	-10.42	1.446	0.1975	0.8696	24.69
10	54.40	-10.32	1.471	0.1981	0.8703	24.30
20	55.31	-10.22	1.504	0.1990	0.8717	23.80
30	56.50	-10.07	1.548	0.2001	0.8733	23.15
40	58.10	-9.87	1.608	0.2018	0.8749	22.31
50	60.33	-9.57	1.696	0.2041	0.8762	21.19

c) Results of performance parameter for R134a on condenser fouling at $T_{in,cond}$ = 35^{o} C.

UA_{cond} (%)	**COP_f**	**$Wact_f$ (kW)**	**COP (%)**	**W_{cp} (%)**	**Qevap (%)**	**Є (%)**	**$Qevap_f$ (kW)**
0	1.940	51.54	0	0	0	0	100
10	1.910	51.95	-1.558	0.795	-0.775	-4.365	99.22
20	1.871	52.33	-3.577	1.924	-1.722	-9.493	98.28
30	1.821	53.27	-6.158	3.356	-3.009	-15.52	96.99
40	1.756	54.19	-9.498	5.147	-4.840	-22.59	95.16
50	1.670	55.34	-13.915	7.378	-7.564	-30.90	92.44

UA_{cond} (%)	**T_{1f} (^{o}C)**	**T_{2f} (^{o}C)**	**P_{1f} (MPa)**	**P_{2f} (MPa)**	**$m_{ref,f}$ (kg s^{-1})**	**η_{II} (%)**
0	50.78	-10.42	1.345	0.1975	0.8363	24.88
10	51.46	-10.33	1.368	0.1981	0.8369	24.49
20	52.35	-10.23	1.398	0.1989	0.8383	23.99
30	53.52	-10.10	1.439	0.1999	0.8400	23.34
40	55.09	-9.91	1.496	0.2014	0.8414	22.51
50	57.27	-9.62	1.577	0.2037	0.8363	21.41

Table 4.3

a) Results of performance parameter for R134a on evaporator fouling at $T_{in,cond}$ = 40^{o} C.

UA_{evap} (%)	COP_f	$Wact_f$ (kW)	COP (%)	W_{cp} (%)	Qevap (%)	Є (%)	$Qevap_f$ (kW)
0	1.664	60.11	0	0	0	0	100
10	1.658	59.53	-0.328	-0.965	-1.291	-4.365	98.71
20	1.651	58.80	-0.745	-2.183	-2.912	-9.493	97.09
30	1.642	57.87	-1.288	-3.727	-4.967	-15.52	95.03
40	1.631	56.63	-1.975	-5.804	-7.664	-22.59	92.34
50	1.614	55.06	-2.994	-8.413	-11.16	-30.90	88.84

UA_{evap} (%)	T_{1f} (^{o}C)	T_{2f} (^{o}C)	P_{1f} (MPa)	P_{2f} (MPa)	$m_{ref,f}$ (kg s^{-1})	η_{II} (%)
0	56.68	-10.42	1.554	0.1975	0.9068	24.37
10	56.48	-10.75	1.547	0.1949	0.8942	24.29
20	56.23	-11.17	1.538	0.1916	0.8785	24.19
30	55.92	-11.71	1.526	0.1875	0.8586	24.06
40	55.51	-12.42	1.511	0.1822	0.8325	23.89
50	54.98	-13.39	1.492	0.1752	0.7992	23.64

b) Results of performance parameter for R134a on evaporator fouling at $T_{in,cond}$ = 37.5^{o} C.

UA_{evap} (%)	COP_f	$Wact_f$ (kW)	COP (%)	W_{cp} (%)	Qevap (%)	Є (%)	$Qevap_f$ (kW)
0	1.798	55.63	0	0	0	0	100
10	1.792	55.06	-0.321	-1.023	-1.341	-4.365	98.66
20	1.785	54.34	-0.723	-2.319	-3.026	-9.493	96.97
30	1.775	53.43	-1.248	-3.962	-5.161	-15.52	94.84
40	1.764	52.17	-1.883	-6.224	-7.990	-22.59	92.10
50	1.746	50.63	-2.874	-8.981	-11.60	-30.90	88.40

UA_{evap} (%)	T_{1f} (^{o}C)	T_{2f} (^{o}C)	P_{1f} (MPa)	P_{2f} (MPa)	$m_{ref,f}$ (kg s^{-1})	η_{II} (%)
0	53.71	-10.42	1.446	0.1975	0.8696	24.69
10	53.51	-10.74	1.439	0.1949	0.8571	24.61
20	53.26	-11.16	1.430	0.1917	0.8414	24.51
30	52.94	-11.69	1.419	0.1877	0.8216	24.38
40	52.51	-12.38	1.404	0.1825	0.7954	24.23
50	51.98	-13.32	1.386	0.1757	0.7625	23.98

c) Results of performance parameter for R134a on evaporator fouling at $T_{in,cond}$ = 35^{o} C.

UA_{evap} (%)	COP_f	$Wact_f$ (kW)	COP (%)	W_{cp} (%)	Qevap (%)	Є (%)	$Qevap_f$ (kW)
0	1.940	51.54	0	0	0	0	100
10	1.934	50.98	-0.314	-1.077	-1.388	-4.365	98.61
20	1.927	50.26	-0.689	-2.482	-3.154	-9.493	96.85
30	1.918	49.30	-1.142	-4.330	-5.434	-15.52	94.57
40	1.906	48.10	-1.777	-6.667	-8.326	-22.59	91.67
50	1.888	46.57	-2.706	-9.633	-12.079	-30.90	87.92

UA_{evap} (%)	T_{1f} (^{o}C)	T_{2f} (^{o}C)	P_{1f} (MPa)	P_{2f} (MPa)	$m_{ref,f}$ (kg s^{-1})	η_{II} (%)
0	50.78	-10.42	1.345	0.1975	0.8363	24.88
10	50.58	-10.74	1.338	0.1949	0.8239	24.80
20	50.32	-11.14	1.329	0.1918	0.8080	24.70
30	49.98	-11.66	1.318	0.1879	0.7876	24.59
40	49.56	-12.33	1.304	0.1829	0.7619	24.43
50	49.00	-13.25	1.286	0.1762	0.7290	24.20

Table 4.4

a) Result of performance parameter for R134a on condenser and evaporator fouling at $T_{in,cond}$ = 40^{o} C.

$UA_{cond,evap}$ (%)	COP_f	$Wact_f$ (kW)	COP (%)	W_{cp} (%)	Qevap (%)	Є (%)	$Qevap_f$ (kW)
0	1.664	60.11	0	0	0	0	100
10	1.632	59.97	-1.918	-0.247	-2.160	-4.365	97.84
20	1.593	59.76	-4.276	-0.586	-4.828	-9.493	95.17
30	1.544	59.52	-7.204	-0.989	-8.120	-15.52	91.88
40	1.483	59.13	-10.861	-1.636	-12.32	-22.59	87.68
50	1.405	58.59	-15.54	-2.541	-17.69	-30.90	82.31

$UA_{cond,evap}$ (%)	T_{1f} (^{o}C)	T_{2f} (^{o}C)	P_{1f} (MPa)	P_{2f} (MPa)	$m_{ref,f}$ (kg s^{-1})	η_{II} (%)
0	56.68	-10.42	1.554	0.1975	0.9068	24.37
10	57.18	-10.65	1.574	0.1956	0.8950	23.91
20	57.83	-10.95	1.598	0.1933	0.8804	23.33
30	58.66	-11.32	1.630	0.1904	0.8625	22.62
40	59.75	-11.79	1.673	0.1869	0.8393	21.73
50	61.24	-12.40	1.733	0.1823	0.8094	20.59

b) Results of performance parameter for R134a on condenser and evaporator fouling at $T_{in,cond}$ = 37.5^{o} C.

$UA_{cond,evap}$ (%)	COP_f	$Wact_f$ (kW)	COP (%)	W_{cp} (%)	Qevap (%)	Є (%)	$Qevap_f$ (kW)
0	1.798	55.63	0	0	0	0	100
10	1.764	55.49	-1.886	-0.250	-2.131	-4.365	97.87
20	1.722	55.30	-4.190	-0.601	-4.767	-9.493	95.23
30	1.672	54.99	-7.012	-1.151	-8.082	-15.52	91.92
40	1.608	54.58	-10.56	-1.886	-12.25	-22.59	87.75
50	1.524	54.13	-15.19	-2.702	-17.49	-30.90	82.51

$UA_{cond,evap}$ (%)	T_{1f} (^{o}C)	T_{2f} (^{o}C)	P_{1f} (MPa)	P_{2f} (MPa)	$m_{ref,f}$ (kg s^{-1})	η_{II} (%)
0	53.71	-10.42	1.446	0.1975	0.8696	24.69
10	54.20	-10.66	1.464	0.1956	0.8580	24.23
20	54.82	-10.96	1.486	0.1932	0.8435	23.66
30	55.61	-11.33	1.515	0.1904	0.8250	22.96
40	56.65	-11.80	1.553	0.1868	0.8016	22.08
50	58.09	-12.43	1.608	0.1821	0.7728	20.94

c) Results of performance parameter for R134a on condenser and evaporator fouling at $T_{in,cond}$ = 35^{o} C.

$UA_{cond,evap}$ (%)	COP_f	$Wact_f$ (kW)	COP (%)	W_{cp} (%)	Qevap (%)	Є (%)	$Qevap_f$ (kW)
0	1.940	51.54	0	0	0	0	100
10	1.904	51.41	-1.864	-0.253	-2.111	-4.365	97.89
20	1.860	51.21	-4.124	-0.641	-4.739	-9.493	95.26
30	1.807	50.90	-6.884	-1.248	-8.045	-15.52	91.95
40	1.738	50.54	-10.404	-1.932	-12.14	-22.59	87.86
50	1.654	50.02	-14.876	-2.953	-17.389	-30.90	82.61

$UA_{cond,evap}$ (%)	T_{1f} (^{o}C)	T_{2f} (^{o}C)	P_{1f} (MPa)	P_{2f} (MPa)	$m_{ref,f}$ (kg s^{-1})	η_{II} (%)
0	50.78	-10.42	1.345	0.1975	0.8363	24.88
10	51.26	-10.66	1.361	0.1955	0.8248	24.41
20	51.85	-10.96	1.381	0.1932	0.8102	23.85
30	52.61	-11.33	1.407	0.1904	0.7916	23.16
40	53.62	-11.82	1.443	0.1867	0.7689	22.29
50	54.99	-12.45	1.492	0.1820	0.7394	21.17

Table 4.5

a) Results of performance parameter for R1234yf on condenser fouling at $T_{in,cond}$ = 40° C**.**

UA_{cond} (%)	COP_f	$Wact_f$ (kW)	COP (%)	W_{cp} (%)	Qevap (%)	Є (%)	$Qevap_f$ (kW)
0	1.338	74.75	0	0	0	0	100
10	1.311	75.17	-2.014	0.568	-1.458	-4.365	98.54
20	1.272	76.14	-4.881	1.864	-3.108	-9.493	96.89
30	1.225	77.16	-8.395	3.223	-5.443	-15.52	94.56
40	1.163	78.56	-13.06	5.091	-8.63	-22.59	91.37
50	1.080	80.34	-19.29	7.477	-13.25	-30.90	86.75

UA_{cond} (%)	T_{1f} (°C)	T_{2f} (°C)	P_{1f} (MPa)	P_{2f} (MPa)	$m_{ref,f}$ (kg s^{-1})	η_{II} (%)
0	58.20	-10.42	1.575	0.2186	1.414	19.60
10	58.92	-10.26	1.601	0.2198	1.415	19.21
20	59.91	-10.09	1.638	0.2212	1.424	18.64
30	61.17	-9.84	1.684	0.2232	1.431	17.96
40	62.86	-9.51	1.749	0.2259	1.442	17.04
50	65.18	-9.03	1.841	0.2300	1.456	15.82

b) Results of performance parameter for R1234yf on condenser fouling at $T_{in,cond}$ = 37.5^{o} C**.**

UA_{cond} (%)	COP_f	$Wact_f$ (kW)	COP (%)	W_{cp} (%)	Qevap (%)	Є (%)	$Qevap_f$ (kW)
0	1.495	66.91	0	0	0	0	100
10	1.466	67.37	-1.930	0.685	-1.258	-4.365	98.74
20	1.427	68.18	-4.551	1.902	-2.736	-9.493	97.26
30	1.376	69.27	-7.951	3.533	-4.699	-15.52	95.30
40	1.310	70.62	-12.337	5.542	-7.479	-22.59	92.52
50	1.222	72.43	-18.25	8.246	-11.51	-30.90	88.49

UA_{cond} (%)	T_{1f} (^{o}C)	T_{2f} (^{o}C)	P_{1f} (MPa)	P_{2f} (MPa)	$m_{ref,f}$ (kg s^{-1})	η_{II} (%)
0	54.88	-10.42	1.460	0.2186	1.311	20.53
10	55.59	-10.28	1.484	0.2196	1.313	20.13
20	56.54	-10.13	1.517	0.2209	1.319	19.60
30	57.79	-9.92	1.561	0.2226	1.328	18.90
40	59.45	-9.63	1.621	0.2250	1.338	18.00
50	61.75	-9.21	1.707	0.2284	1.351	16.78

c) Results of performance parameter for R1234yf on condenser fouling at $T_{in,cond}$ = 35° C**.**

UA_{cond} (%)	COP_f	$Wact_f$ (kW)	COP (%)	W_{cp} (%)	Qevap (%)	Є (%)	$Qevap_f$ (kW)
0	1.656	60.40	0	0	0	0	100
10	1.625	60.84	-1.847	0.742	-1.119	-4.365	98.88
20	1.584	61.57	-4.316	1.952	-2.448	-9.493	97.55
30	1.530	62.65	-7.590	3.732	-4.141	-15.52	95.86
40	1.459	64.08	-11.88	6.099	-6.512	-22.59	93.49
50	1.365	65.90	-17.55	9.122	-10.058	-30.90	89.94

UA_{cond} (%)	T_{1f} (°C)	T_{2f} (°C)	P_{1f} (MPa)	P_{2f} (MPa)	$m_{ref,f}$ (kg s^{-1})	η_{II} (%)
0	51.70	-10.42	1.355	0.2186	1.228	21.23
10	52.39	-10.30	1.377	0.2195	1.230	20.84
20	53.31	-10.16	1.407	0.2206	1.235	20.31
30	54.54	-9.98	1.448	0.2221	1.243	19.62
40	56.20	-9.73	1.405	0.2241	1.254	18.70
50	58.49	-9.36	1.586	0.2272	1.267	17.50

Table 4.6

a) Results of performance parameter for R1234yf on evaporator fouling at $T_{in,cond}$ = 40^{o} C.

UA_{evap} (%)	COP_f	$Wact_f$ (kW)	COP (%)	W_{cp} (%)	Qevap (%)	€ (%)	$Qevap_f$ (kW)
0	1.338	74.75	0	0	0	0	100
10	1.332	74.22	-0.414	-0.714	-1.13	-4.365	98.87
20	1.326	73.51	-0.917	-1.658	-2.56	-9.493	97.44
30	1.317	72.59	-1.555	-2.892	-4.402	-15.52	95.60
40	1.306	71.37	-2.394	-4.524	-6.81	-22.59	93.19
50	1.290	69.79	-3.590	-6.640	-9.99	-30.90	90.01

UA_{evap} (%)	T_{1f} (^{o}C)	T_{2f} (^{o}C)	P_{1f} (MPa)	P_{2f} (MPa)	$m_{ref,f}$ (kg s^{-1})	η_{II} (%)
0	58.20	-10.42	1.575	0.2186	1.414	19.60
10	58.03	-10.76	1.569	0.2157	1.397	19.52
20	57.80	-11.21	1.561	0.2122	1.375	19.42
30	57.51	-11.78	1.551	0.2077	1.348	19.30
40	57.14	-12.54	1.538	0.2019	1.312	19.13
50	56.64	-13.56	1.520	0.1942	1.265	18.90

b) Results of performance parameter for R1234yf on evaporator fouling at $T_{in,cond}$ = 37.5^{o} C.

UA_{evap} (%)	COP_f	$Wact_f$ (kW)	COP (%)	W_{cp} (%)	Qevap (%)	€ (%)	$Qevap_f$ (kW)
0	1.495	66.91	0	0	0	0	100
10	1.489	66.38	-0.400	-0.791	-1.190	-4.365	98.81
20	1.482	65.65	-0.859	-1.879	-2.722	-9.493	97.28
30	1.473	64.72	-1.452	-3.274	-4.678	-15.52	95.32
40	1.462	63.44	-2.192	-5.183	-7.260	-22.59	92.74
50	1.445	61.90	-3.345	-7.490	-10.59	-30.90	89.41

UA_{evap} (%)	T_{1f} (^{o}C)	T_{2f} (^{o}C)	P_{1f} (MPa)	P_{2f} (MPa)	$m_{ref,f}$ (kg s^{-1})	η_{II} (%)
0	54.88	-10.42	1.460	0.2186	1.311	20.53
10	54.70	-10.76	1.454	0.2158	1.295	20.45
20	54.47	-11.19	1.446	0.2124	1.273	20.35
30	54.17	-11.75	1.436	0.2080	1.246	20.23
40	53.76	-12.47	1.422	0.2024	1.210	20.08
50	53.26	-13.47	1.406	0.1949	1.164	19.84

c) Results of performance parameter for R1234yf on evaporator fouling at $T_{in,cond}$ = 35° C**.**

UA_{evap} (%)	COP_f	$Wact_f$ (kW)	COP (%)	W_{cp} (%)	Qevap (%)	Є (%)	$Qevap_f$ (kW)
0	1.656	60.40	0	0	0	0	100
10	1.649	59.88	-0.390	-0.857	-1.240	-4.365	98.16
20	1.642	59.15	-0.817	-2.068	-2.870	-9.493	97.13
30	1.634	58.15	-1.312	-3.725	-4.988	-15.52	95.10
40	1.622	56.94	-2.053	-5.724	-7.659	-22.59	92.34
50	1.605	55.34	-3.081	-8.307	-11.190	-30.90	88.81

UA_{evap} (%)	T_{1f} (°C)	T_{2f} (°C)	P_{1f} (MPa)	P_{2f} (MPa)	$m_{ref,f}$ (kg s^{-1})	η_{II} (%)
0	51.70	-10.42	1.355	0.2186	1.228	21.23
10	51.52	-10.75	1.349	0.2159	1.212	21.15
20	51.27	-11.17	1.342	0.2125	1.190	21.05
30	50.95	-11.71	1.331	0.2083	1.162	20.95
40	50.54	-12.45	1.319	0.2028	1.127	20.79
50	50.01	-13.38	1.302	0.1956	1.082	20.57

Table 4.7

a) Results of performance parameter for R1234yf on condenser and evaporator fouling at $T_{in,cond}$ = 40^{o} C**.**

$UA_{cond,evap}$ (%)	COP_f	$Wact_f$ (kW)	COP (%)	W_{cp} (%)	Qevap (%)	Є (%)	$Qevap_f$ (kW)
0	1.338	74.75	0	0	0	0	100
10	1.306	74.61	-2.377	-0.183	-2.56	-4.365	97.44
20	1.267	74.40	-5.276	-0.463	-5.715	-9.493	94.28
30	1.219	74.16	-8.902	-0.785	-9.618	-15.52	90.38
40	1.158	73.75	-13.406	-1.337	-14.56	-22.59	85.44
50	1.081	73.22	-19.209	-2.054	-20.87	-30.90	79.13

$UA_{cond,evap}$ (%)	T_{1f} (^{o}C)	T_{2f} (^{o}C)	P_{1f} (MPa)	P_{2f} (MPa)	$m_{ref,f}$ (kg s^{-1})	η_{II} (%)
0	58.20	-10.42	1.575	0.2186	1.414	19.60
10	58.74	-10.61	1.595	0.2170	1.398	19.14
20	59.41	-10.85	1.619	0.2151	1.379	18.57
30	60.28	-11.14	1.651	0.2128	1.355	17.86
40	61.42	-11.49	1.694	0.2100	1.325	16.97
50	62.96	-11.92	1.753	0.2066	1.287	15.84

b) Results of performance parameter for R1234yf on condenser and evaporator fouling at $T_{in,cond}$ = 37.5^{o} C**.**

$UA_{cond,evap}$ (%)	COP_f	$Wact_f$ (kW)	COP (%)	W_{cp} (%)	Qevap (%)	Є (%)	$Qevap_f$ (kW)
0	1.495	66.91	0	0	0	0	100
10	1.461	66.79	-2.259	-0.185	-2.440	-4.365	97.56
20	1.420	66.54	-4.971	-0.545	-5.489	-9.493	94.51
30	1.368	66.36	-8.441	-0.816	-9.188	-15.52	90.81
40	1.306	65.90	-12.640	-1.504	-13.95	-22.59	86.05
50	1.224	65.39	-18.109	-2.275	-19.97	-30.90	80.03

$UA_{cond,evap}$ (%)	T_{1f} (^{o}C)	T_{2f} (^{o}C)	P_{1f} (MPa)	P_{2f} (MPa)	$m_{ref,f}$ (kg s^{-1})	η_{II} (%)
0	54.88	-10.42	1.460	0.2186	1.311	20.53
10	55.40	-10.62	1.477	0.2169	1.296	20.07
20	56.03	-10.87	1.499	0.2149	1.276	19.51
30	56.87	-11.19	1.528	0.2124	1.254	18.80
40	57.94	-11.57	1.566	0.2094	1.223	17.93
50	59.42	-12.06	1.619	0.2056	1.185	16.81

c) Results of performance parameter for R1234yf on condenser and evaporator fouling at $T_{in,cond}$ = 35^{o} C**.**

$UA_{cond,evap}$ (%)	COP_f	$Wact_f$ (kW)	COP (%)	W_{cp} (%)	Qevap (%)	Є (%)	$Qevap_f$ (kW)
0	1.656	60.40	0	0	0	0	100
10	1.620	60.26	-2.155	-0.222	-2.37	-4.365	97.63
20	1.577	60.04	-4.760	-0.591	-5.323	-9.493	94.68
30	1.523	59.80	-8.030	-0.988	-8.939	-15.52	91.06
40	1.456	59.40	-12.075	-1.651	-13.53	-22.59	86.47
50	1.370	58.86	-17.254	-2.549	-19.36	-30.90	80.64

$UA_{cond,evap}$ (%)	T_{1f} (^{o}C)	T_{2f} (^{o}C)	P_{1f} (MPa)	P_{2f} (MPa)	$m_{ref,f}$ (kg s^{-1})	η_{II} (%)
0	51.70	-10.42	1.355	0.2186	1.228	21.23
10	52.19	-10.63	1.371	0.2168	1.213	20.77
20	52.80	-10.89	1.391	0.2147	1.193	20.22
30	53.60	-11.22	1.417	0.2121	1.170	19.52
40	54.62	-11.63	1.451	0.2089	1.140	18.66
50	56.02	-12.15	1.499	0.2049	1.102	17.57

Table 4.8

a) Results of performance parameter for R1234ze on condenser fouling at $T_{in,cond}$ = 40^{o} C.

UA_{cond} (%)	COP_f	$Wact_f$ (kW)	COP (%)	W_{cp} (%)	Qevap (%)	Є (%)	$Qevap_f$ (kW)
0	1.675	59.76	0	0	0	0	100
10	1.647	60.18	-1.593	0.697	-0.908	-4.365	99.09
20	1.612	60.75	-3.645	1.658	-2.048	-9.493	97.95
30	1.569	61.47	-6.264	2.855	-3.588	-15.52	96.41
40	1.510	62.46	-9.740	4.515	-5.665	-22.59	94.34
50	1.431	63.84	-14.47	6.826	-8.628	-30.90	91.37

UA_{cond} (%)	T_{1f} (^{o}C)	T_{2f} (^{o}C)	P_{1f} (MPa)	P_{2f} (MPa)	$m_{ref,f}$ (kg s^{-1})	η_{II} (%)
0	56.64	-10.42	1.177	0.1466	0.9992	24.52
10	57.34	-10.32	1.197	0.1472	1.000	24.13
20	58.26	-10.20	1.224	0.1479	1.001	23.62
30	59.46	-10.04	1.260	0.1488	1.003	22.98
40	61.09	-9.82	1.310	0.1501	1.005	22.13
50	63.39	-9.51	1.383	0.1520	1.008	20.97

b) Results of performance parameter for R1234ze on condenser fouling at $T_{in,cond}$ = 37.5^{o} C**.**

UA_{cond} (%)	COP_f	$Wact_f$ (kW)	COP (%)	W_{cp} (%)	Qevap (%)	€ (%)	$Qevap_f$ (kW)
0	1.808	55.32	0	0	0	0	100
10	1.779	55.76	-1.591	0.796	-0.808	-4.365	99.19
20	1.743	56.31	-3.596	1.792	-1.869	-9.493	98.13
30	1.696	57.03	-6.180	3.096	-3.276	-15.52	96.72
40	1.634	58.04	-9.617	4.923	-5.168	-22.59	94.83
50	1.551	59.32	-14.179	7.227	-7.977	-30.90	92.02

UA_{cond} (%)	T_{1f} (^{o}C)	T_{2f} (^{o}C)	P_{1f} (MPa)	P_{2f} (MPa)	$m_{ref,f}$ (kg s^{-1})	η_{II} (%)
0	53.67	-10.42	1.094	0.1466	0.9591	24.83
10	54.37	-10.33	1.113	0.1471	0.9591	24.44
20	55.27	-10.22	1.138	0.1478	0.9603	23.94
30	56.45	-10.07	1.172	0.1486	0.9619	23.30
40	58.07	-9.87	1.218	0.1498	0.9646	22.44
50	60.31	-9.58	1.286	0.1515	0.9669	21.31

c) Results of performance parameter for R1234ze on condenser fouling at $T_{in,cond}$ = 35^{o} C**.**

UA_{cond} (%)	COP_f	$Wact_f$ (kW)	COP (%)	W_{cp} (%)	Qevap (%)	Є (%)	$Qevap_f$ (kW)
0	1.951	51.26	0	0	0	0	100
10	1.920	51.70	-1.587	0.872	-0.729	-4.365	99.27
20	1.881	52.24	-3.566	1.923	-1.711	-9.493	98.29
30	1.831	53.00	-6.154	3.391	-2.972	-15.52	97.03
40	1.765	53.94	-9.506	5.236	-4.767	-22.59	95.23
50	1.680	55.06	-13.884	7.414	-7.500	-30.90	92.50

UA_{cond} (%)	T_{1f} (^{o}C)	T_{2f} (^{o}C)	P_{1f} (MPa)	P_{2f} (MPa)	$m_{ref,f}$ (kg s^{-1})	η_{II} (%)
0	50.75	-10.42	1.017	0.1466	0.9211	25.01
10	51.44	-10.34	1.035	0.1471	0.9224	24.62
20	52.32	-10.24	1.058	0.1477	0.9235	24.12
30	53.49	-10.10	1.089	0.1484	0.9256	23.47
40	55.07	-9.92	1.132	0.1495	0.9277	22.63
50	57.24	-9.63	1.194	0.1512	0.9281	21.49

Table 4.9

a) Results of performance parameter for R1234ze on evaporator fouling at $T_{in,cond}$ = 40^{o} C.

UA_{evap} (%)	COP_f	$Wact_f$ (kW)	COP (%)	W_{cp} (%)	Qevap (%)	€ (%)	$Qevap_f$ (kW)
0	1.675	59.76	0	0	0	0	100
10	1.668	59.19	-0.338	-0.961	-1.295	-4.365	98.70
20	1.661	58.46	-0.765	-2.173	-2.921	-9.493	97.08
30	1.651	57.54	-1.319	-3.715	-4.985	-15.52	95.02
40	1.640	56.26	-1.985	-5.791	-7.730	-22.59	92.27
50	1.623	54.71	-3.036	-8.445	-11.225	-30.90	88.77

UA_{evap} (%)	T_{1f} (^{o}C)	T_{2f} (^{o}C)	P_{1f} (MPa)	P_{2f} (MPa)	$m_{ref,f}$ (kg s^{-1})	η_{II} (%)
0	56.64	-10.42	1.177	0.1466	0.9992	24.52
10	56.44	-10.75	1.171	0.1447	0.9854	24.43
20	56.20	-11.17	1.164	0.1422	0.9682	24.33
30	55.89	-11.71	1.155	0.1391	0.9464	24.19
40	55.47	-12.41	1.144	0.1352	0.9173	24.03
50	54.94	-13.38	1.129	0.1300	0.8810	23.77

b) Results of performance parameter for R1234ze on evaporator fouling at $T_{in,cond}$ = 37.5^{o} C**.**

UA_{evap} (%)	COP_f	$Wact_f$ (kW)	COP (%)	W_{cp} (%)	Qevap (%)	€ (%)	$Qevap_f$ (kW)
0	1.808	55.32	0	0	0	0	100
10	1.802	54.72	-0.304	-1.074	-1.374	-4.365	98.63
20	1.795	54.01	-0.715	-2.368	-3.064	-9.493	96.94
30	1.786	53.06	-1.215	-4.080	-5.250	-15.52	94.75
40	1.774	51.84	-1.886	-6.288	-8.056	-22.59	91.94
50	1.755	50.32	-2.90	-9.035	-11.67	-30.90	88.33

UA_{evap} (%)	T_{1f} (^{o}C)	T_{2f} (^{o}C)	P_{1f} (MPa)	P_{2f} (MPa)	$m_{ref,f}$ (kg s^{-1})	η_{II} (%)
0	53.67	-10.42	1.094	0.1466	0.9591	24.83
10	53.47	-10.74	1.088	0.1447	0.9440	24.76
20	53.22	-11.15	1.082	0.1428	0.9268	24.65
30	52.89	-11.68	1.073	0.1393	0.9046	24.53
40	52.47	-12.37	1.062	0.1355	0.8762	24.36
50	51.94	-13.31	1.048	0.1303	0.8402	24.11

c) Results of performance parameter for R1234ze on evaporator fouling at $T_{in,cond}$ = 35^{o} C**.**

UA_{evap} (%)	COP_f	$Wact_f$ (kW)	COP (%)	W_{cp} (%)	Qevap (%)	€ (%)	$Qevap_f$ (kW)
0	1.951	51.26	0	0	0	0	100
10	1.946	50.66	-0.277	-1.173	-1.446	-4.365	98.55
20	1.938	49.92	-0.643	-2.608	-3.235	-9.493	96.77
30	1.928	49.02	-1.152	-4.358	-5.460	-15.52	94.54
40	1.917	47.76	-1.735	-6.821	-8.440	-22.59	91.56
50	1.898	46.31	-2.737	-9.657	-12.13	-30.90	87.87

UA_{evap} (%)	T_{1f} (^{o}C)	T_{2f} (^{o}C)	P_{1f} (MPa)	P_{2f} (MPa)	$m_{ref,f}$ (kg s^{-1})	η_{II} (%)
0	50.75	-10.42	1.017	0.1466	0.9211	25.01
10	50.54	-10.73	1.0110	0.1447	0.9068	24.94
20	50.27	-11.13	1.0050	0.1424	0.8893	24.85
30	49.95	-11.65	0.9963	0.1395	0.8676	24.72
40	49.51	-12.32	0.9852	0.1358	0.8386	24.58
50	48.97	-13.24	0.9718	0.1307	0.8032	24.33

Table 4.10

a) Results of performance parameter for R1234ze on condenser and evaporator fouling at $T_{in,cond}$ = 40^{o} C**.**

$UA_{cond,evap}$ (%)	COP_f	$Wact_f$ (kW)	COP (%)	W_{cp} (%)	Qevap (%)	Є (%)	$Qevap_f$ (kW)
0	1.675	59.76	0	0	0	0	100
10	1.641	59.64	-1.933	-0.210	-2.139	-4.365	97.86
20	1.602	59.41	-4.266	-0.583	-4.824	-9.493	95.18
30	1.553	59.19	-7.212	-0.963	-8.106	-15.52	91.89
40	1.492	58.78	-10.86	-1.634	-12.31	-22.59	87.69
50	1.413	58.25	-15.54	-2.525	-17.67	-30.90	82.32

$UA_{cond,evap}$ (%)	T_{1f} (^{o}C)	T_{2f} (^{o}C)	P_{1f} (MPa)	P_{2f} (MPa)	$m_{ref,f}$ (kg s^{-1})	η_{II} (%)
0	56.64	-10.42	1.177	0.1466	0.9992	24.52
10	57.15	-10.65	1.192	0.1452	0.9866	24.04
20	57.79	-10.95	1.210	0.1435	0.9704	23.47
30	58.62	-11.33	1.235	0.1413	0.9511	22.75
40	59.71	-11.79	1.267	0.1387	0.9255	21.86
50	61.19	-12.41	1.313	0.1353	0.8931	20.71

b) Results of performance parameter for R1234ze on condenser and evaporator fouling at $T_{in,cond}$ = 37.5^{o} C**.**

$UA_{cond,evap}$ (%)	COP_f	$Wact_f$ (kW)	COP (%)	W_{cp} (%)	Qevap (%)	Є (%)	$Qevap_f$ (kW)
0	1.808	55.32	0	0	0	0	100
10	1.773	55.19	-1.895	-0.230	-2.121	-4.365	97.88
20	1.732	54.97	-4.180	-0.624	-4.779	-9.493	95.22
30	1.680	54.74	-7.063	-1.037	-8.027	-15.52	91.97
40	1.616	54.36	-10.63	-1.738	-12.18	-22.59	87.82
50	1.533	53.84	-15.20	-2.673	-17.47	-30.90	82.53

$UA_{cond,evap}$ (%)	T_{1f} (^{o}C)	T_{2f} (^{o}C)	P_{1f} (MPa)	P_{2f} (MPa)	$m_{ref,f}$ (kg s^{-1})	η_{II} (%)
0	53.67	-10.42	1.094	0.1466	0.9591	24.83
10	54.17	-10.66	1.108	0.1452	0.9455	24.36
20	54.78	-10.95	1.124	0.1434	0.9294	23.79
30	55.58	-11.34	1.147	0.1413	0.9101	23.08
40	56.63	-11.81	1.177	0.1386	0.8848	22.19
50	58.05	-12.44	1.218	0.1351	0.8526	21.06

c) Results of performance parameter for R1234ze on condenser and evaporator fouling at $T_{in,cond}$ = 35^{o} C**.**

$UA_{cond,evap}$ (%)	COP_f	$Wact_f$ (kW)	COP (%)	W_{cp} (%)	Qevap (%)	Є (%)	$Qevap_f$ (kW)
0	1.951	51.26	0	0	0	0	100
10	1.915	51.12	-1.861	-0.259	-2.114	-4.365	97.89
20	1.871	50.90	-4.104	-0.688	-4.764	-9.493	95.24
30	1.815	50.69	-6.946	-1.111	-7.980	-15.52	92.02
40	1.748	50.28	-10.415	-1.911	-12.127	-22.59	87.87
50	1.660	49.76	-14.896	-2.913	-17.375	-30.90	82.63

$UA_{cond,evap}$ (%)	T_{1f} (^{o}C)	T_{2f} (^{o}C)	P_{1f} (MPa)	P_{2f} (MPa)	$m_{ref,f}$ (kg s^{-1})	η_{II} (%)
0	50.75	-10.42	1.017	0.1466	0.9211	25.01
10	51.22	-10.66	1.029	0.1452	0.9085	24.55
20	51.81	-10.96	1.044	0.1434	0.8924	23.99
30	52.59	-11.34	1.065	0.1412	0.8732	23.27
40	53.58	-11.82	1.092	0.1385	0.8477	22.41
50	54.95	-12.45	1.129	0.1350	0.8156	21.29

4.3 Performance curves

The tables are represented in the form of performance curves. The curves are shown between the percentage decrease in condenser and evaporator conductances individually and simultaneously vs. i) COP, ii) Compressor work (W_{cp}), iii) Percentage change in compressor power, iv) Percentage change in cooling capacity, v) Percentage change in COP, vi) Percentage change in effectiveness vii) Second –law efficiency. These performance curves are shown in figures 4.1 to 4.72.

It is found that the performance curves obtained from the present thermodynamic model for R134a are nearly same, as obtained for the actual system in Qureshi and Zubair [19]. This indicates the validity of the present thermodynamic model.

Figures 4.1-4.6 shows the variation of compressor work, COP and percentage changes (%) in Q_{evap}, W_{cp}, COP, Є with percentage decrease in condenser conductance for R134a.

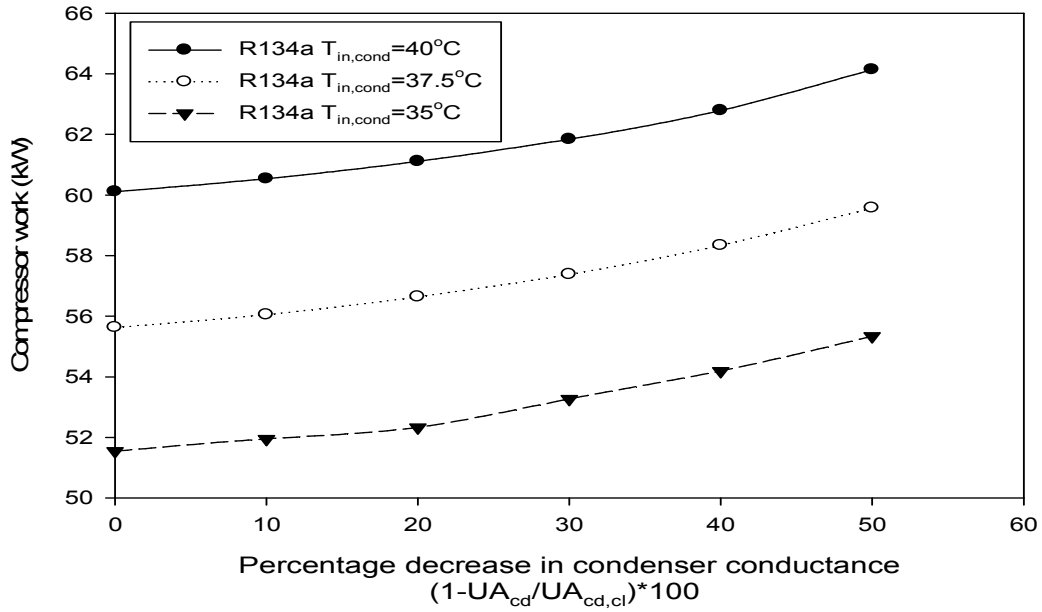

Figure 4.1 Compressor work vs. Percentage decrease in condenser conductance for R134a.

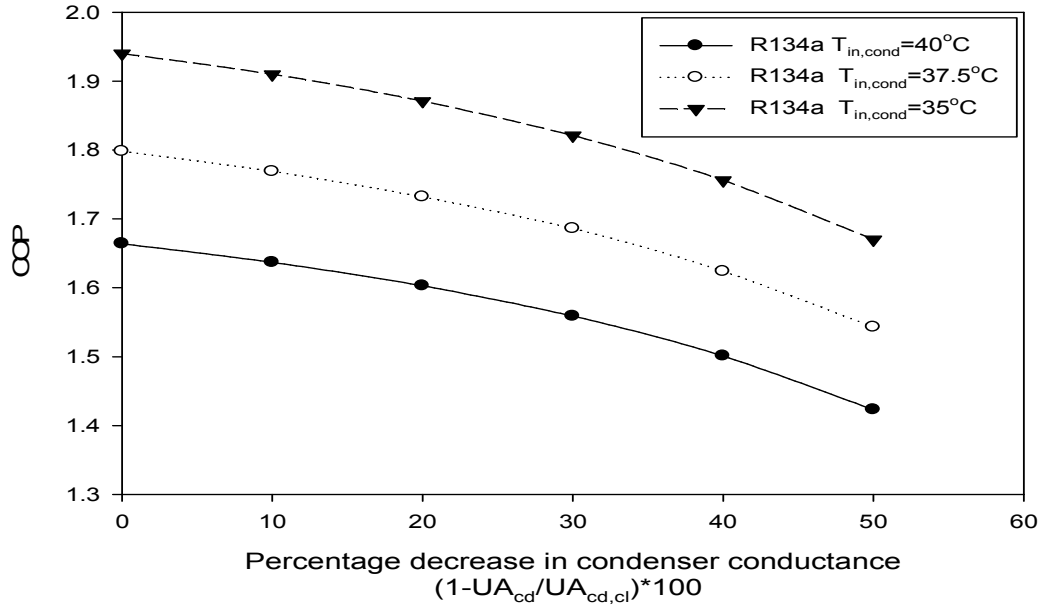

Figure 4.2 COP vs. Percentage decrease in condenser conductance for R134a.

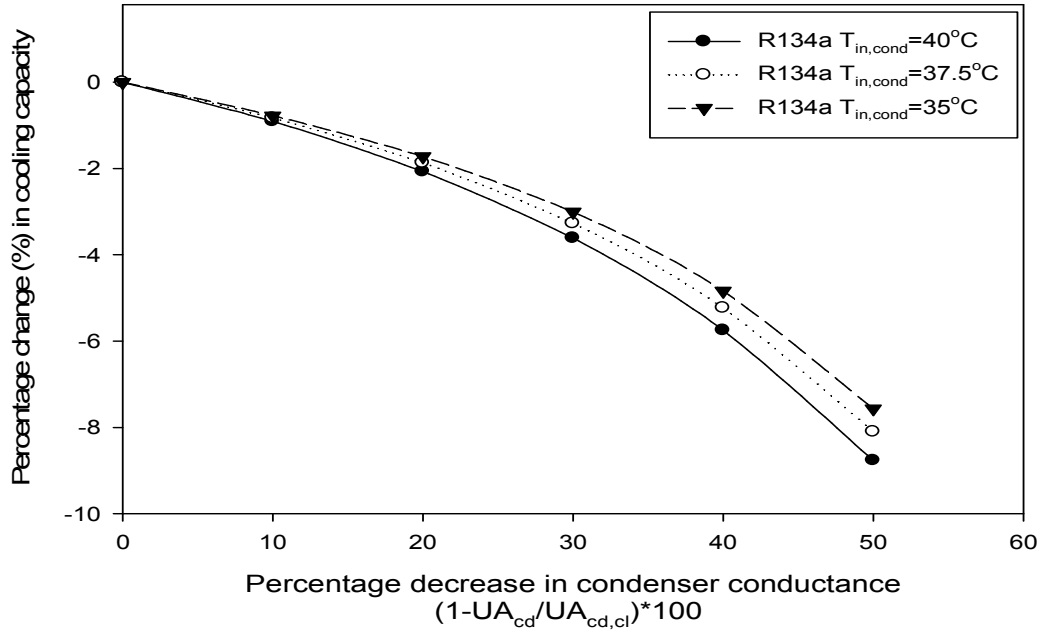

Figure 4.3 Percentage change in cooling capacity vs. Percentage decrease in condenser conductance for R134a.

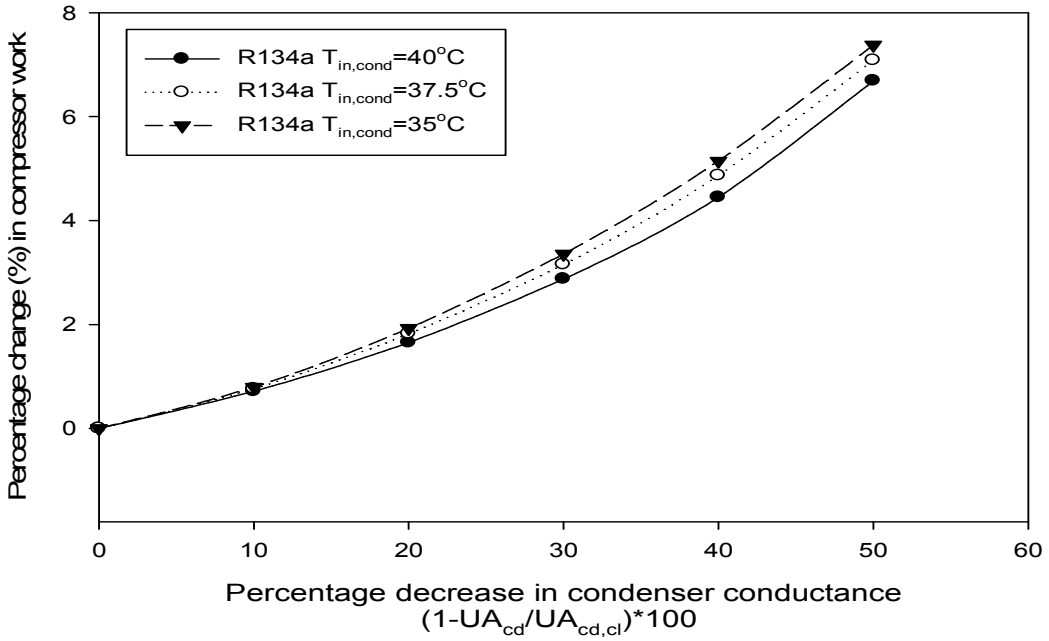

Figure 4.4 Percentage change in compressor work vs. Percentage decrease in condenser conductance for R134a.

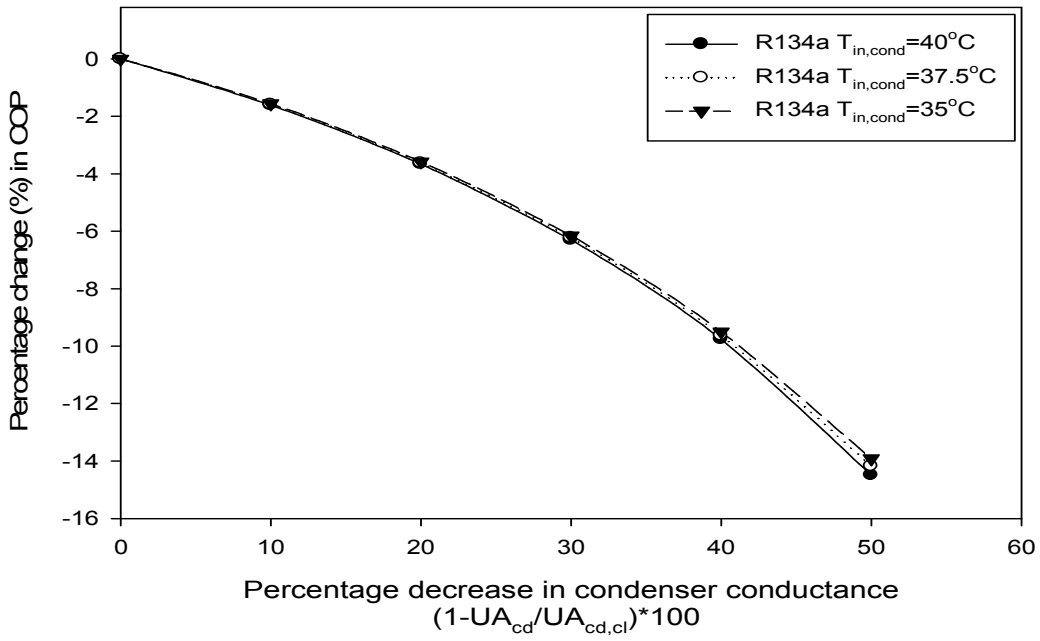

Figure 4.5 Percentage change in COP vs. Percentage decrease in condenser conductance for R134a.

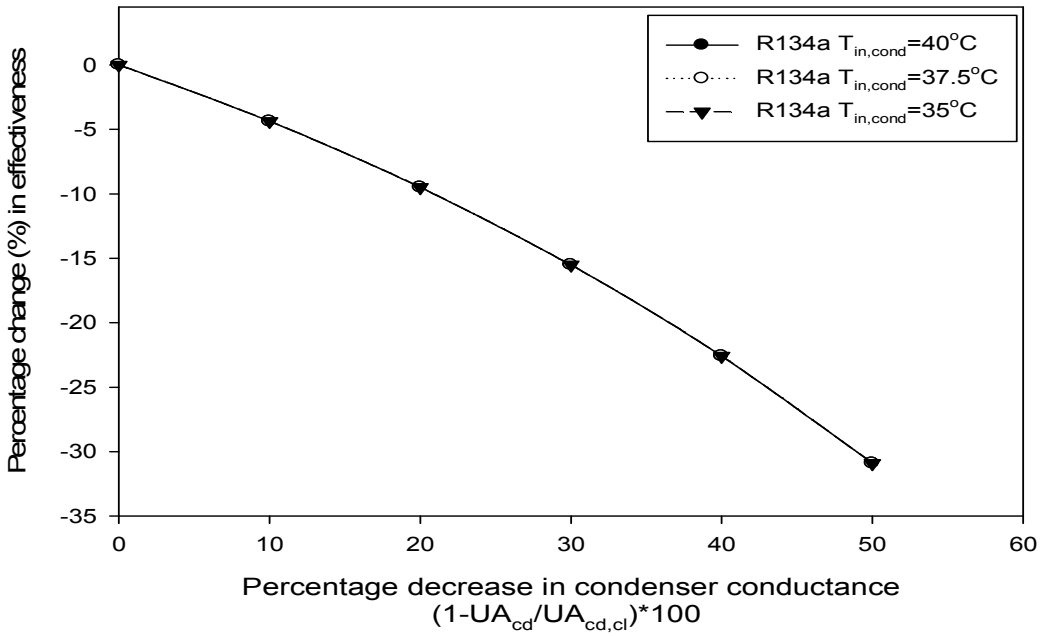

Figure 4.6 Percentage change in effectiveness vs. Percentage decrease in condenser conductance for R134a.

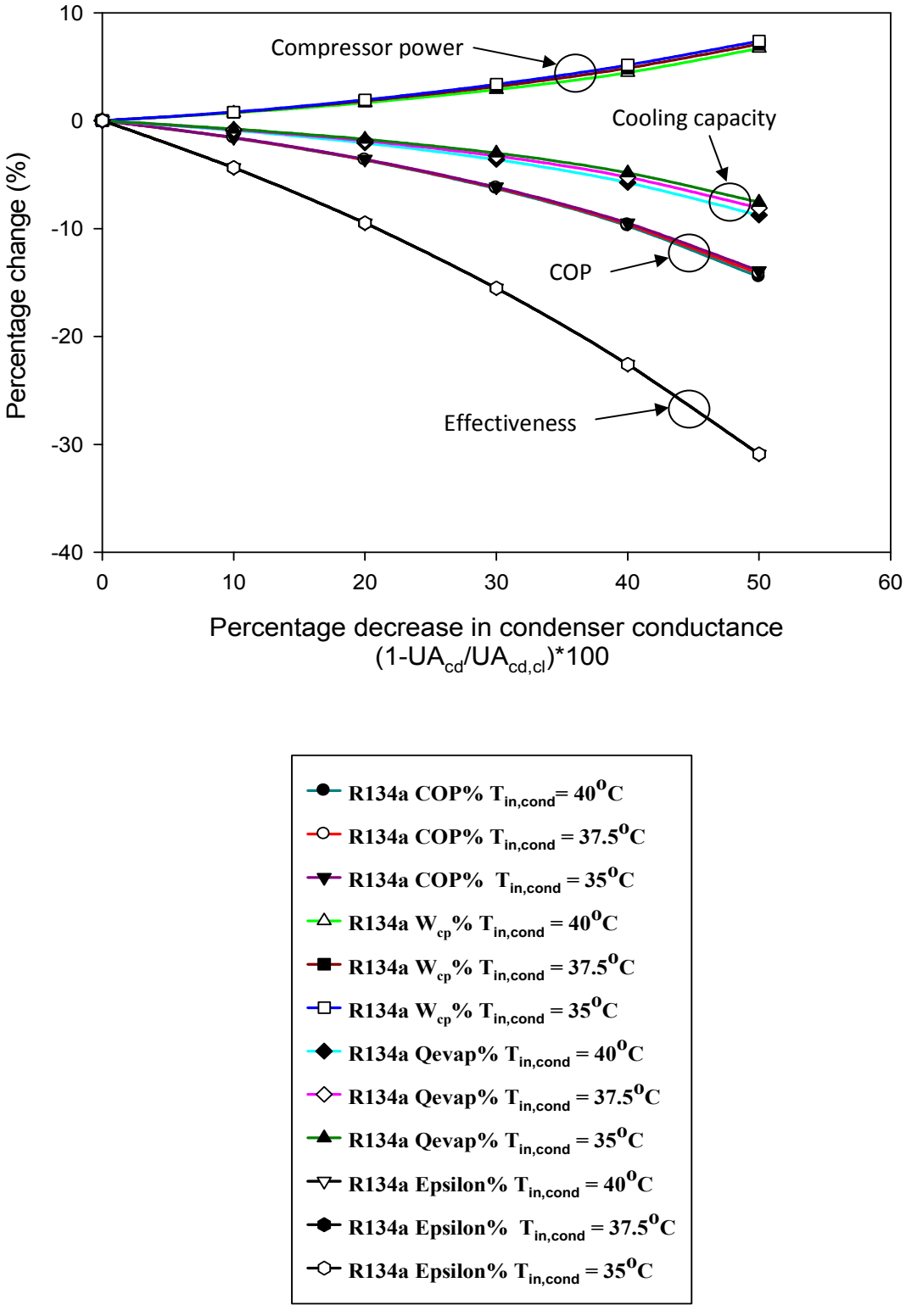

Figure 4.7 Percentage change (%) vs. Percentage decrease in condenser conductance for R134a.

The effect of condenser fouling with variation in condenser coolant temperature, decreases the COP because with percentage decrease in condenser conductance ((1-$UA_{cd}/UA_{cd,cl}$)*100), cooling capacity decreases and compressor work goes on increasing, as it is clear from the tables 4.2 a), b), and c) and figure 4.7a.

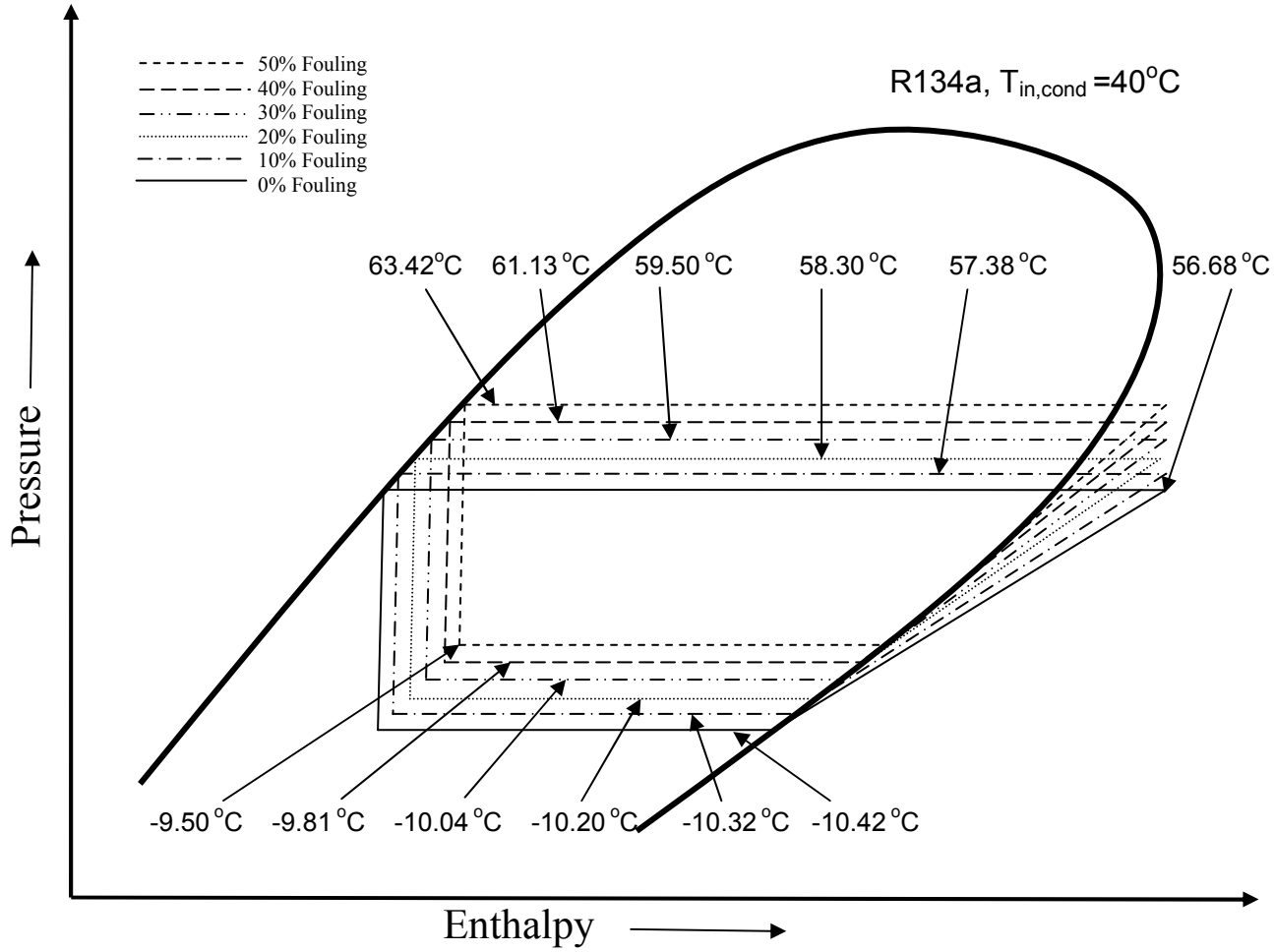

Figure 4.7a Pressure - Enthalpy diagram of condenser fouling for VCRS.

Figures 4.8-4.13 shows the variation of compressor work, COP and percentage changes (%) in Q_{evap}, W_{cp}, COP, Є with percentage decrease in evaporator conductance for R134a.

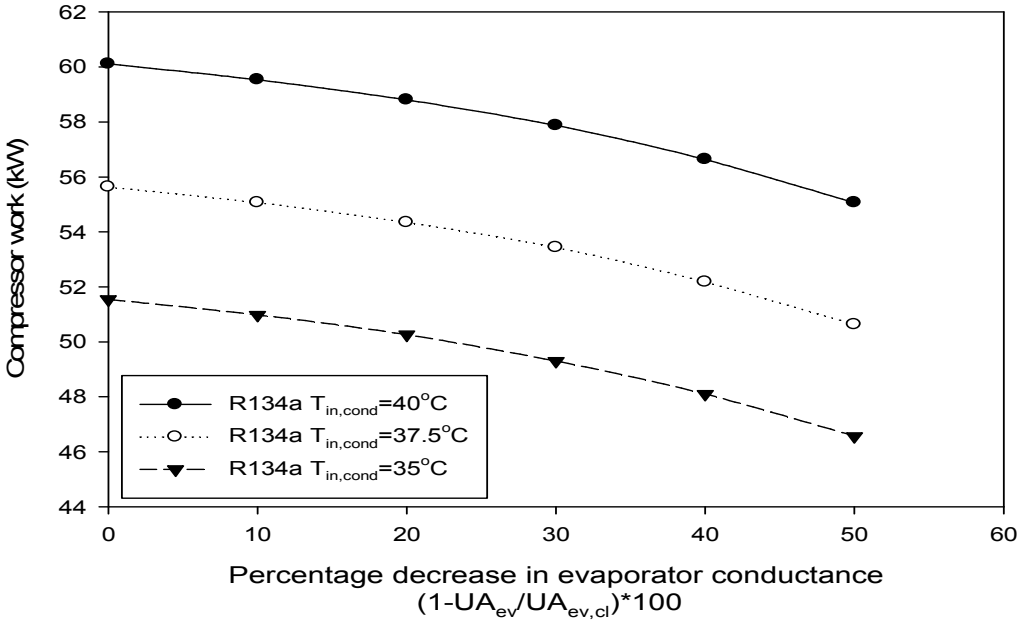

Figure 4.8 Compressor work vs. percentage decrease in evaporator conductance for R134a.

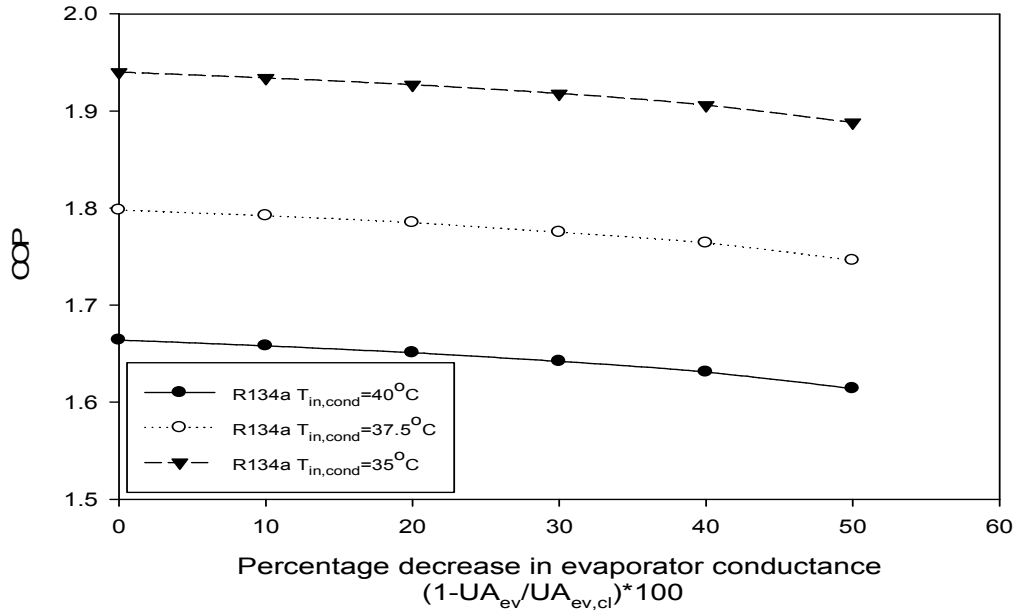

Figure 4.9 COP vs. Percentage decrease in evaporator conductance for R134a.

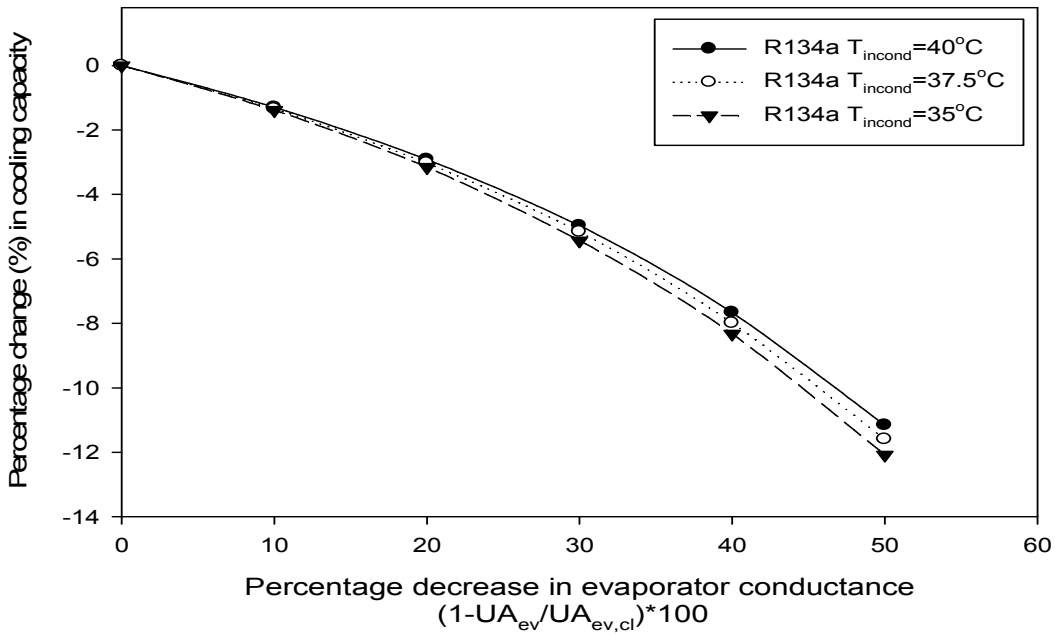

Figure 4.10 Percentage change in cooling capacity vs. Percentage decrease in evaporator conductance for R134a.

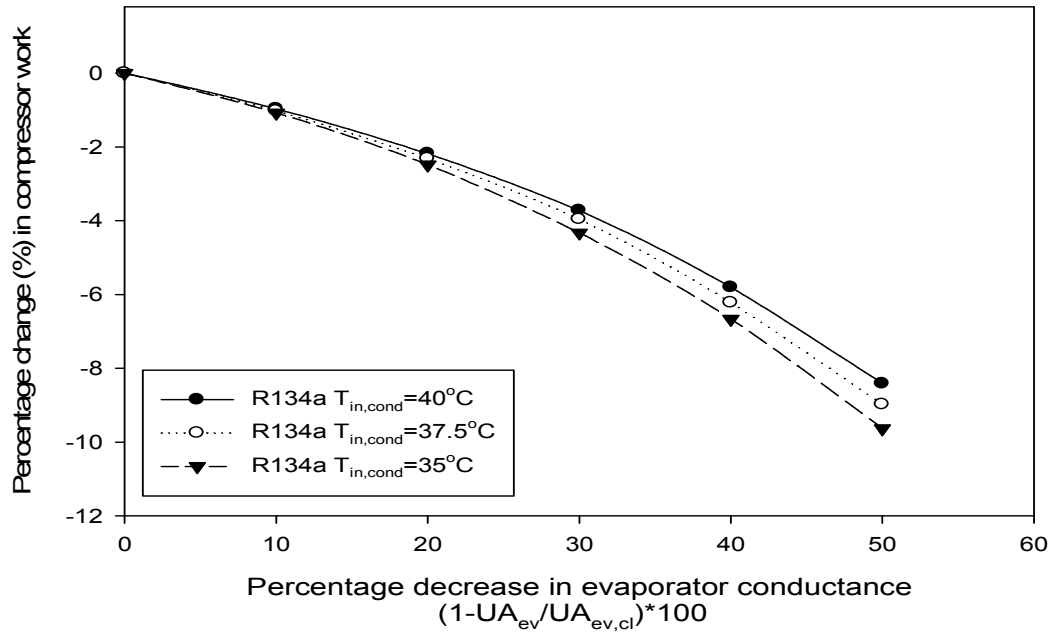

Figure 4.11 Percentage change in compressor work vs. Percentage decrease in evaporator conductance for R134a.

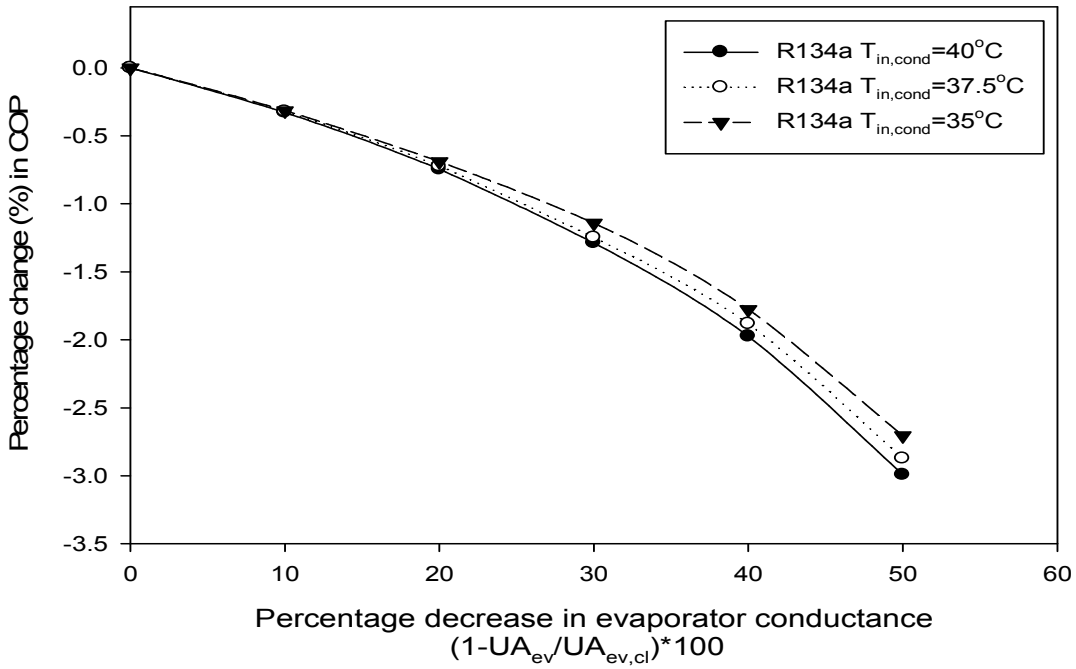

Figure 4.12 Percentage change in COP vs. Percentage decrease in evaporator conductance for R134a.

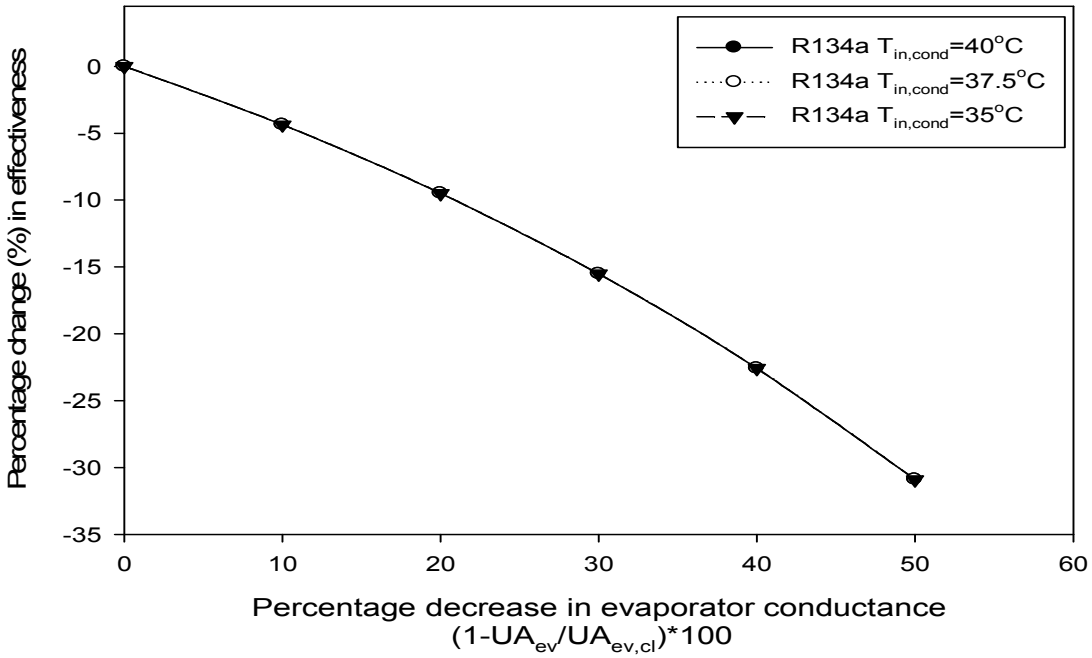

Figure 4.13 Percentage change in effectiveness vs. Percentage decrease in evaporator conductance for R134a.

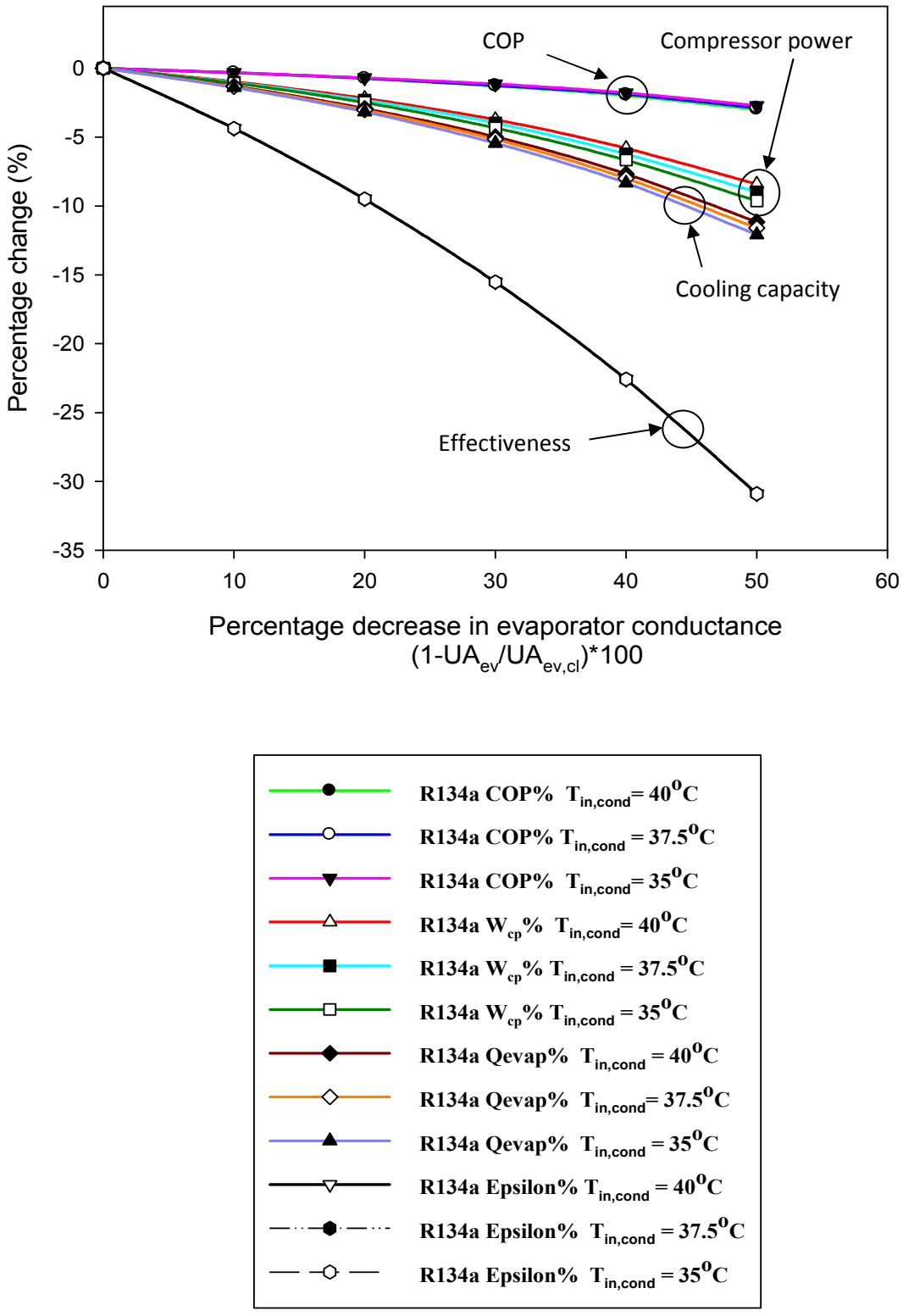

Figure 4.14 Percentage change (%) vs. Percentage decrease in evaporator conductance for R134a.

The effect of evaporator fouling with variation in condenser coolant temperature decreases the COP at a lower rate as compared to condenser fouling, because with percentage decrease in evaporator conductance ((1-$UA_{ev}/UA_{ev,cl}$)*100), cooling capacity and compressor work decreases, However cooling capacity decrease at a higher rate as compare to condenser fouling, as it is clear from the table 4.3 a), b), and c) and figure 4.14a.

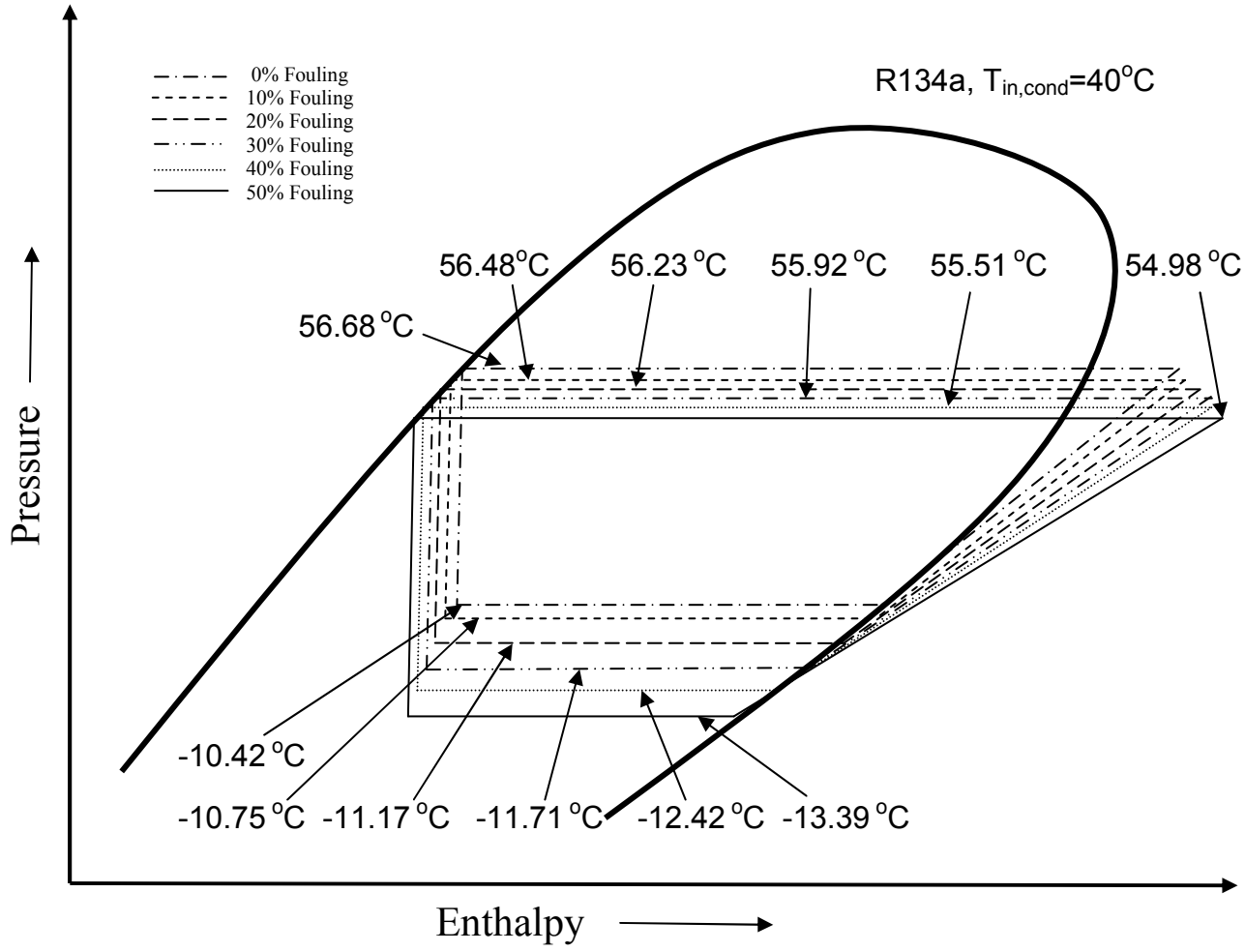

Figure 4.14a Pressure - Enthalpy diagram of evaporator fouling for VCRS.

Figures 4.15-4.20 shows the variation of compressor work, COP and percentage changes (%) in Q_{evap}, W_{cp}, COP, Є with percentage decrease in condenser and evaporator conductances for R134a.

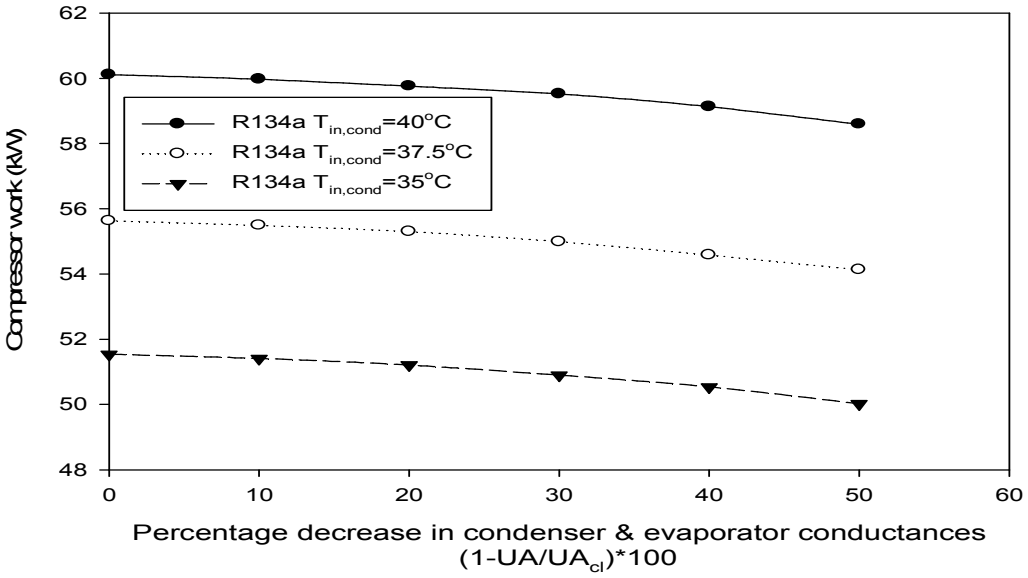

Figure 4.15 Compressor work vs. Percentage decrease in condenser and evaporator conductances for R134a.

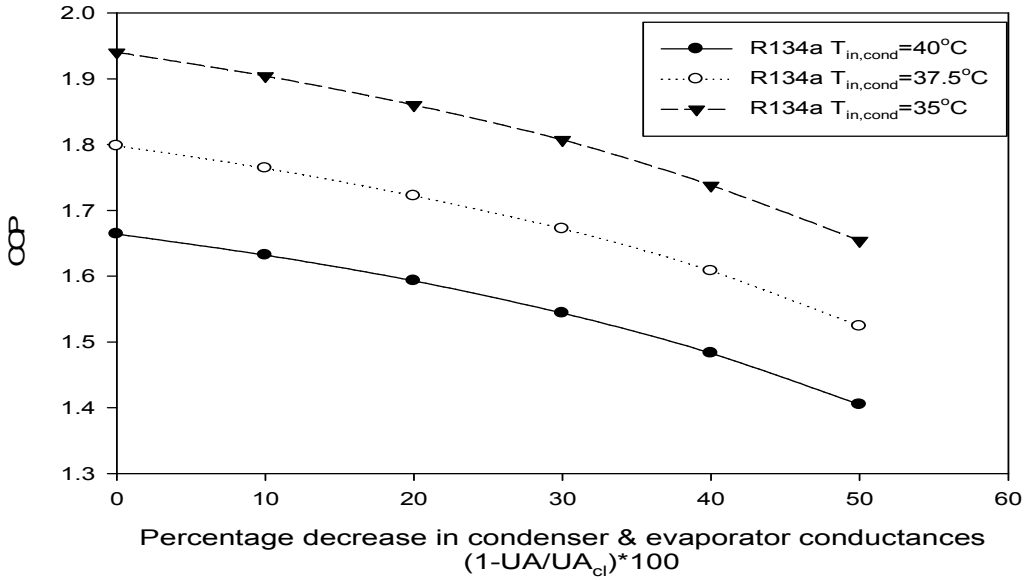

Figure 4.16 COP vs. Percentage decrease in condenser and evaporator conductances for R134a.

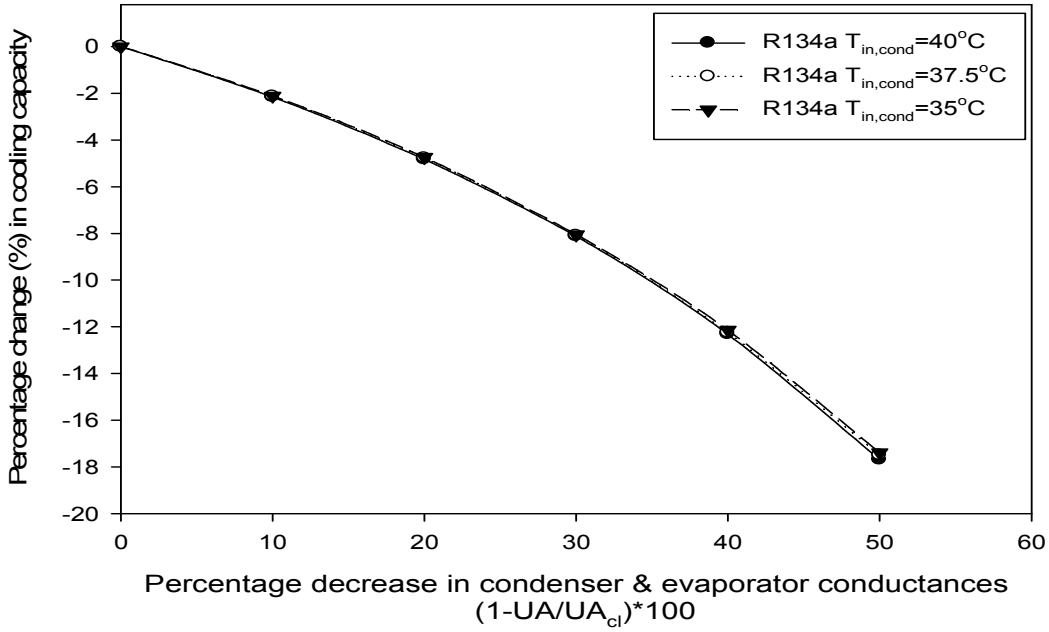

Figure 4.17 Percentage change in cooling capacity vs. Percentage decrease in condenser and evaporator conductances for R134a.

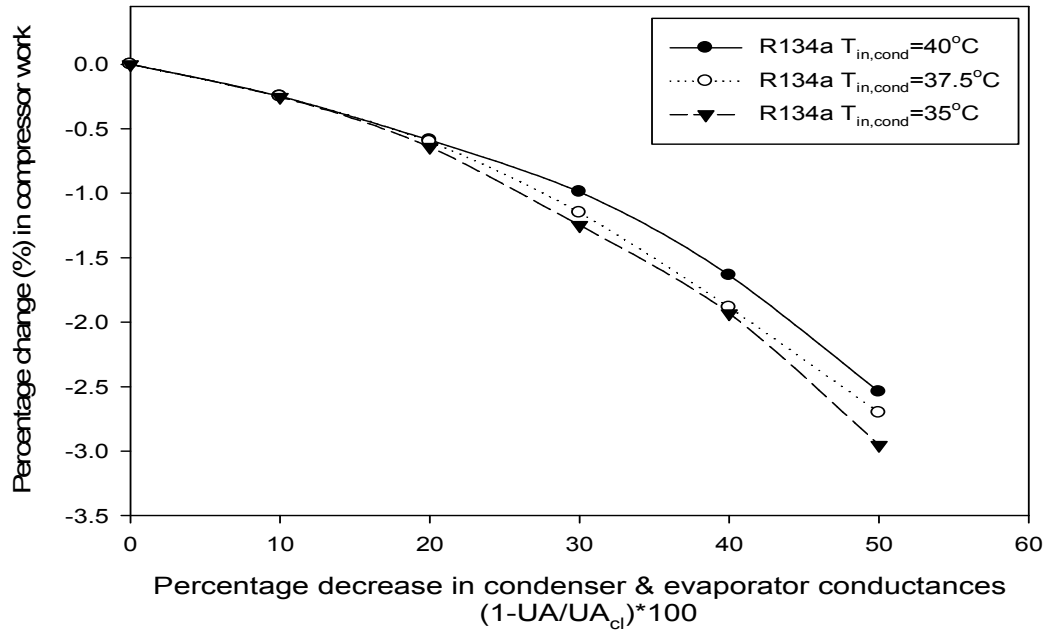

Figure 4.18 Percentage change in compressor work vs. Percentage decrease in condenser and evaporator conductances for R134a.

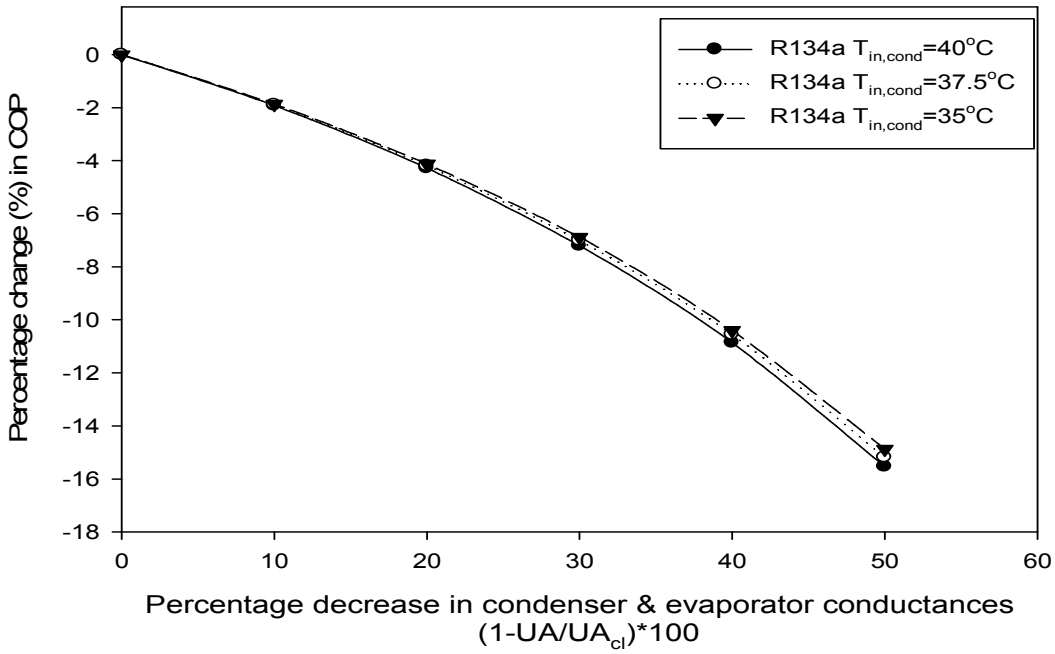

Figure 4.19 Percentage change in COP vs. Percentage decrease in condenser and evaporator conductances for R134a.

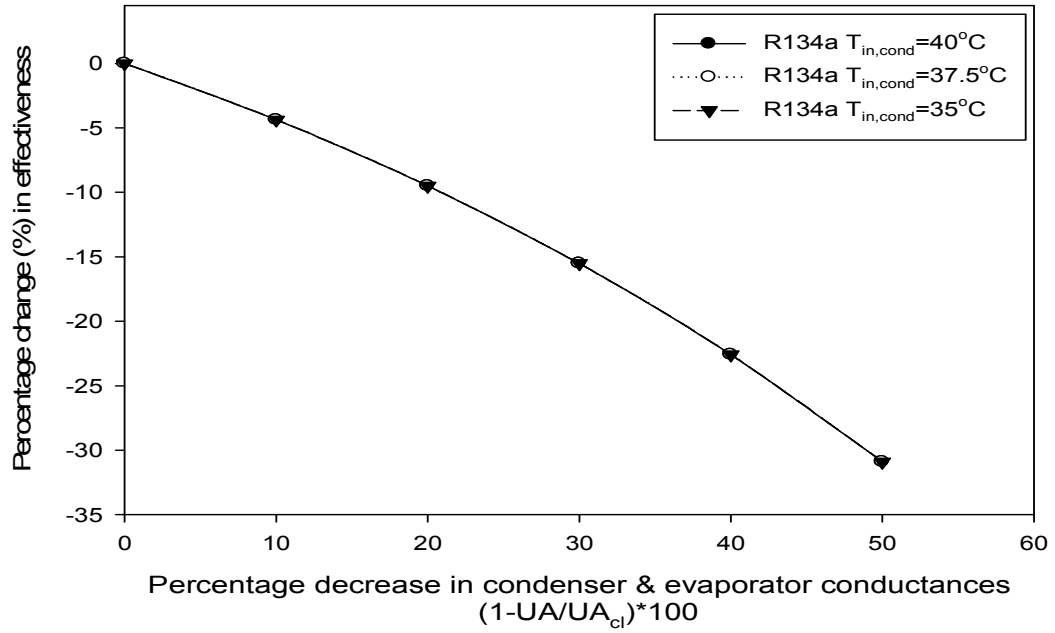

Figure 4.20 Percentage change in effectiveness vs. Percentage decrease in condenser and evaporator conductances for R134a.

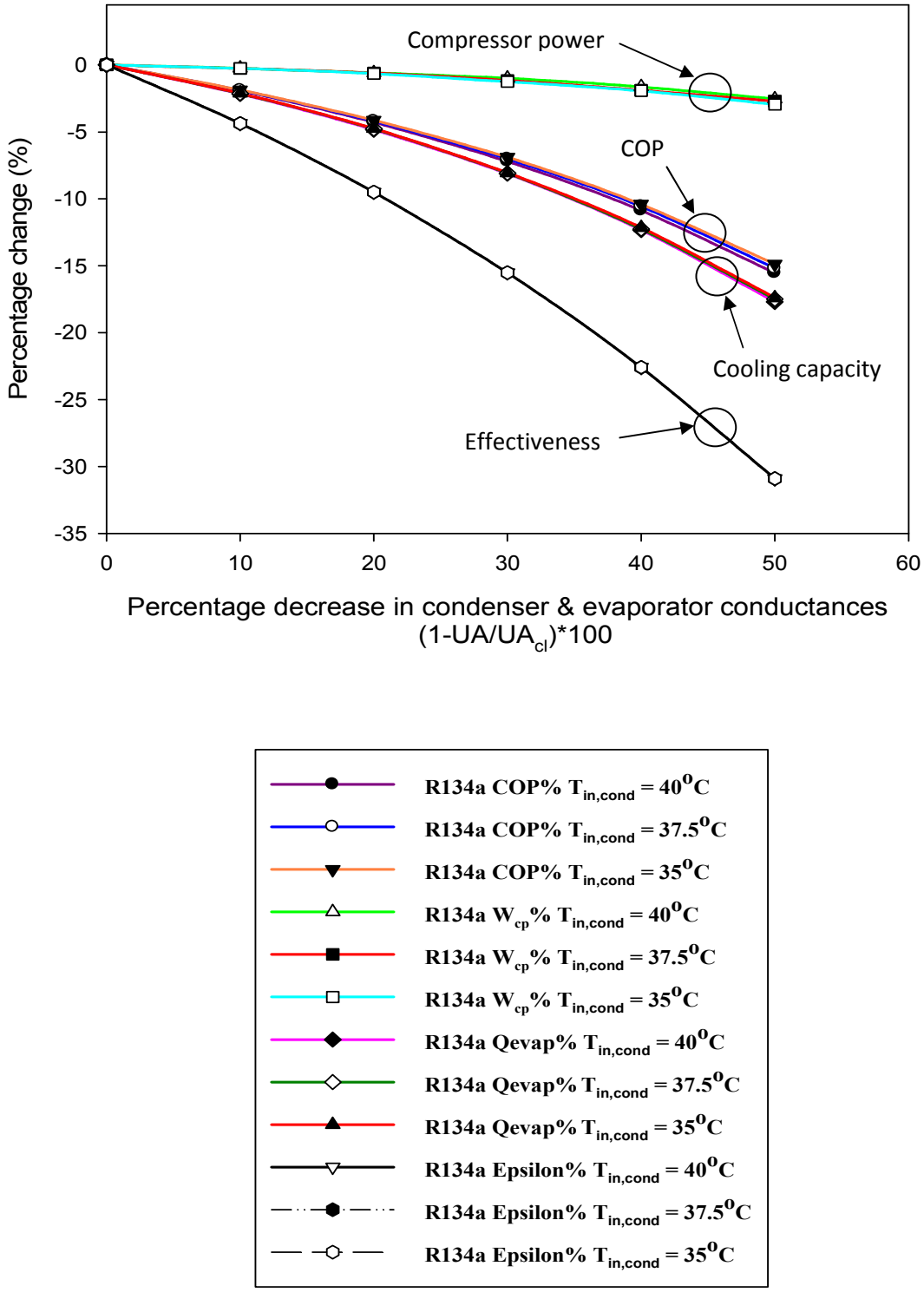

Figure 4.21 Percentage change (%) vs. Percentage decrease in condenser and evaporator conductances for R134a.

The combined effect of fouling on condenser and evaporator with variation in condenser coolant temperature decrease the COP at a higher rate as compared to condenser and evaporator fouling considered individually, because with percentage decrease in condenser and evaporator conductances simultaneously (((1-UA/UA_{cl})*100), cooling capacity decreases at a higher rate as compared to condenser and evaporator fouling considered individually and compressor work decreases at a lower rate. as it is clear from the table 4.4 a), b), and c) and figure 4.21a.

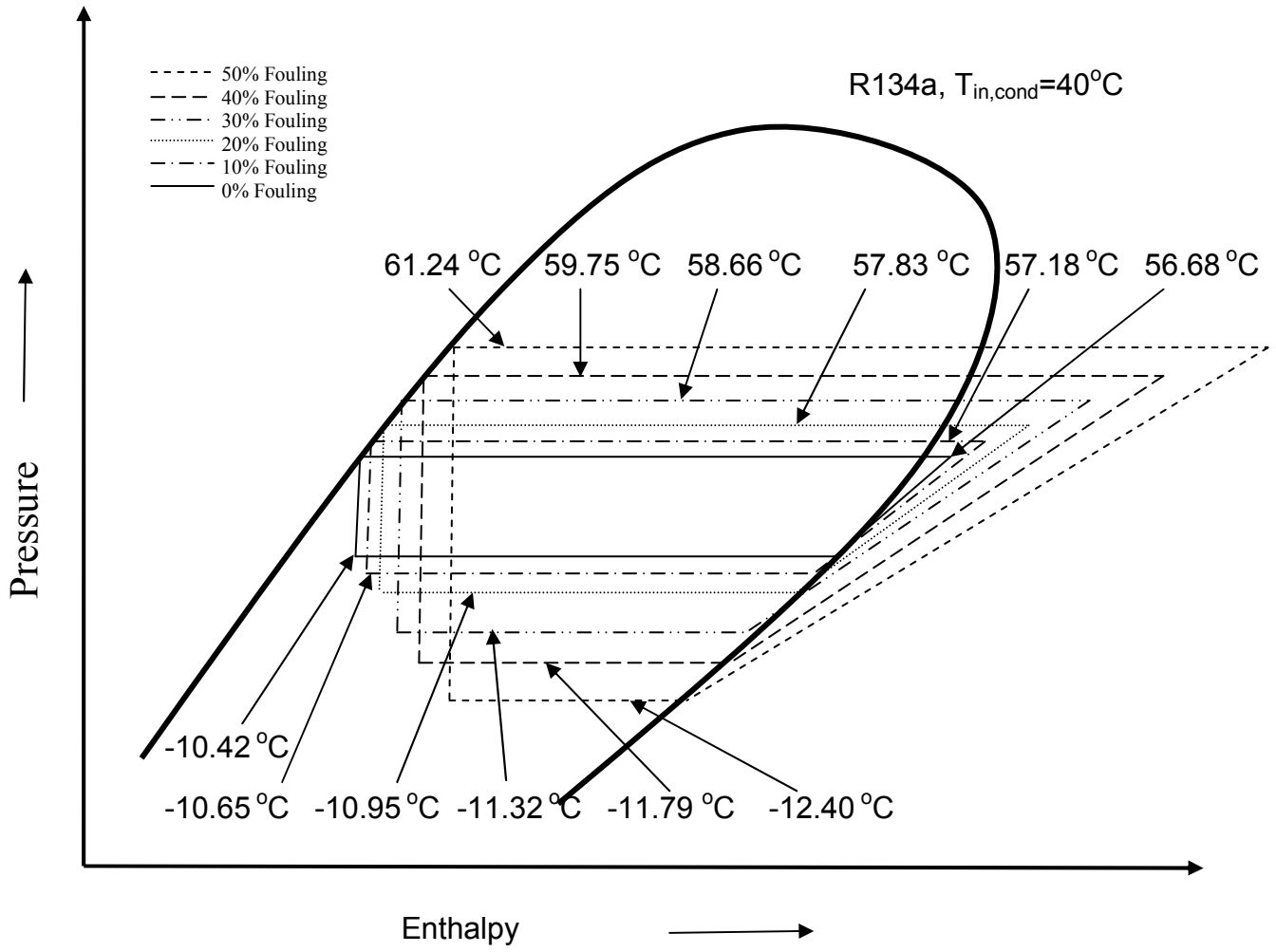

Figure 4.21a. Pressure - Enthalpy diagram of condenser and evaporator fouling for VCRS.

Figures 4.22-4.27 shows the variation of compressor work, COP and percentage changes (%) in Q_{evap}, W_{cp}, COP, Є with percentage decrease in condenser conductance for R1234yf.

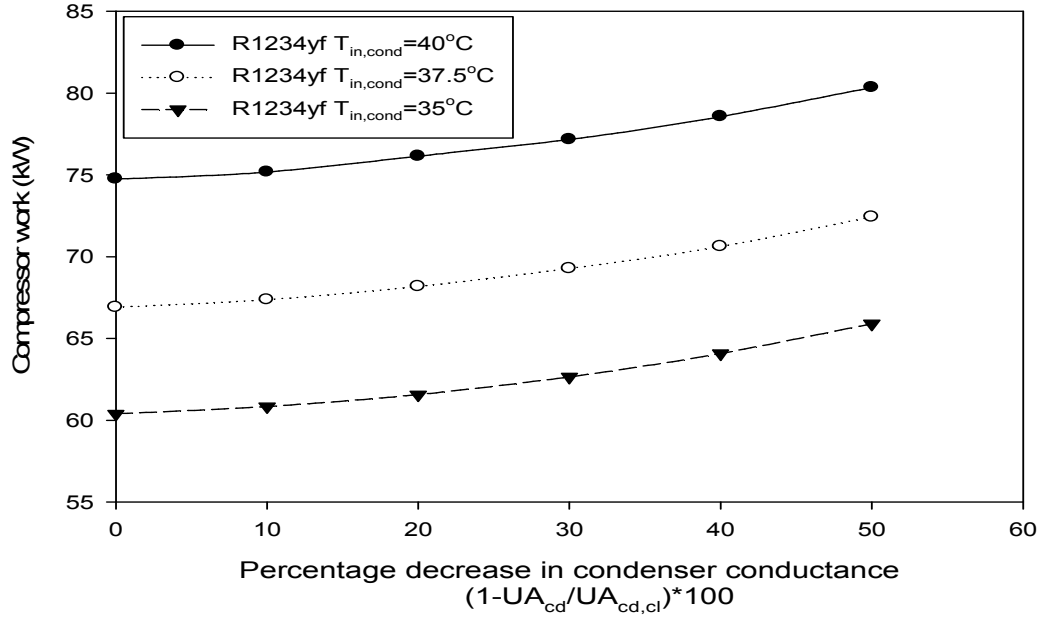

Figure 4.22 Compressor work vs. Percentage decrease in condenser conductance for R1234yf.

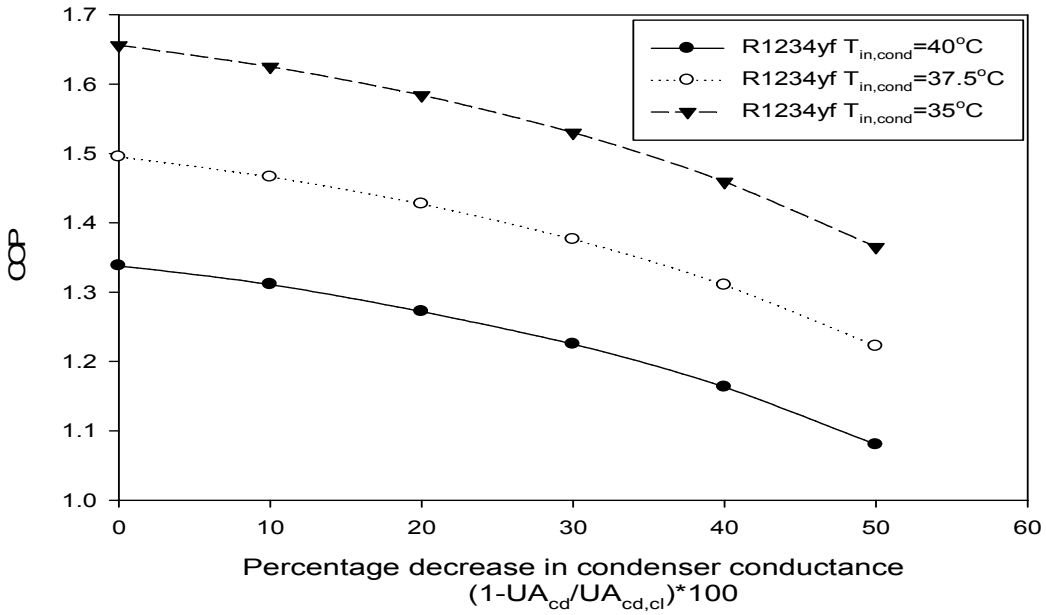

Figure 4.23 COP vs. Percentage decrease in condenser conductance for R1234yf.

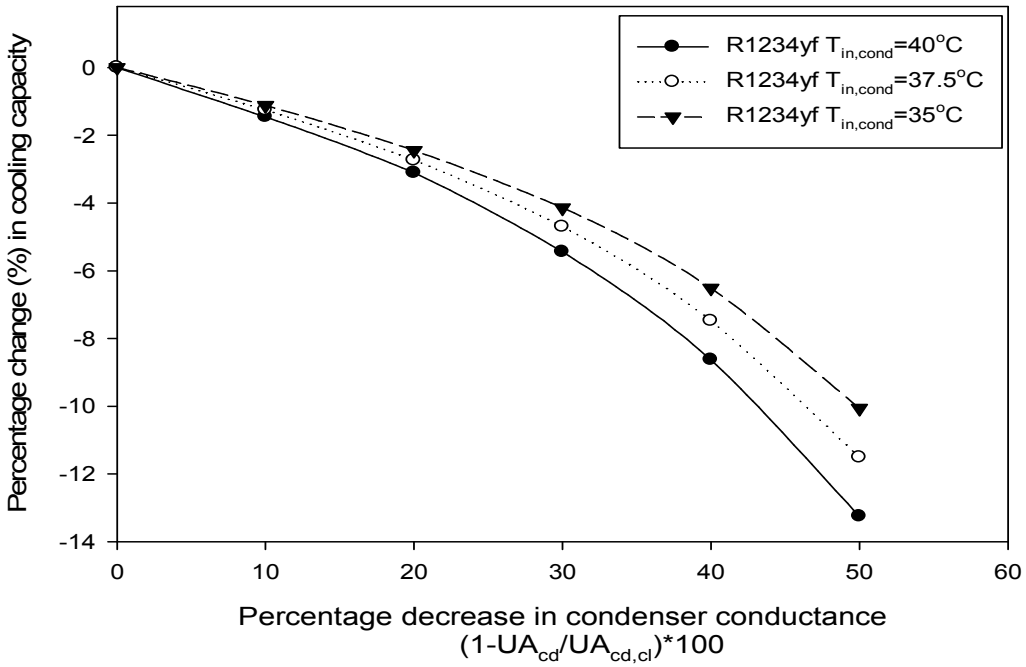

Figure 4.24 Percentage change in cooling capacity vs. Percentage decrease in condenser conductance for R1234yf.

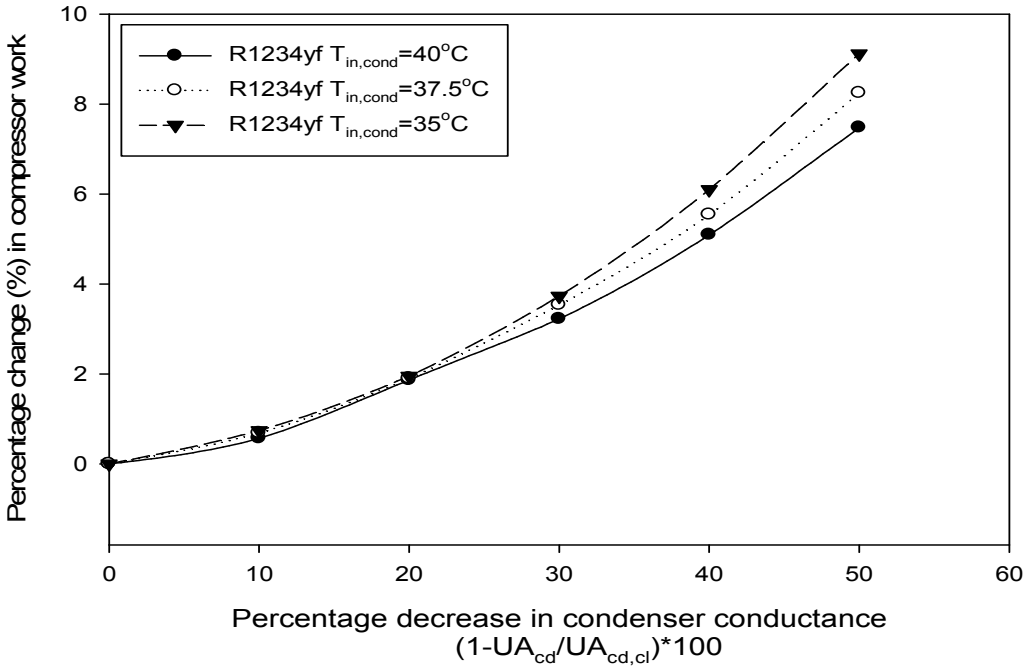

Figure 4.25 Percentage change in compressor work vs. Percentage decrease in condenser conductance for R1234yf.

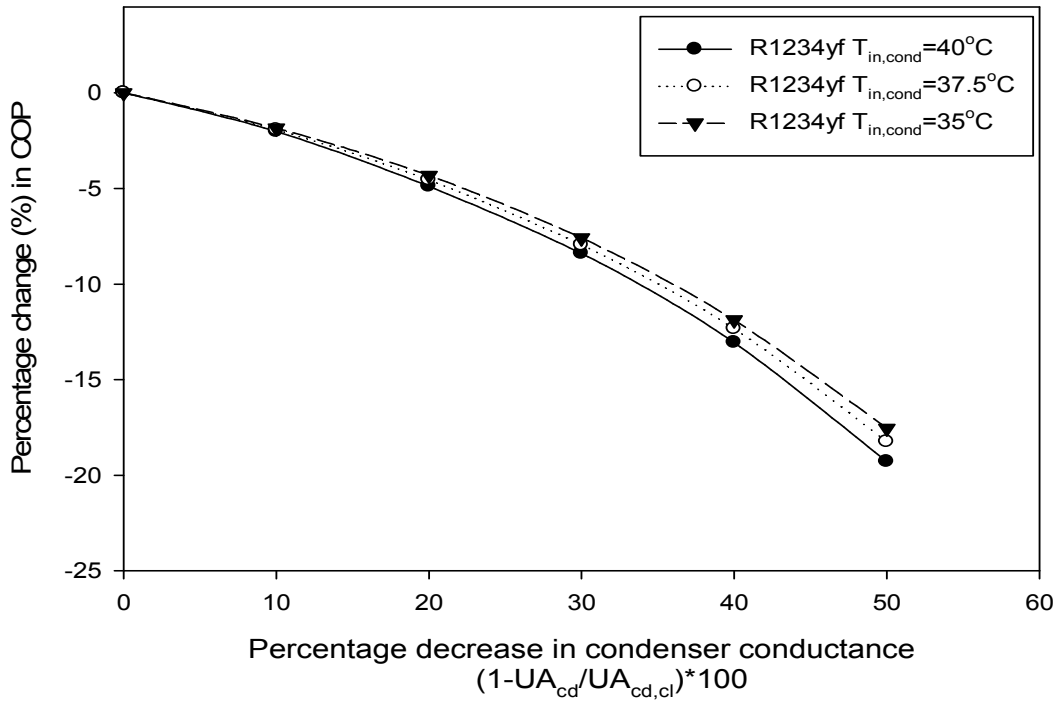

Figure 4.26 Percentage change in COP vs. Percentage decrease in condenser conductance for R1234yf.

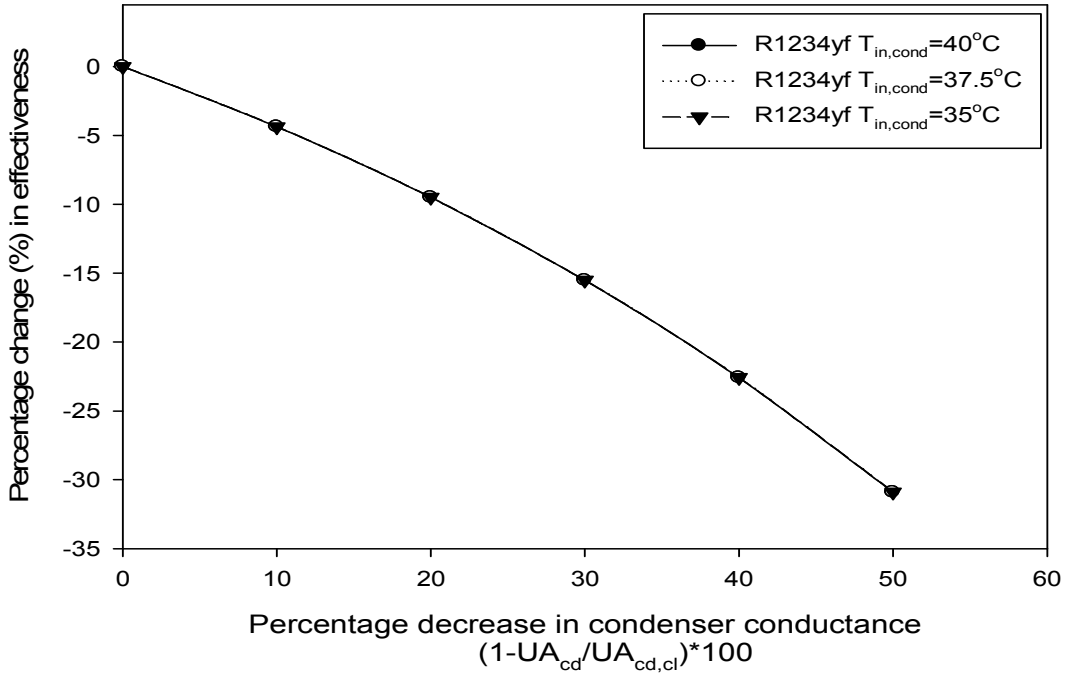

Figure 4.27 Percentage change in effectiveness vs. Percentage decrease in condenser conductance for R1234yf.

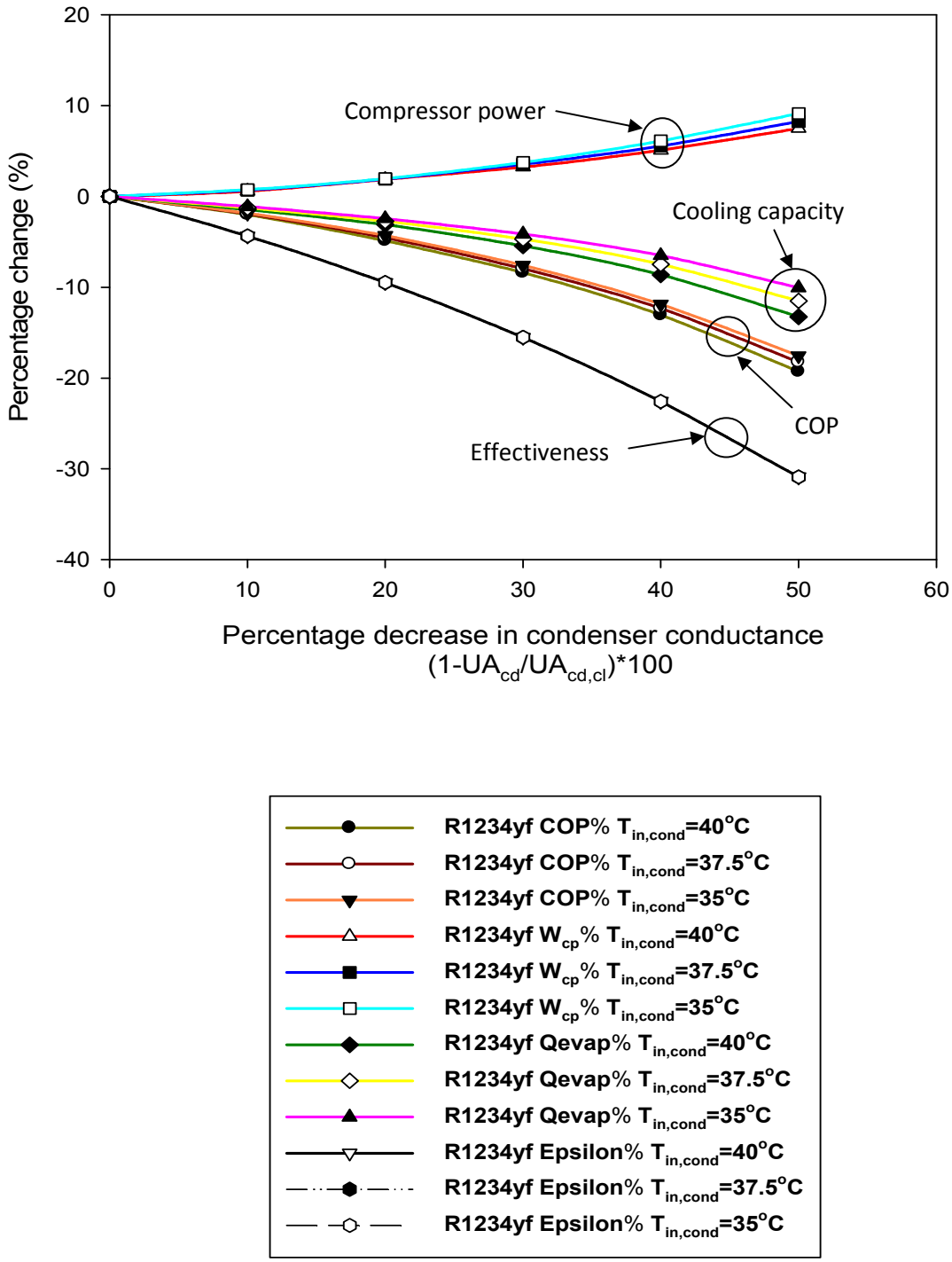

Figure 4.28 Percentage change (%) vs. Percentage decrease in condenser conductance for R1234yf.

The trends are similar in figures 4.22 to 4.28 for R1234yf as compared with figures 4.1 to 4.7 for R134a; hence it does not require explanation.

Figures 4.29-4.34 shows the variation of compressor work, COP and percentage changes (%) in Q_{evap}, W_{cp}, COP, Є with percentage decrease in evaporator conductance for R1234yf.

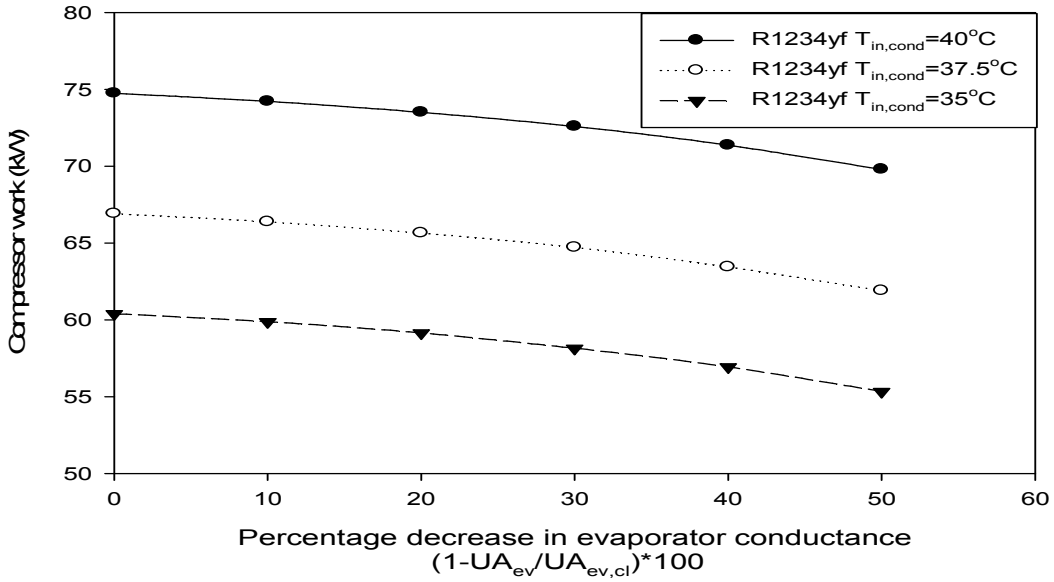

Figure 4.29 Compressor work vs. Percentage decrease in evaporator conductance for R1234yf.

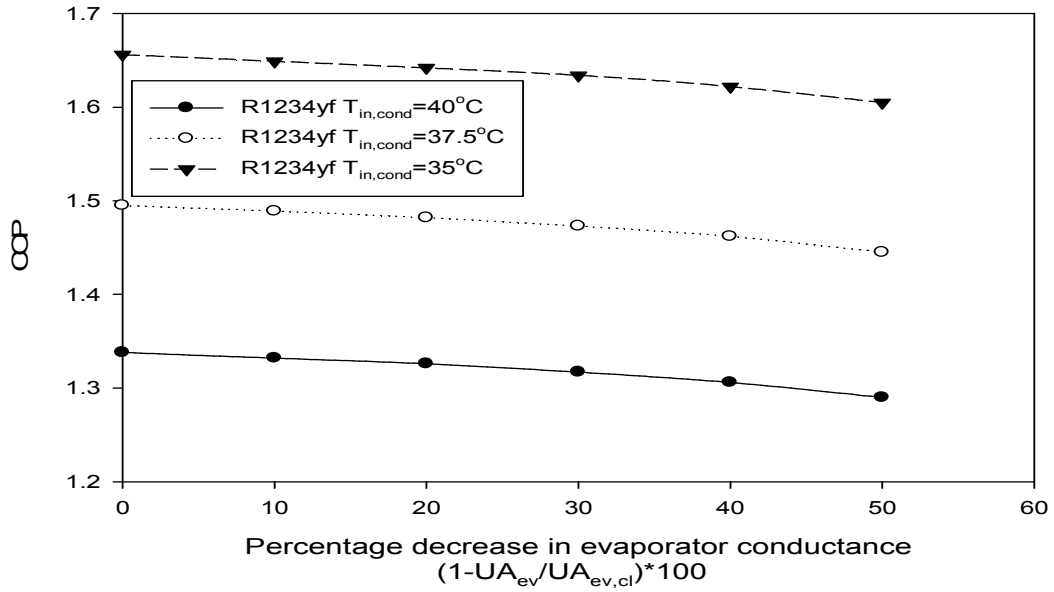

Figure 4.30 COP vs. Percentage decrease in evaporator conductance for R1234yf.

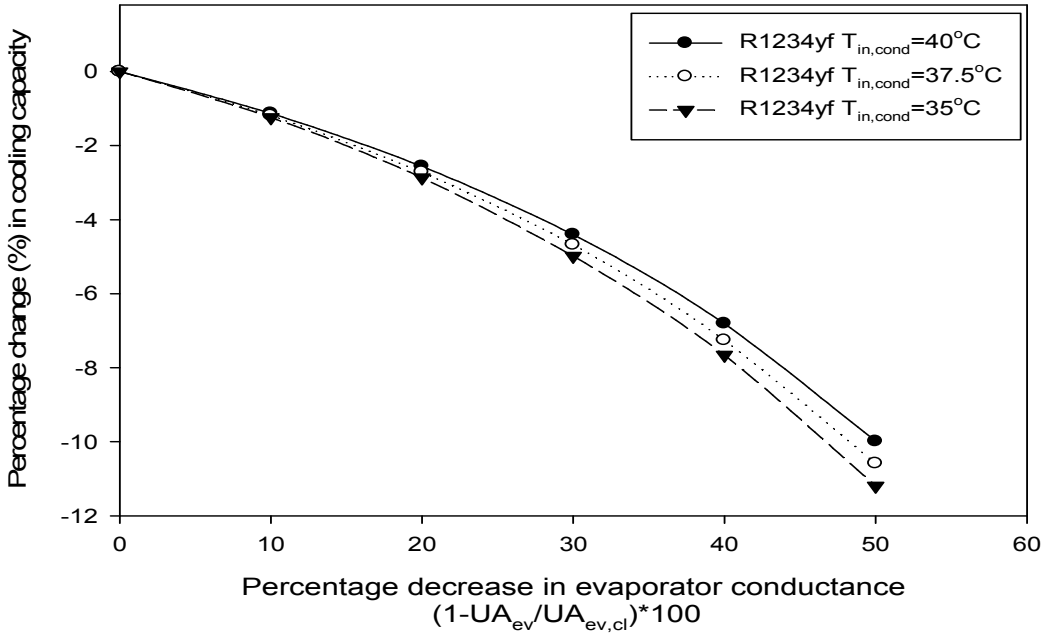

Figure 4.31 Percentage change in cooling capacity vs. Percentage decrease in evaporator conductance for R1234yf.

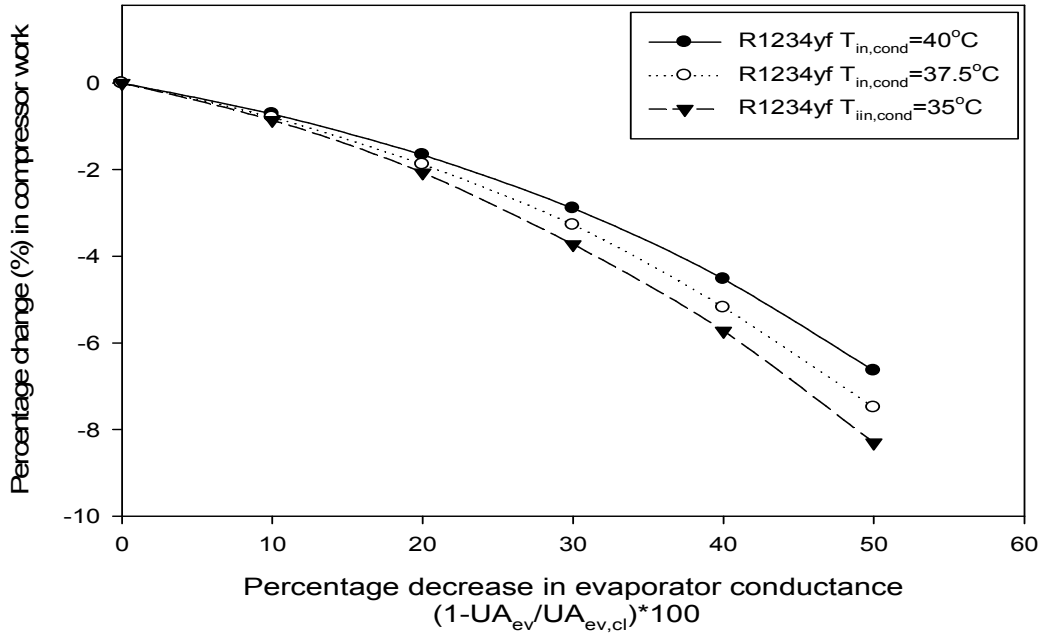

Figure 4.32 Percentage change in compressor work vs. Percentage decrease in evaporator conductance for R1234yf.

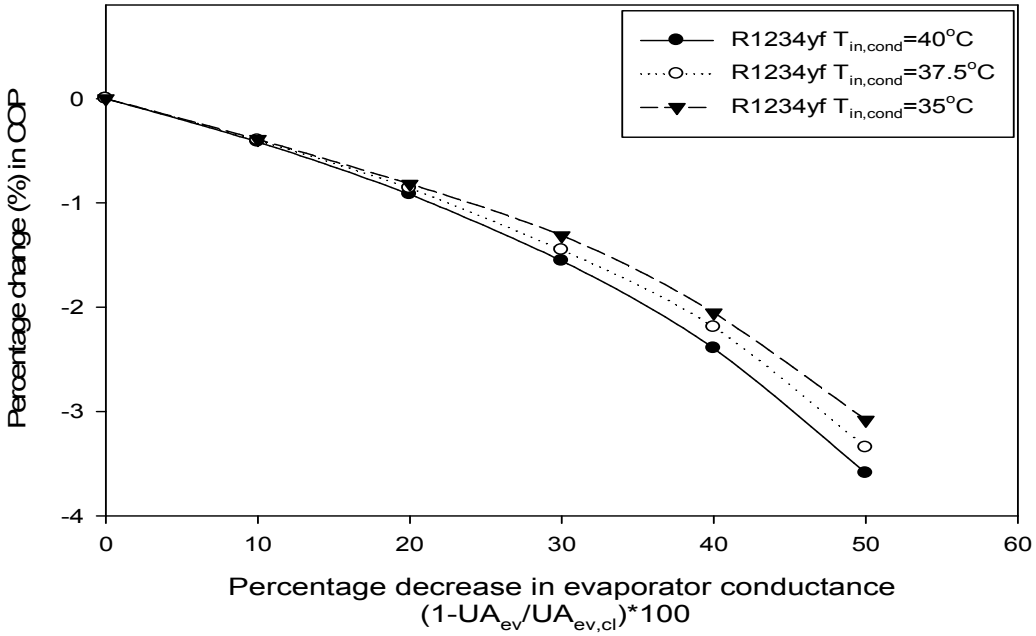

Figure 4.33 Percentage change in COP vs. Percentage decrease in evaporator conductance for R1234yf.

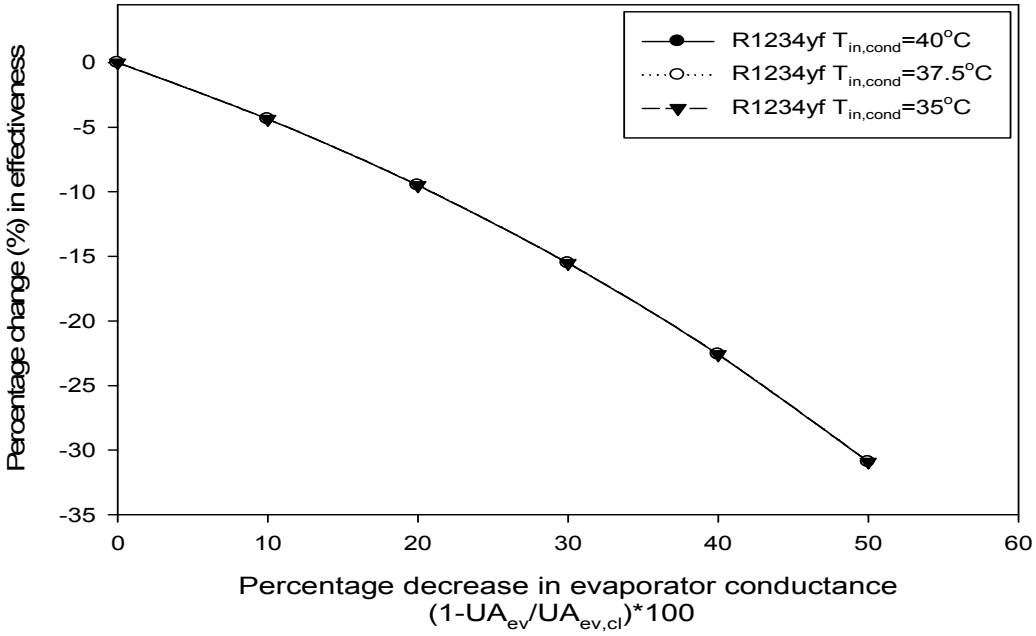

Figure 4.34 Percentage change in effectiveness vs. Percentage decrease in evaporator conductance for R1234yf.

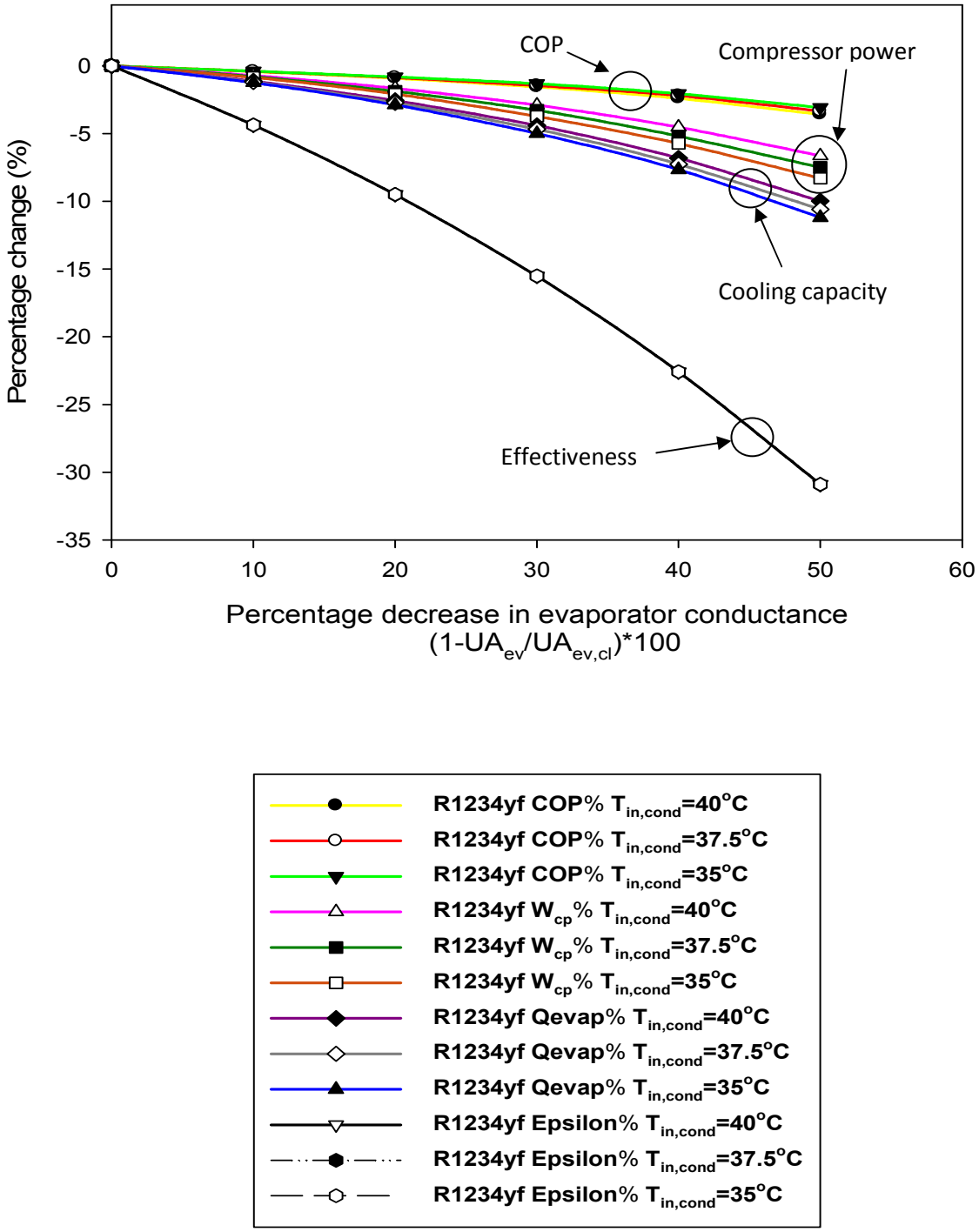

Figure 4.35 Percentage change (%) vs. Percentage decrease in evaporator conductance for R1234yf.

The trends are similar in figures 4.29 to 4.35 for R1234yf as compared with figures 4.8 to 4.14 for R134a; hence it does not require explanation.

Figures 4.36-4.41 shows the variation of compressor work, COP and percentage changes (%) in Q_{evap}, W_{cp}, COP, Є with percentage decrease in condenser and evaporator conductances for R1234yf.

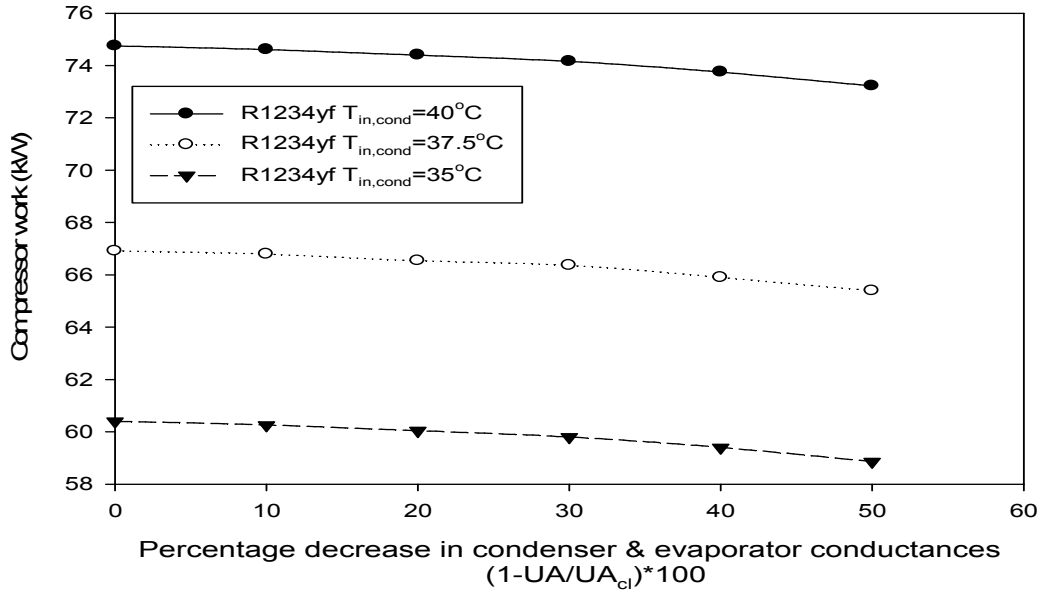

Figure 4.36 Compressor work vs. Percentage decrease in condenser and evaporator conductances for R1234yf.

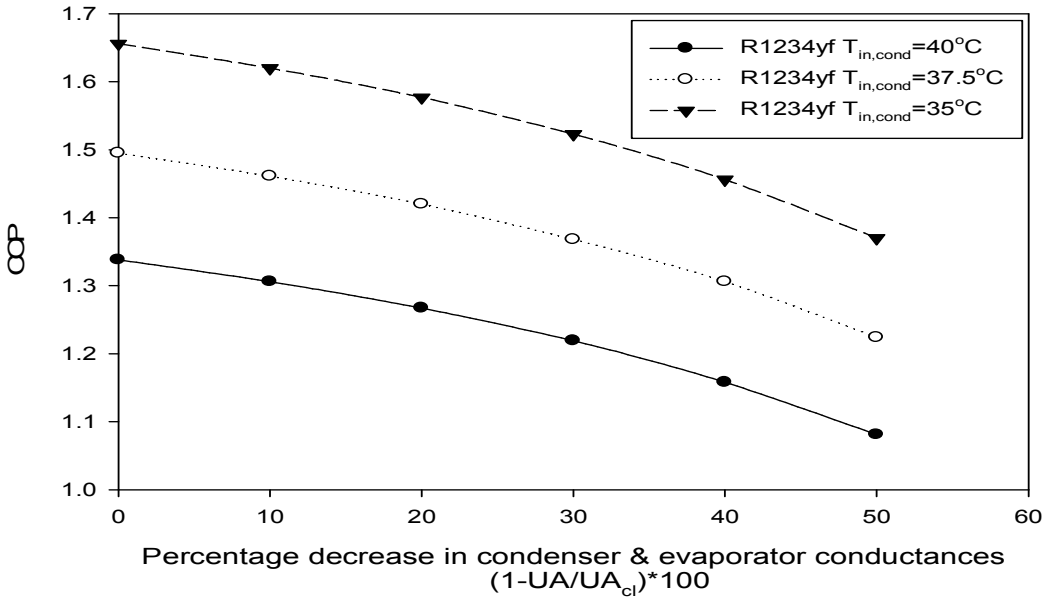

Figure 4.37 COP vs. Percentage decrease in condenser and evaporator Conductances for R1234yf.

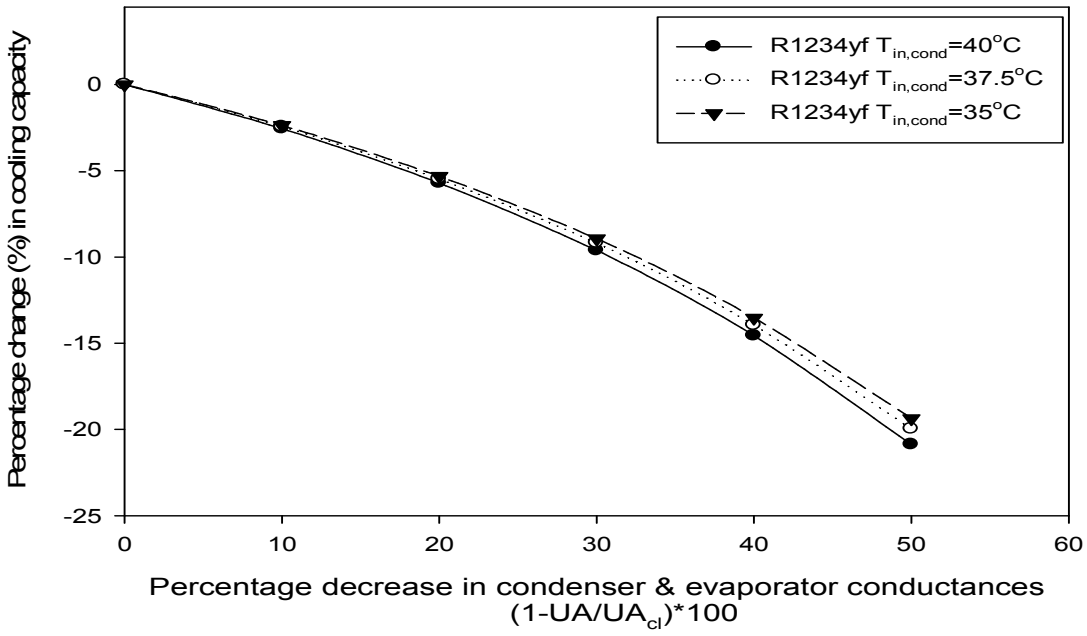

Figure 4.38 Percentage change in cooling capacity vs. Percentage decrease in condenser and evaporator conductances for R1234yf.

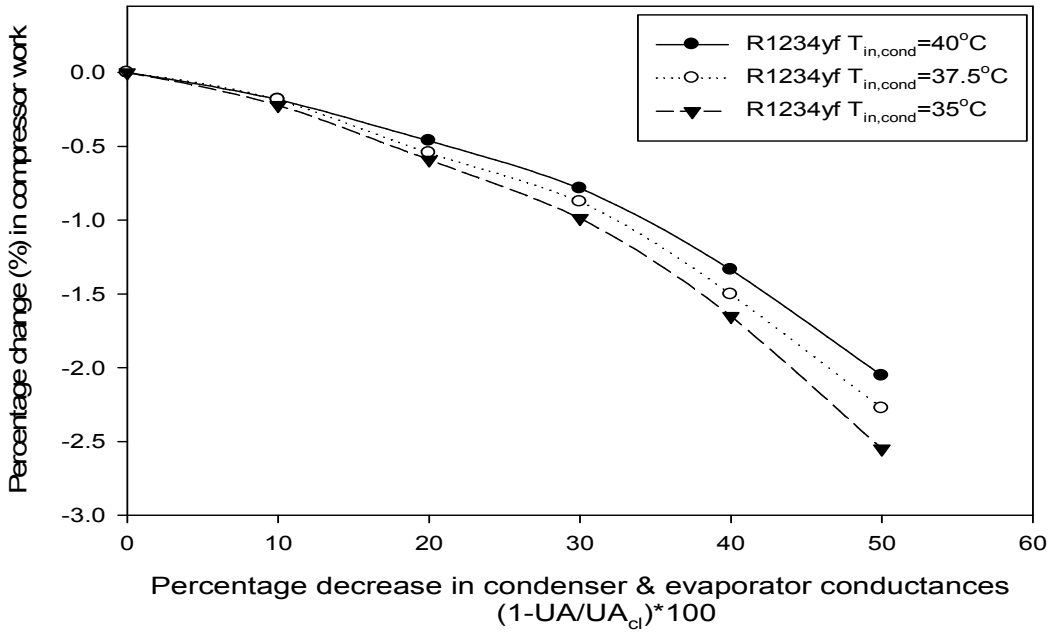

Figure 4.39 Percentage change in compressor work vs. Percentage decrease in condenser and evaporator conductances for R1234yf.

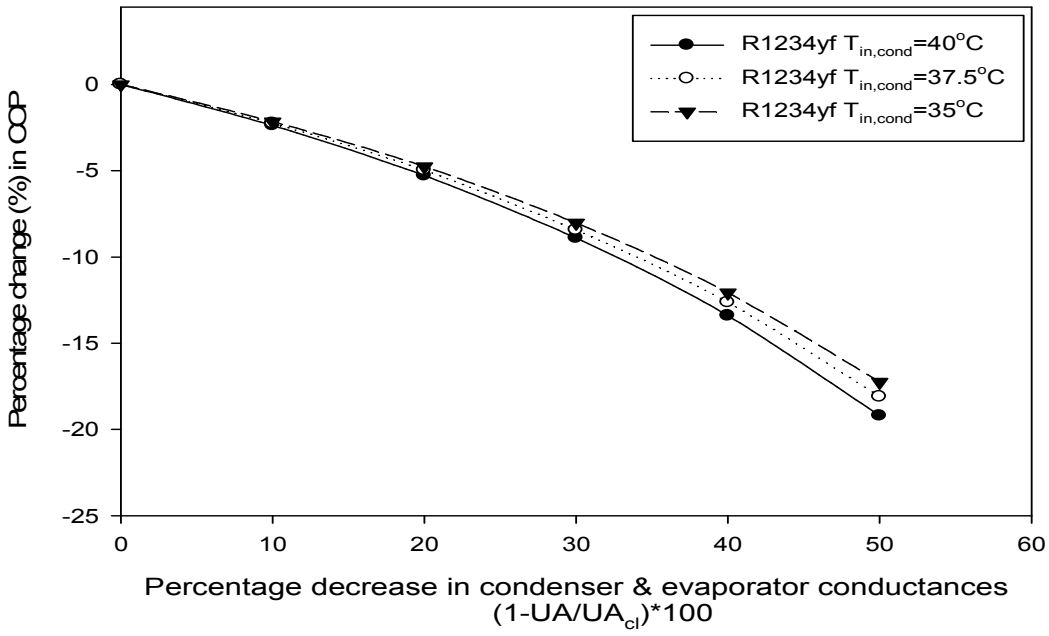

Figure 4.40 Percentage change in COP vs. Percentage decrease in condenser and evaporator conductances for R1234yf.

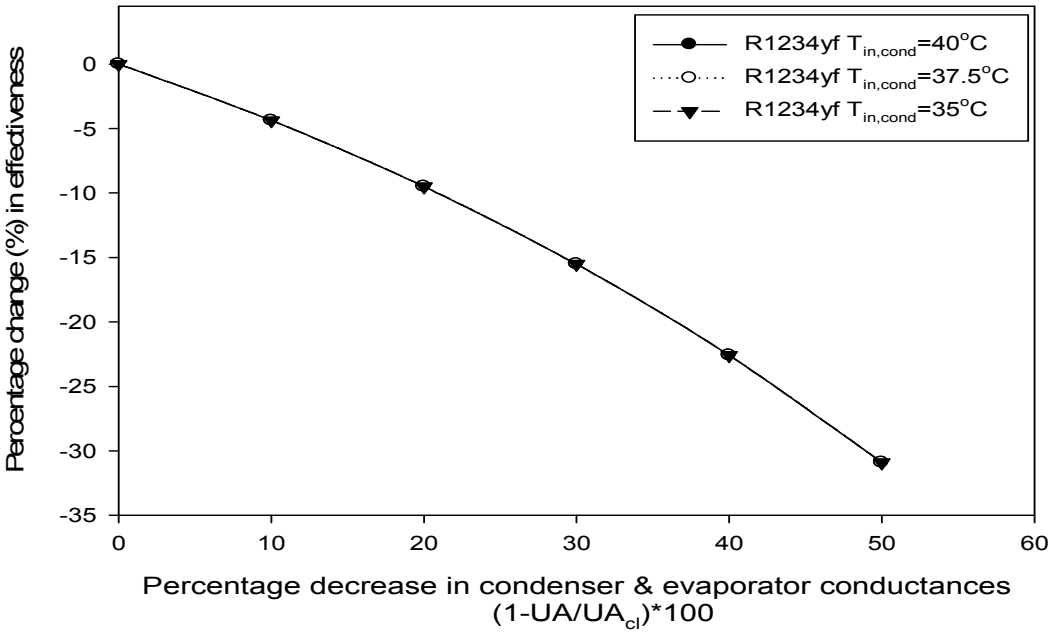

Figure 4.41 Percentage change in effectiveness vs. Percentage decrease in condenser and evaporator conductances for R1234yf.

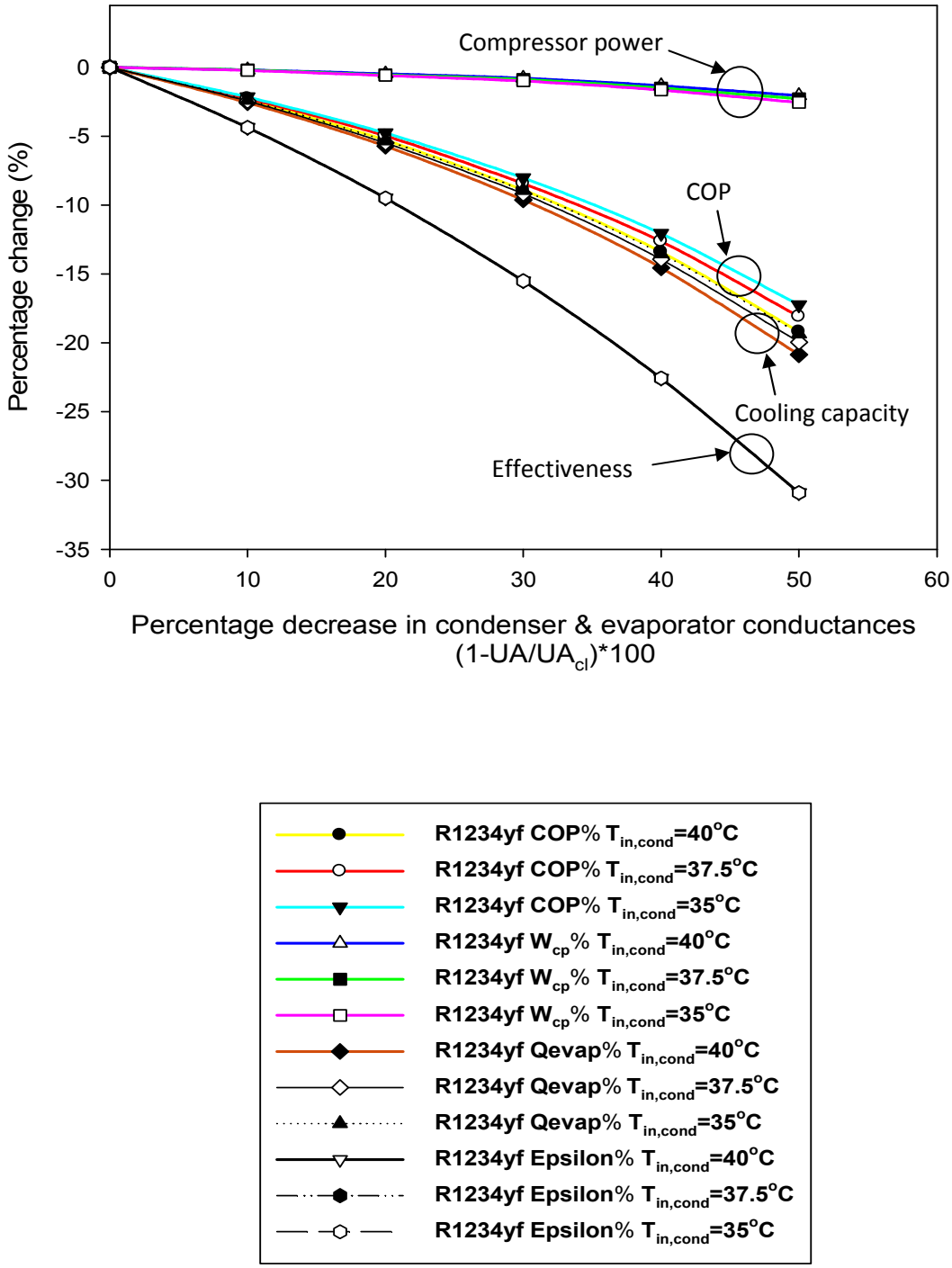

Figure 4.42 Percentage change (%) vs. Percentage decrease in condenser and evaporator conductances for R1234yf.

The trends are similar in figures 4.36 to 4.42 for R1234yf as compared with figures 4.15 to 4.21 for R134a; hence it does not require explanation.

Figures 4.43-4.48 shows the variation of compressor work, COP and percentage changes (%) in Q_{evap}, W_{cp}, COP, Є with percentage decrease in condenser conductance for R1234ze.

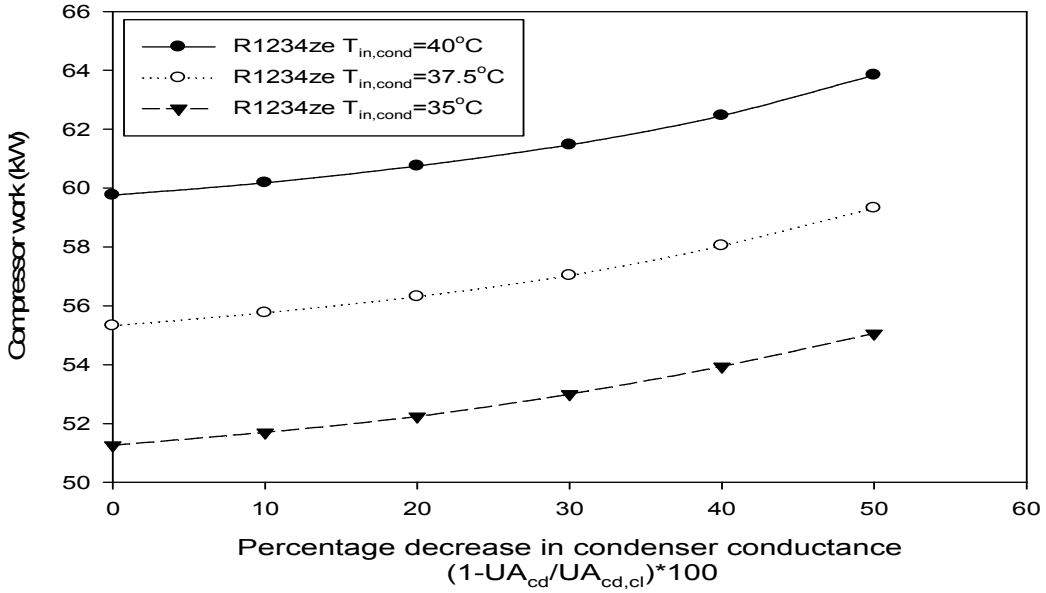

Figure 4.43 Compressor work vs. Percentage decrease in condenser conductance for R1234ze.

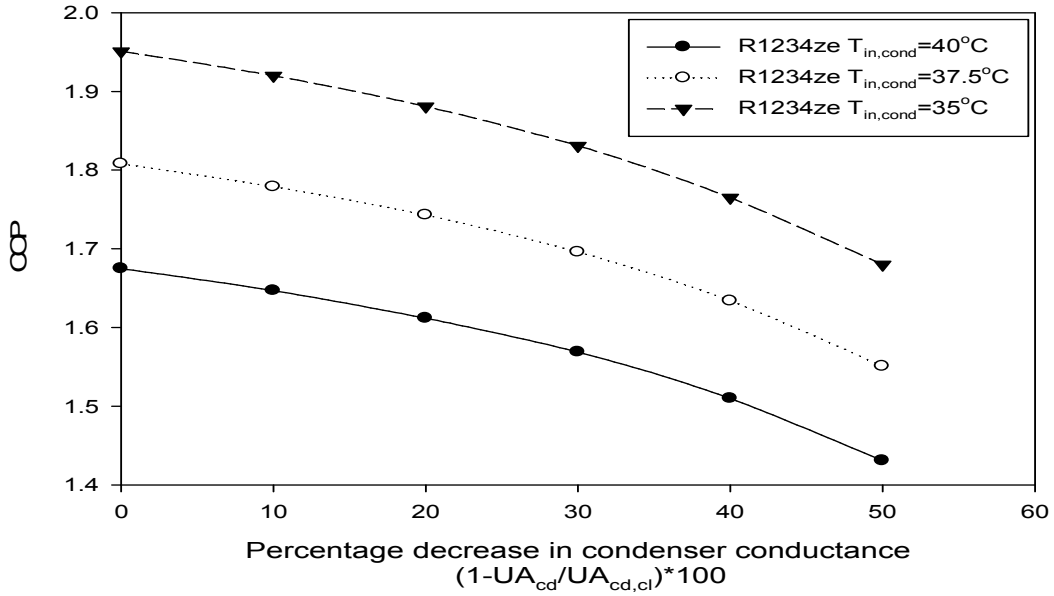

Figure 4.44 COP vs. Percentage decrease in condenser conductance for R1234ze.

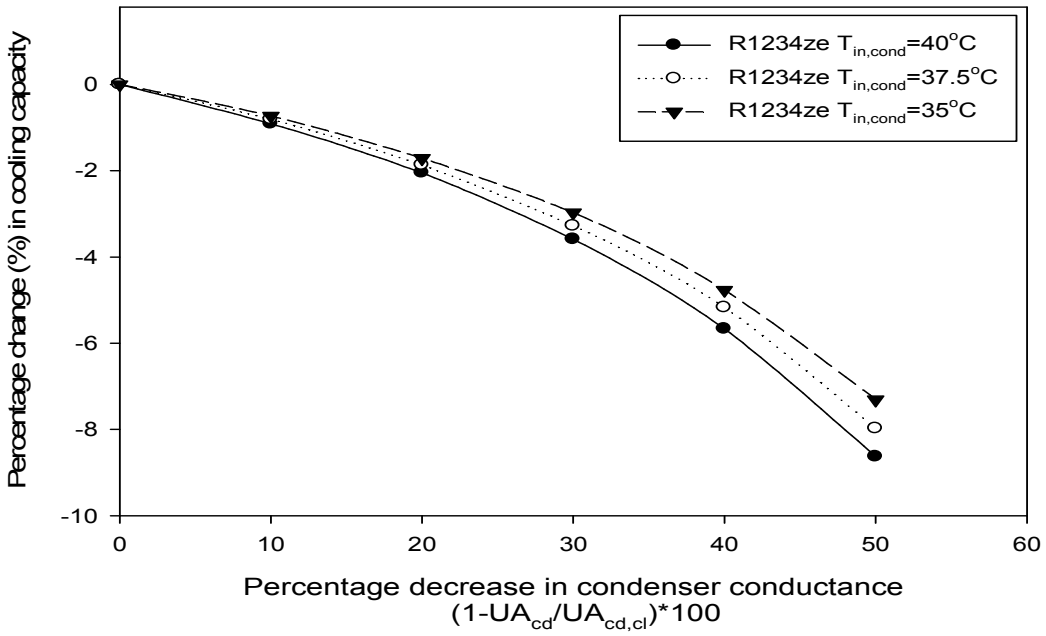

Figure 4.45 Percentage change in cooling capacity vs. Percentage decrease in condenser conductance for R1234ze.

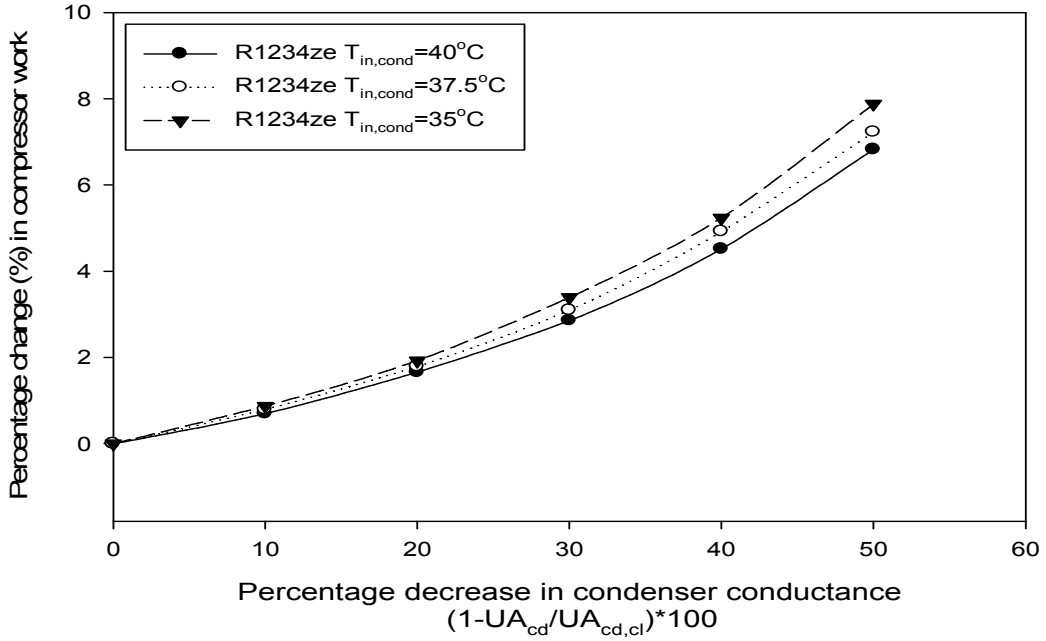

Figure 4.46 Percentage change in compressor work vs. Percentage decrease in condenser conductance for R1234ze.

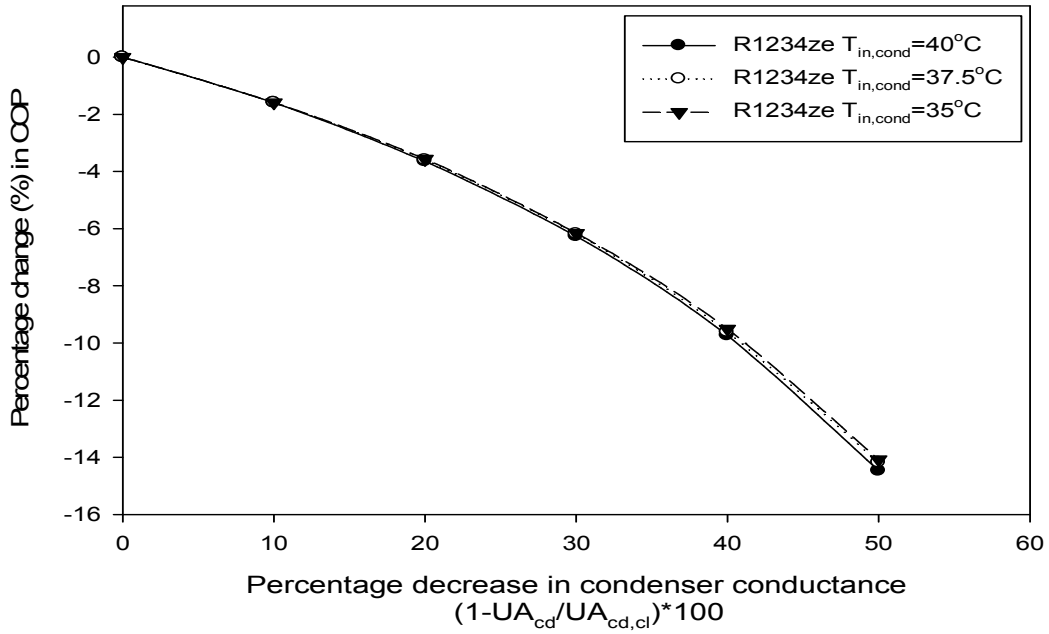

Figure 4.47 Percentage change in COP vs. Percentage decrease in condenser conductance for R1234ze.

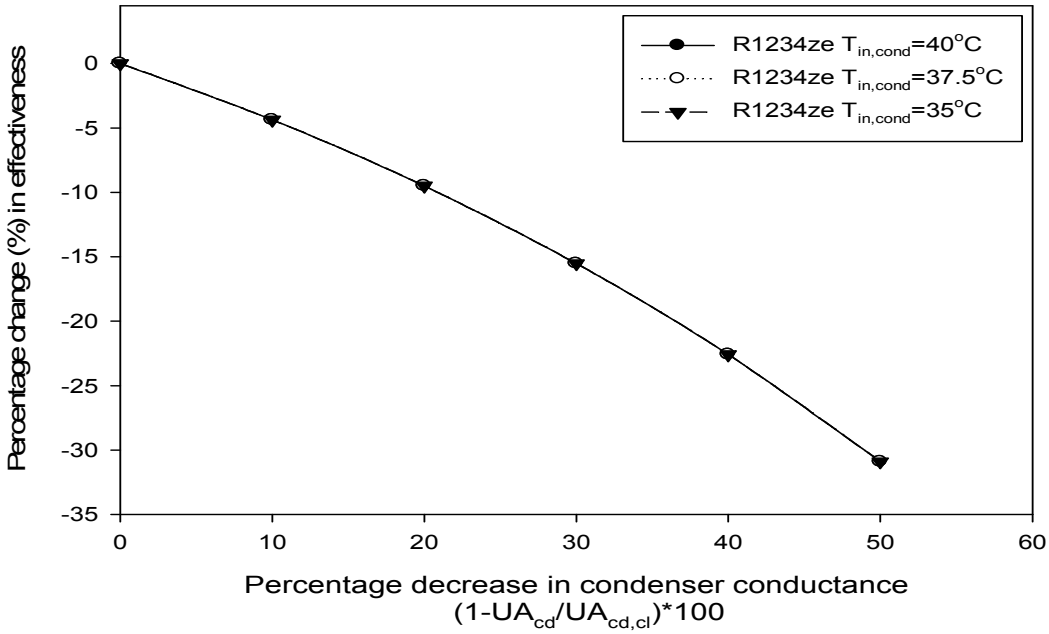

Figure 4.48 Percentage change in effectiveness vs. Percentage decrease in condenser conductance for R1234ze.

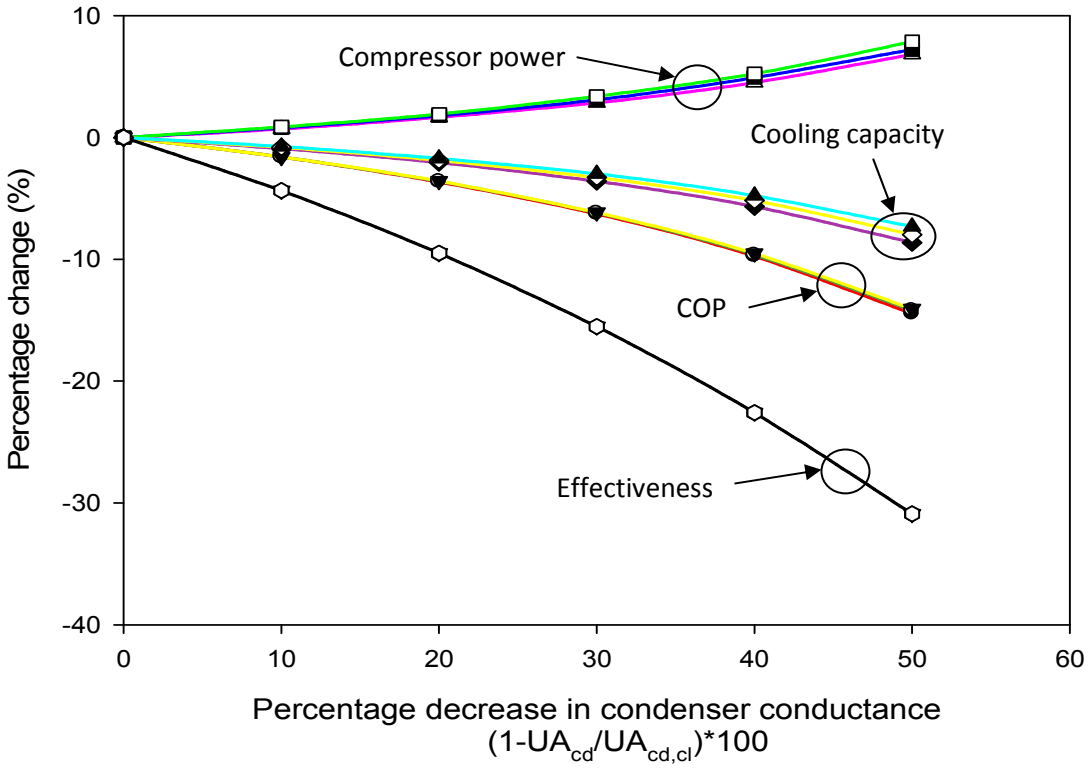

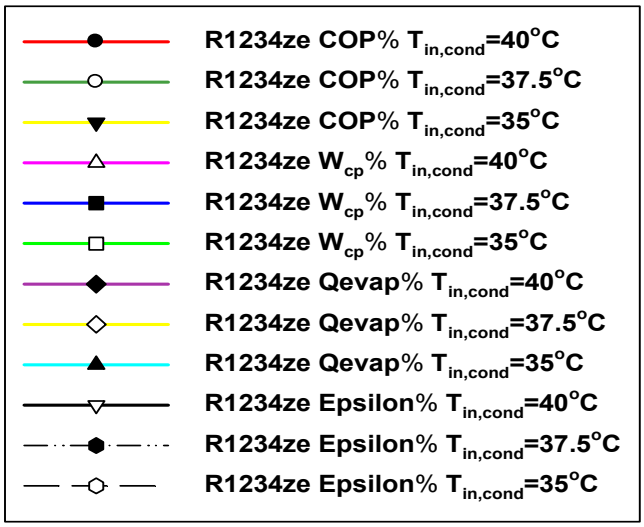

Figure 4.49 Percentage change (%) vs. Percentage decrease in condenser conductance for R1234ze.

The trends are similar in figures 4.43 to 4.49 for R1234ze as compared with figures 4.1 to 4.7 for R134a; hence it does not require explanation.

Figures 4.50-4.55 shows the variation of compressor work, COP and percentage changes (%) in Q_{evap}, W_{cp}, COP, Є with percentage decrease in evaporator conductance for R1234ze.

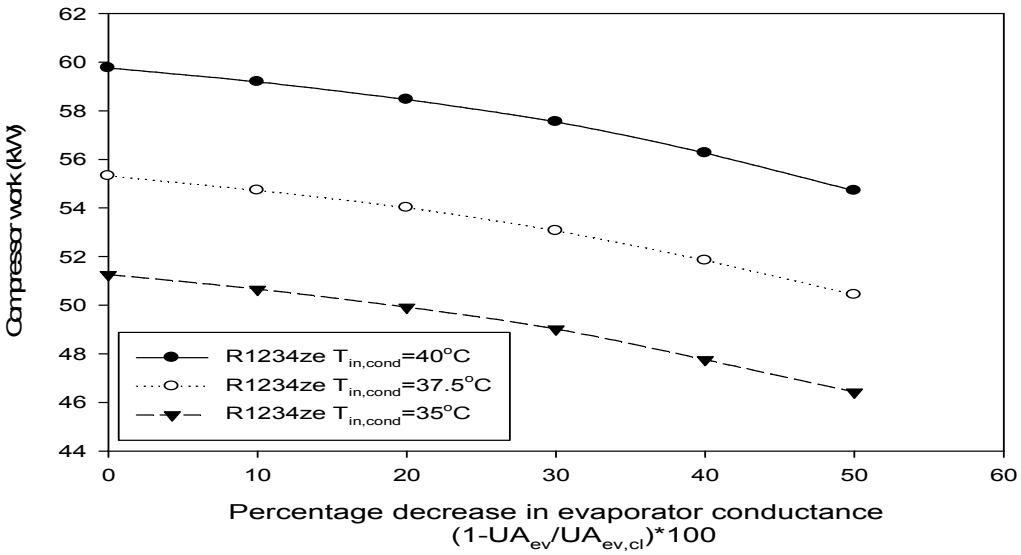

Figure 4.50 Compressor work vs. Percentage decrease in evaporator conductance for R1234ze.

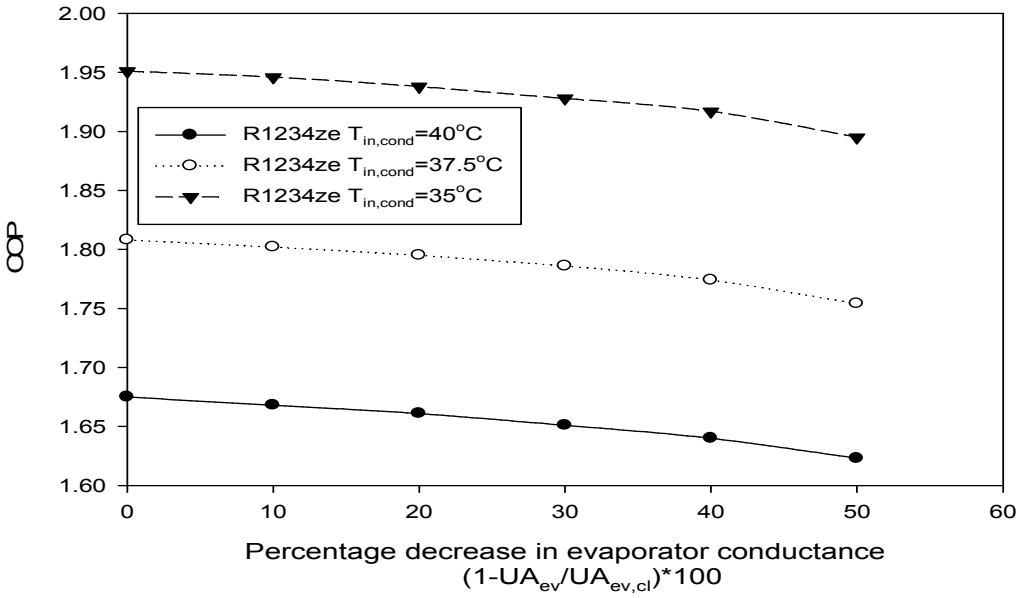

Figure 4.51 COP vs. Percentage decrease in evaporator conductance for R1234ze.

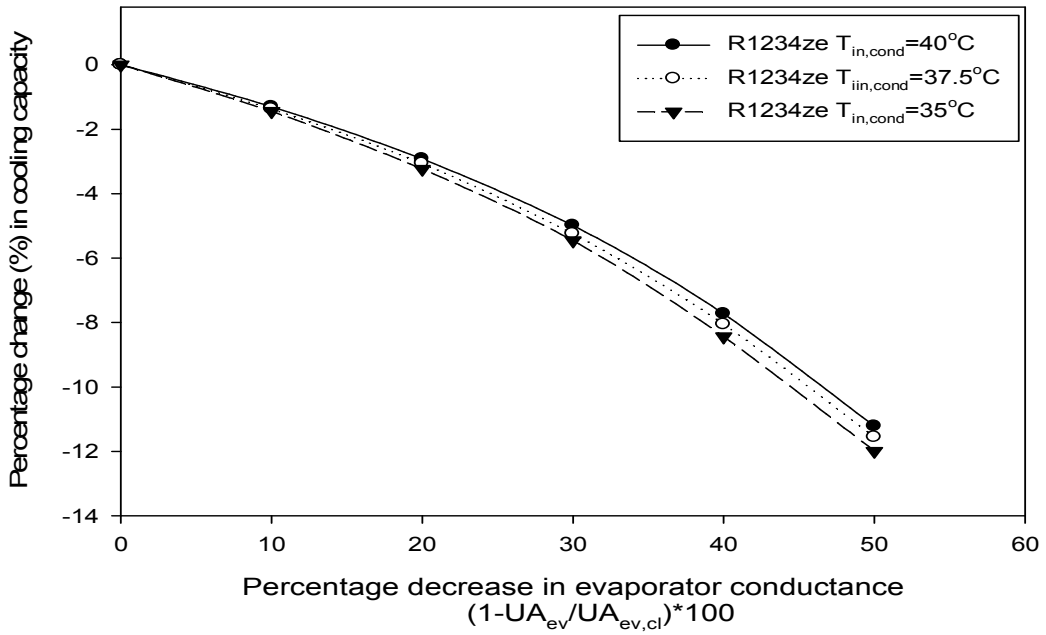

Figure 4.52 Percentage change in cooling capacity vs. Percentage decrease in evaporator conductance for R1234ze.

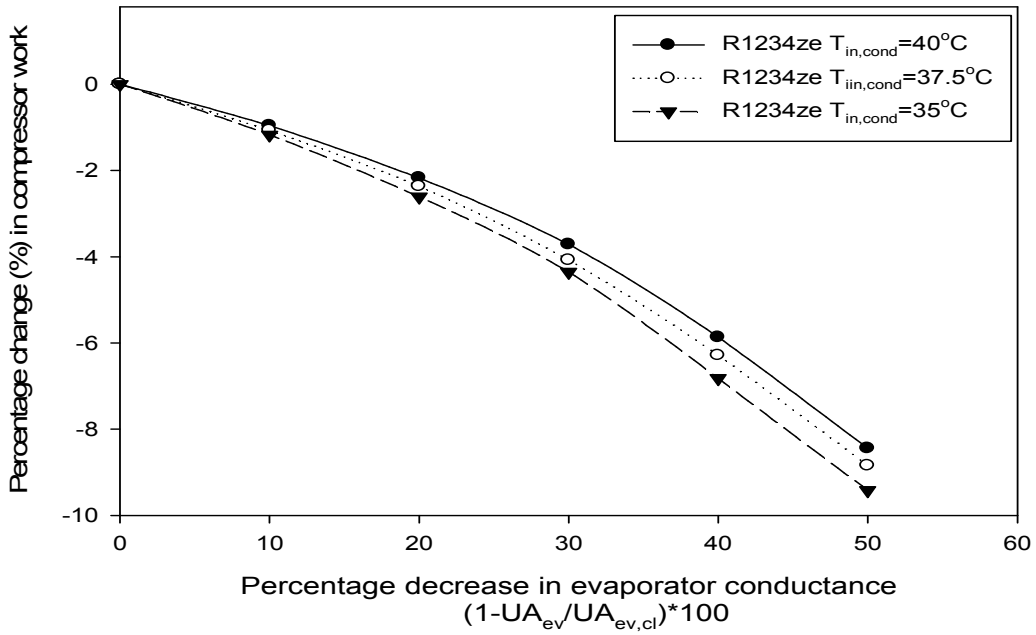

Figure 4.53 Percentage change in Compressor work vs. Percentage decrease in evaporator conductance for R1234ze.

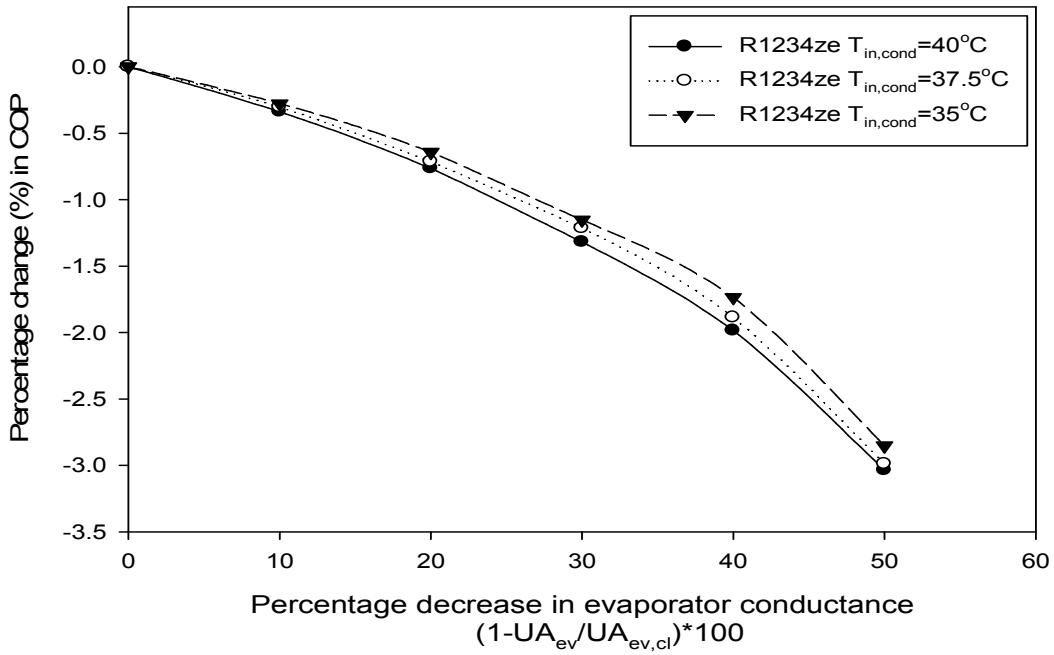

Figure 4.54 Percentage change in COP vs. Percentage decrease in evaporator conductance for R1234ze.

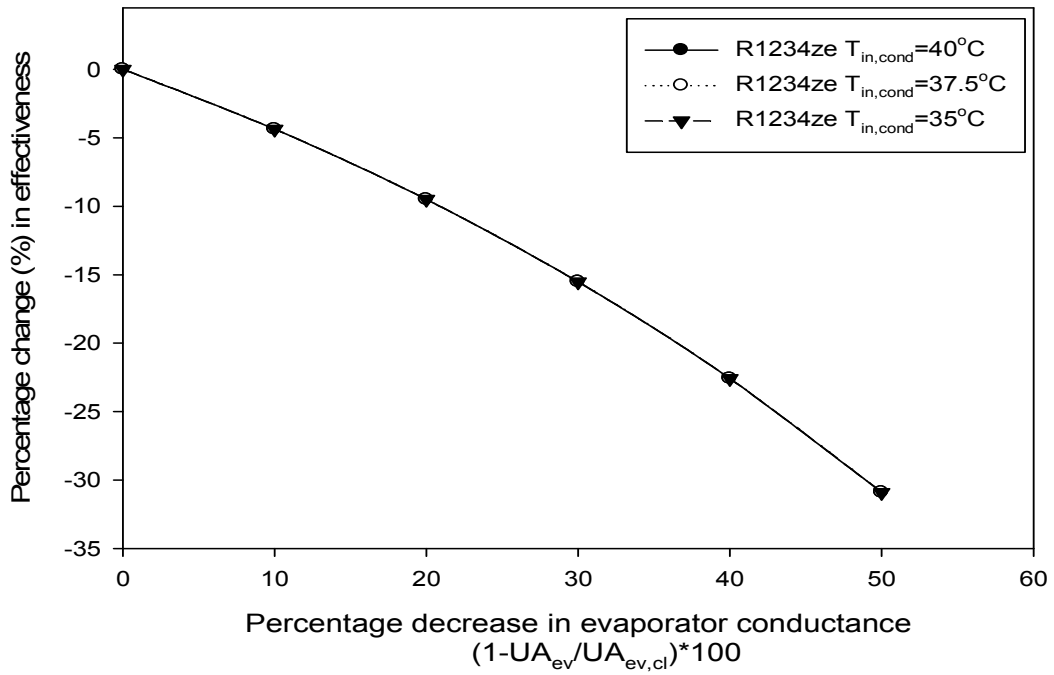

Figure 4.55 Percentage change in effectiveness vs. Percentage decrease in evaporator conductance for R1234ze.

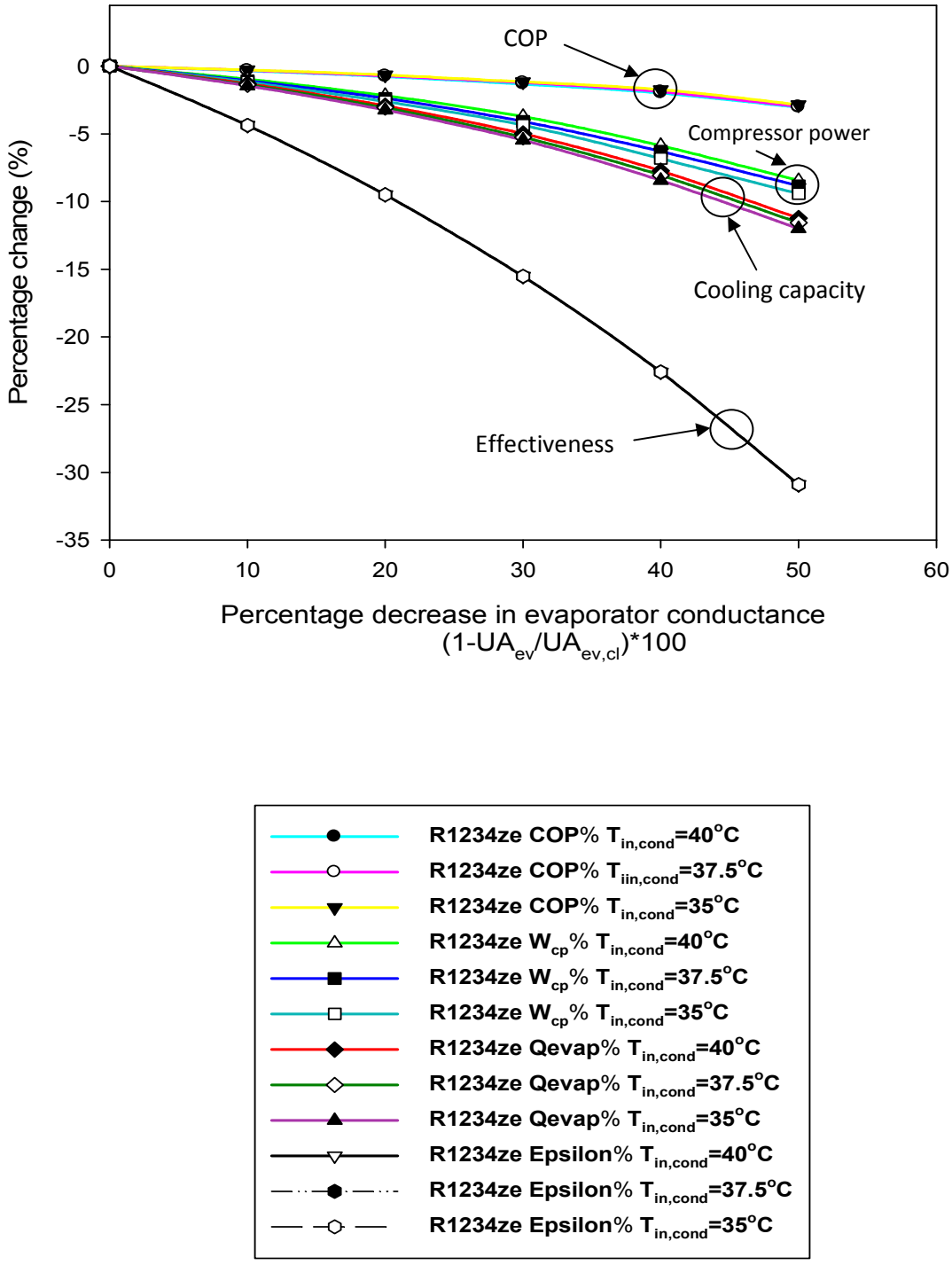

Figure 4.56 Percentage change (%) vs. Percentage decrease in evaporator conductance for R1234ze.

The trends are similar in figures 4.50 to 4.56 for R1234ze as compared with figures 4.7 to 4.14 for R134a; hence it does not require explanation.

Figures 4.57-4.62 shows the variation of compressor work, COP and percentage changes (%) in Q_{evap}, W_{cp}, COP, Є with percentage decrease in condenser and evaporator conductances for R1234ze.

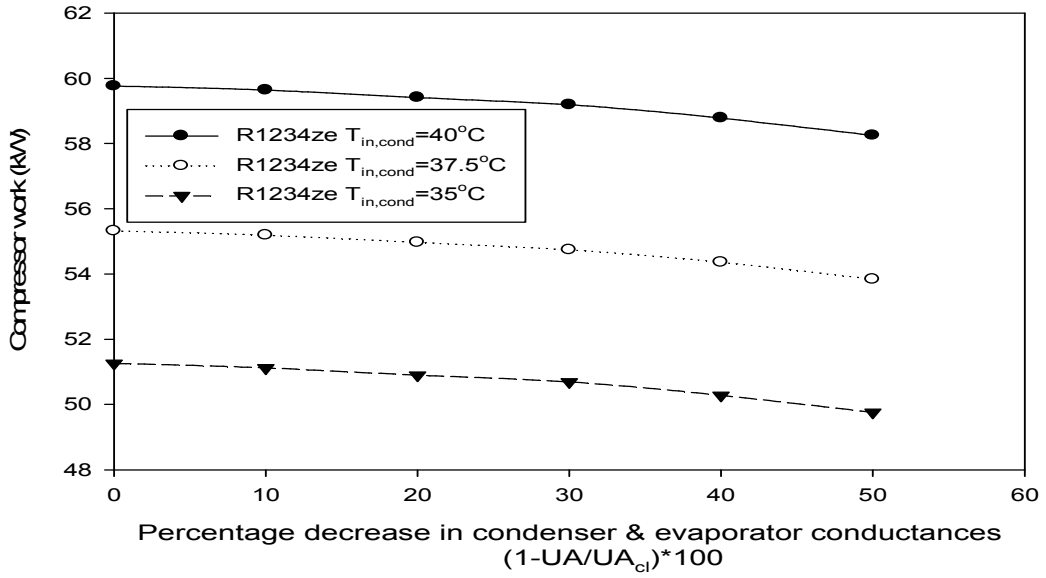

Figure 4.57 Compressor work vs. Percentage decrease in condenser and evaporator conductances for R1234ze.

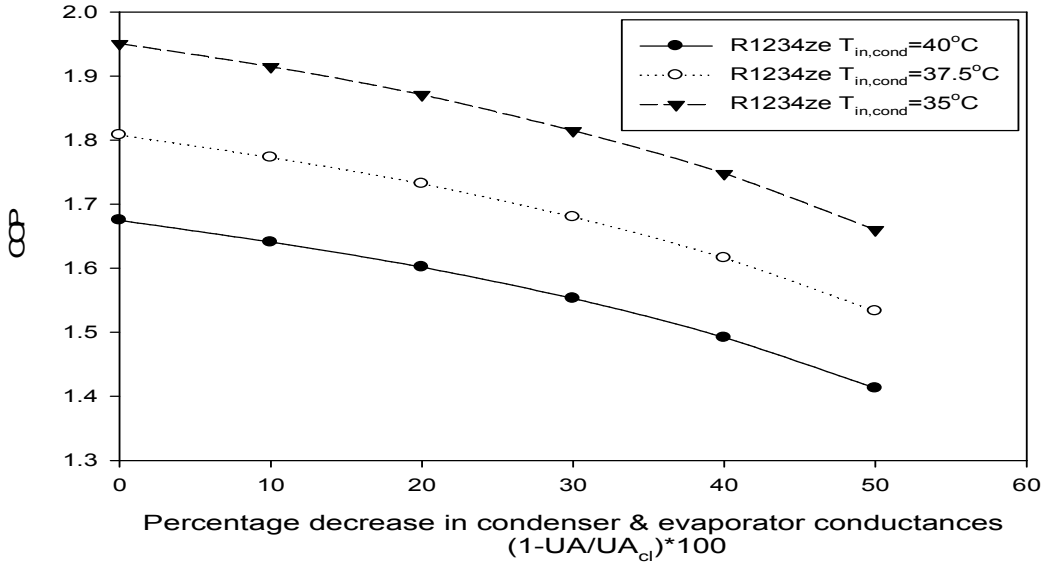

Figure 4.58 COP vs. Percentage decrease in condenser and evaporator conductances for R1234ze.

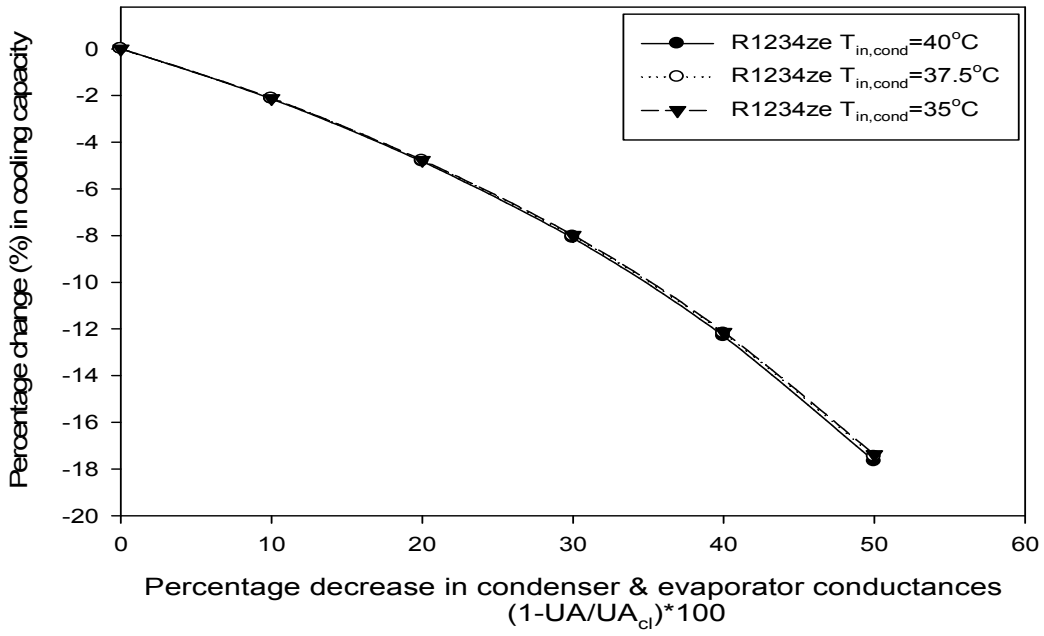

Figure 4.59 Percentage change in cooling capacity vs. Percentage decrease in condenser and evaporator conductances for R1234ze.

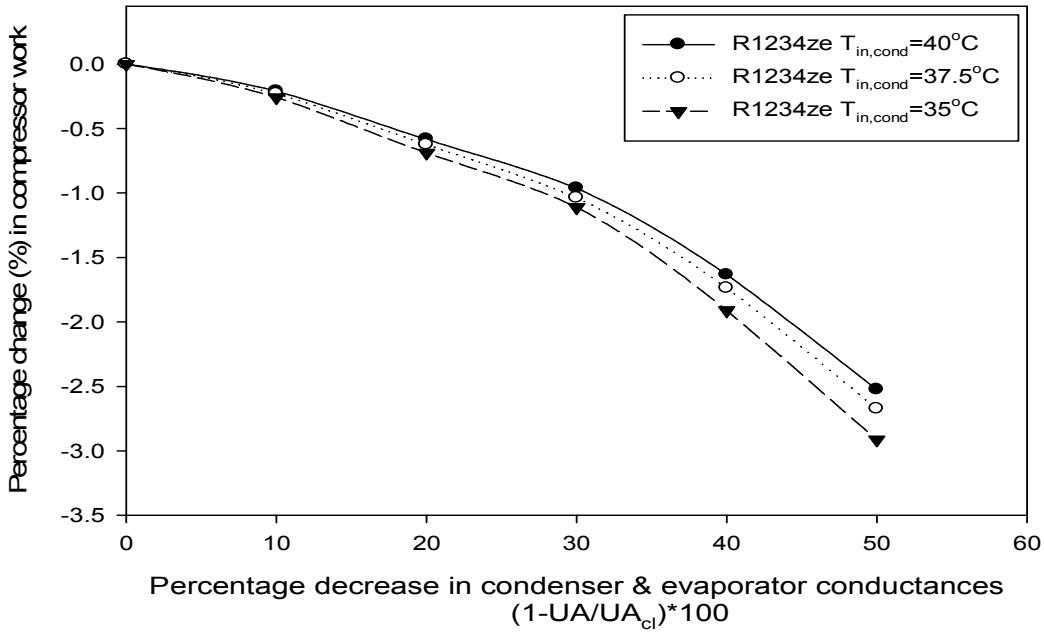

Figure 4.60 Percentage change in compressor work vs. Percentage decrease in condenser and evaporator conductances for R1234ze.

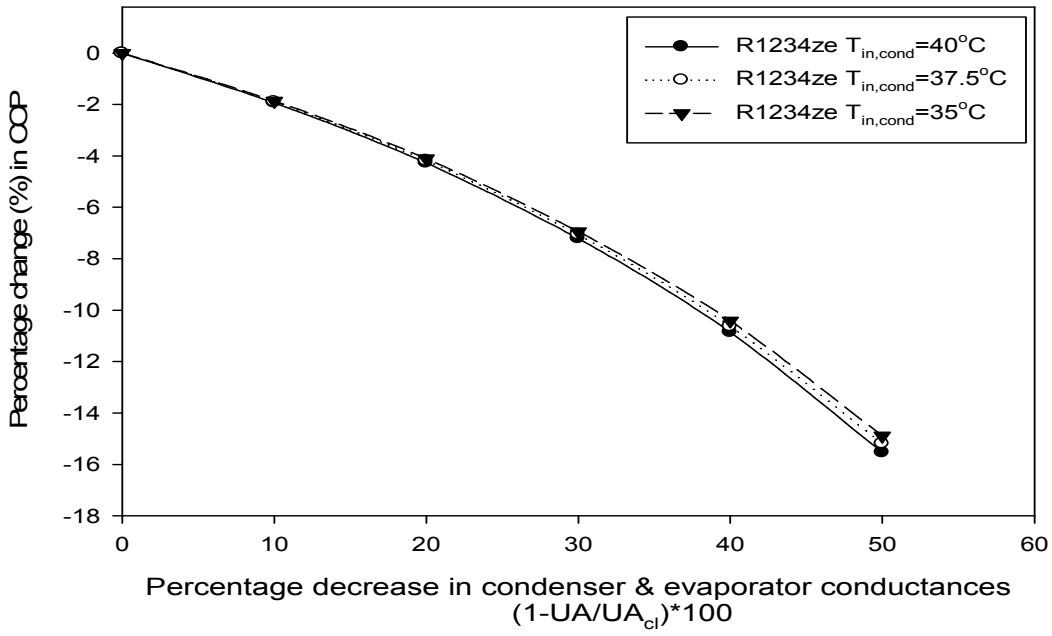

Figure 4.61 Percentage change in COP vs. Percentage decrease in condenser and evaporator conductances for R1234ze.

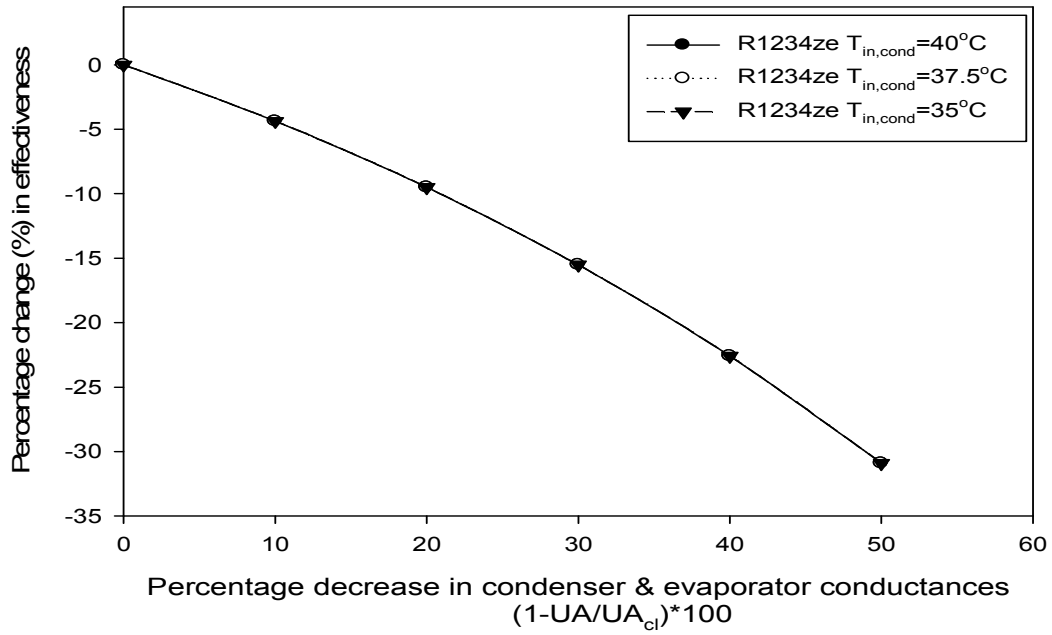

Figure 4.62 Percentage change in effectiveness vs. Percentage decrease in condenser and evaporator conductances for R1234ze.

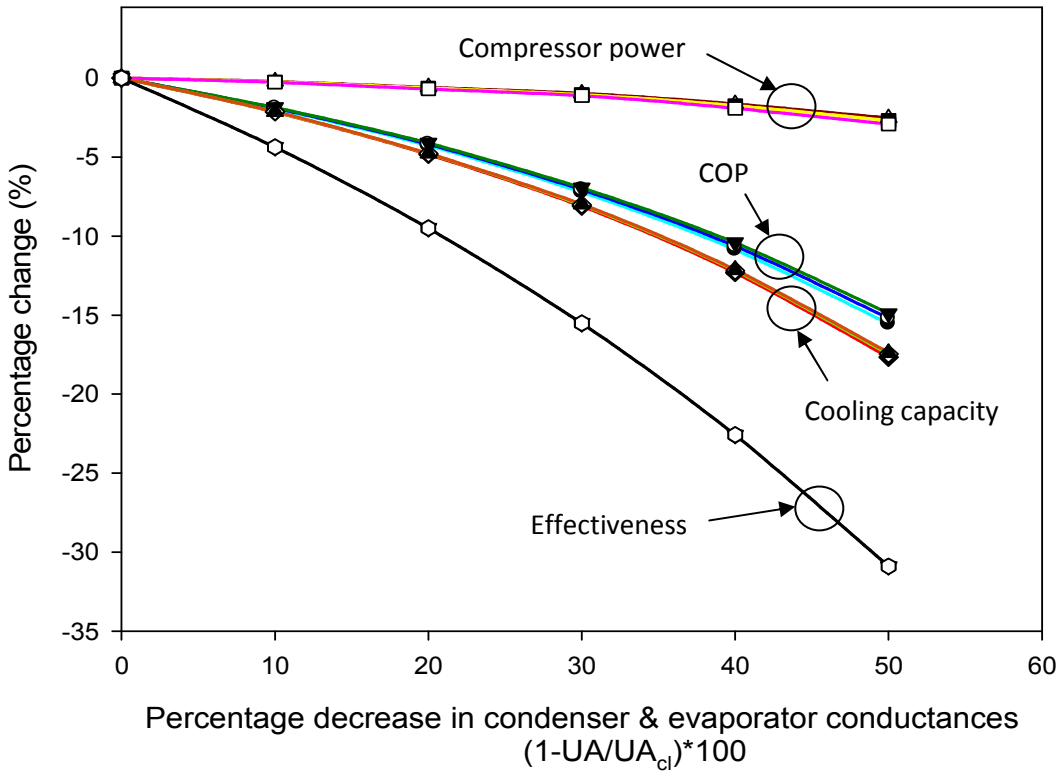

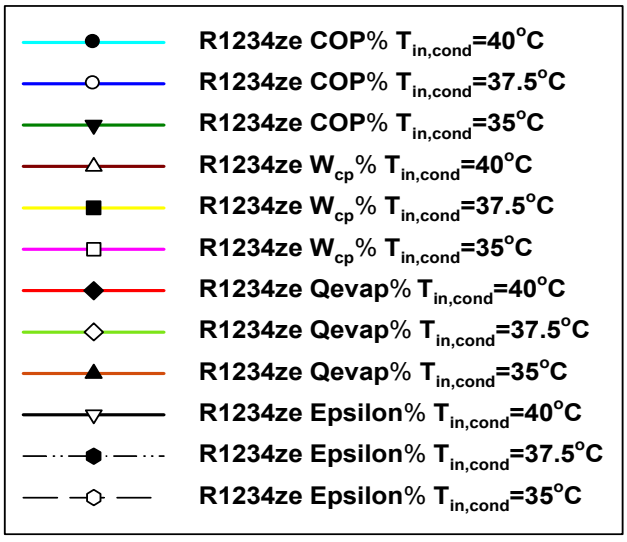

Figure 4.63 Percentage change (%) vs. Percentage decrease in condenser and evaporator conductances for R1234ze.

The trends are similar in figures 4.57 to 4.63 for R1234ze as compared with figures 4.14 to 4.21 for R134a; hence it does not require explanation.

On comparing results of R1234yf, R1234ze with R134a in condenser fouling at $T_{in,cond}$ = 40°C, 37.5 °C, 35 °C, the following results are observed and are shown in tables 4.11a-4.11c.

Table 4.11a Comparison of results for R1234yf, R1234ze with R134a at $T_{in,cond}$ = 40°C.

Refrigerant	UA_{cond}%	W_{cp} %	COP %	Qevap %
R1234yf	50	7.48	-19.29	-13.25
R1234ze	50	6.83	-14.47	-8.63
R134a	50	6.69	-14.49	-8.77

Table 4.11b Comparison of results for R1234yf, R1234ze with R134a at $T_{in,cond}$ = 37.5°C.

Refrigerant	UA_{cond}%	W_{cp} %	COP %	Qevap %
R1234yf	50	8.25	-18.25	-11.51
R1234ze	50	7.22	-14.17	-7.98
R134a	50	7.08	-14.18	-8.09

Table 4.11c Comparison of results for R1234yf, R1234ze with R134a at $T_{in,cond}$ = 35°C.

Refrigerant	UA_{cond}%	W_{cp} %	COP %	Qevap %
R1234yf	50	9.12	-17.55	-10.06
R1234ze	50	7.41	-13.88	-7.50
R134a	50	7.38	-13.91	-7.56

From the above tables it is clear that the refrigerant R1234yf shows maximum increase in value of W_{cp}% at $T_{in,cond}$ = 35°C, and maximum decrease in values of COP %, and Qevap% at $T_{in,cond}$ = 40°C.where as values of R1234ze & R134a are nearly same.

On comparing results of R1234yf, R1234ze with R134a in evaporator fouling at $T_{in,cond}$ = 40^{o}C, 37.5 ^{o}C, 35 ^{o}C, the following results are observed and are shown in tables 4.12a – 4.12c.

Table 4.12a Comparison of results for R1234yf, R1234ze with R134a at $T_{in,cond}$ = 40^{o}C.

Refrigerant	**UA_{evap}%**	**W_{cp} %**	**COP %**	**Qevap %**
R1234yf	50	-6.64	-3.59	-9.99
R1234ze	50	-8.45	-3.04	-11.22
R134a	50	-8.41	-2.99	-11.16

Table 4.12b Comparison of results for R1234yf, R1234ze with R134a at $T_{in,cond}$ = 37.5^{o}C.

Refrigerant	**UA_{evap}%**	**W_{cp} %**	**COP %**	**Qevap %**
R1234yf	50	-7.49	-3.34	-10.59
R1234ze	50	-9.04	-2.90	-11.67
R134a	50	-8.98	-2.87	-11.60

Table 4.12c Comparison of results for R1234yf, R1234ze with R134a at $T_{in,cond}$ = 35^{o}C.

Refrigerant	**UA_{evap}%**	**W_{cp} %**	**COP%**	**Qevap %**
R1234yf	50	-8.31	-3.08	-11.19
R1234ze	50	-9.66	-2.74	-12.13
R134a	50	-9.63	-2.71	-12.08

From the above tables it is clear that the refrigerant R1234ze shows maximum decrease in value of W_{cp}% and Qevap% at $T_{in,cond}$ = 35^{o}C, and R1234yf shows maximum decrease in values of COP % at $T_{in,cond}$ = 40^{o}C.

On comparing results of R1234yf, R1234ze with R134a in condenser and evaporator fouling at $T_{in,cond}$ = 40°C, 37.5 °C, 35 °C, the following results are observed and are shown in tables 4.13a – 4.13c.

Table 4.13a Comparison of results for R1234yf, R1234ze with R134a at $T_{in,cond}$ = 40°C.

Refrigerant	$UA_{cond\&evap}$%	W_{cp}%	COP %	Qevap %
R1234yf	50	-2.05	-19.20	-20.87
R1234ze	50	-2.52	-15.54	-17.67
R134a	50	-2.54	-15.54	-17.69

Table 4.13b Comparison of results for R1234yf, R1234ze with R134a at $T_{in,cond}$ = 37.5°C.

Refrigerant	$UA_{cond\&evap}$%	W_{cp}%	COP %	Qevap %)
R1234yf	50	-2.27	-18.11	-19.97
R1234ze	50	-2.67	-15.20	-17.47
R134a	50	-2.70	-15.19	-17.49

Table 4.13c Comparison of result for R1234yf, R1234ze with R134a at $T_{in,cond}$ = 35°C.

Refrigerant	$UA_{cond\&evap}$%	W_{cp} %	COP %	Qevap %
R1234yf	50	-2.55	-17.25	-19.36
R1234ze	50	-2.91	-14.89	-17.37
R134a	50	-2.95	-14.88	-17.39

From the above tables it is clear that the refrigerant R1234ze shows maximum decrease in value of W_{cp}% at $T_{in,cond}$ = 35°C, and R1234yf shows maximum decrease in values of COP % and Qevap% at $T_{in,cond}$ = 40°C.

Figures 4.64-4.66 shows the variation of second-law efficiency (η_{II}) %, with condenser fouling from 0% to 50%, at $T_{in,cond}$ = 40°C, 37.5 °C, 35 °C, for refrigerants R134a, R1234yf and R1234ze.

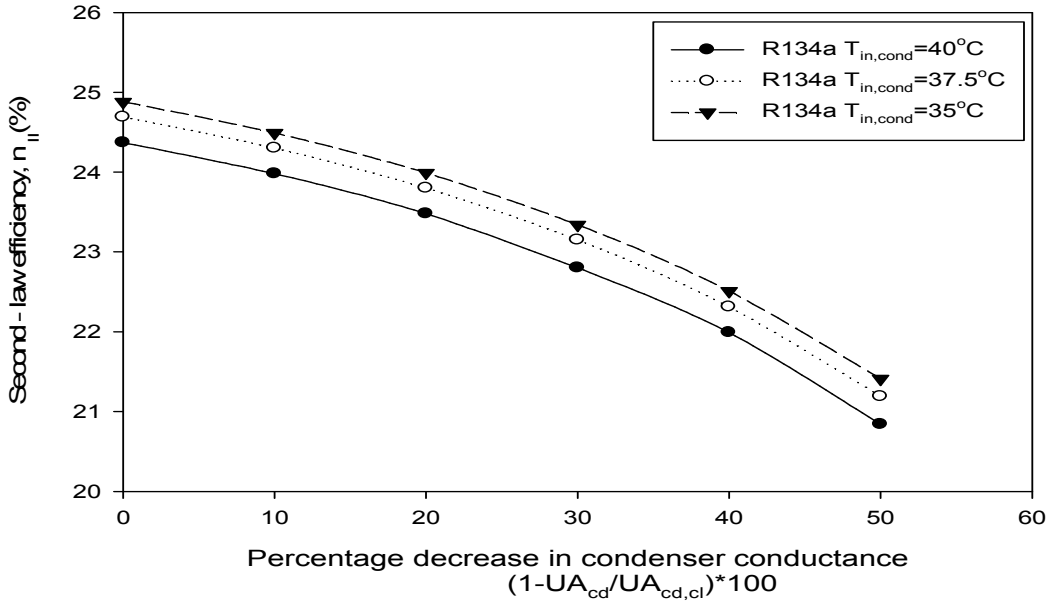

Figure 4.64 Second-law efficiency (%) vs. Percentage decrease in condenser conductance for R134a.

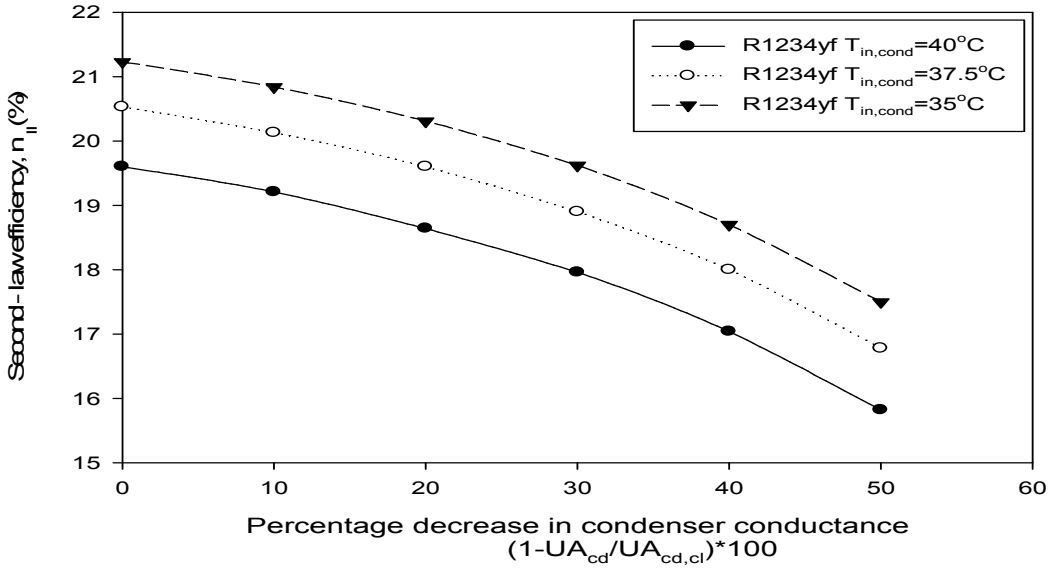

Figure 4.65 Second-law efficiency (%) vs. Percentage decrease in condenser conductance for R1234yf.

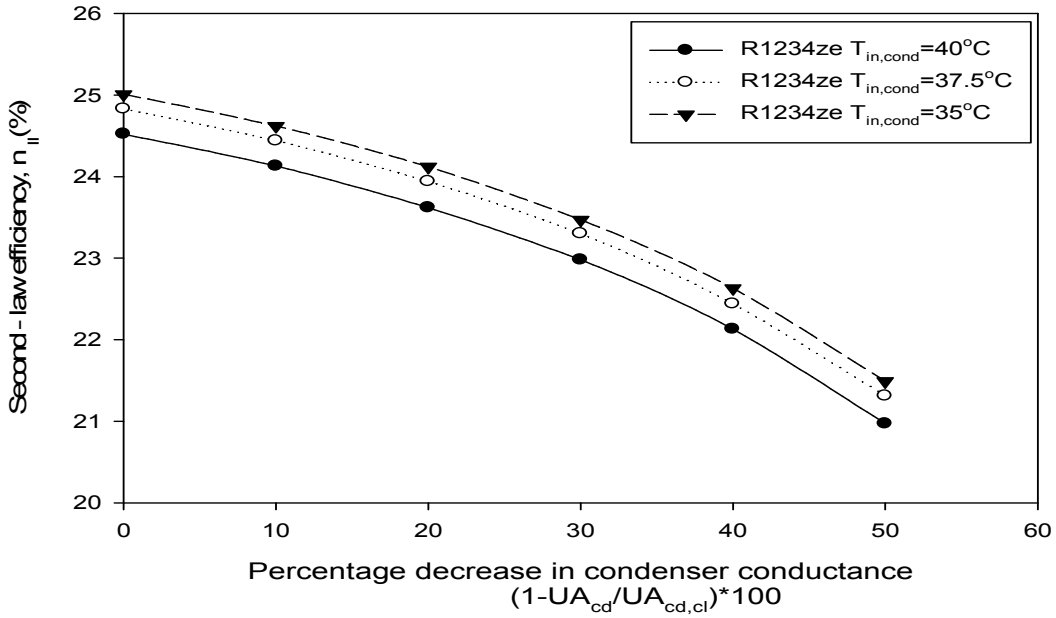

Figure 4.66 Second-law efficiency (%) vs. Percentage decrease in condenser conductance for R1234ze.

On comparing results of R1234yf, R1234ze with R134a in condenser fouling at $T_{in,cond}$ = 40°C, 37.5 °C, 35 °C (50% fouling), the following results are observed as shown in tables 4.14.

Table 4.14 Comparison of second-law efficiency for Refrigerants R1234yf, R1234ze with R134a.

Refrigerant	**UA_{cond}%**	**η_{II} ($T_{in,cond}$=40°C)**	**η_{II} ($T_{in,cond}$=37.5°C)**	**η_{II} ($T_{in,cond}$=35°C)**
R1234ze	50	20.97 %	21.31 %	21.49 %
R1234yf	50	15.82 %	16.78 %	17.50 %
R134a	50	20.84 %	21.19 %	21.41 %

From the above tables it is clear that, the second-law efficiency decreases on comparing R1234yf with R134a, while its value increases on comparing R1234ze with R134a.

Figures 4.67-4.69 shows the variation of second-law efficiency (η_{II}) %, with evaporator fouling from 0% to 50%, at $T_{in,cond}$ = 40°C, 37.5 °C, 35 °C, for refrigerants R134a, R1234yf and R1234ze.

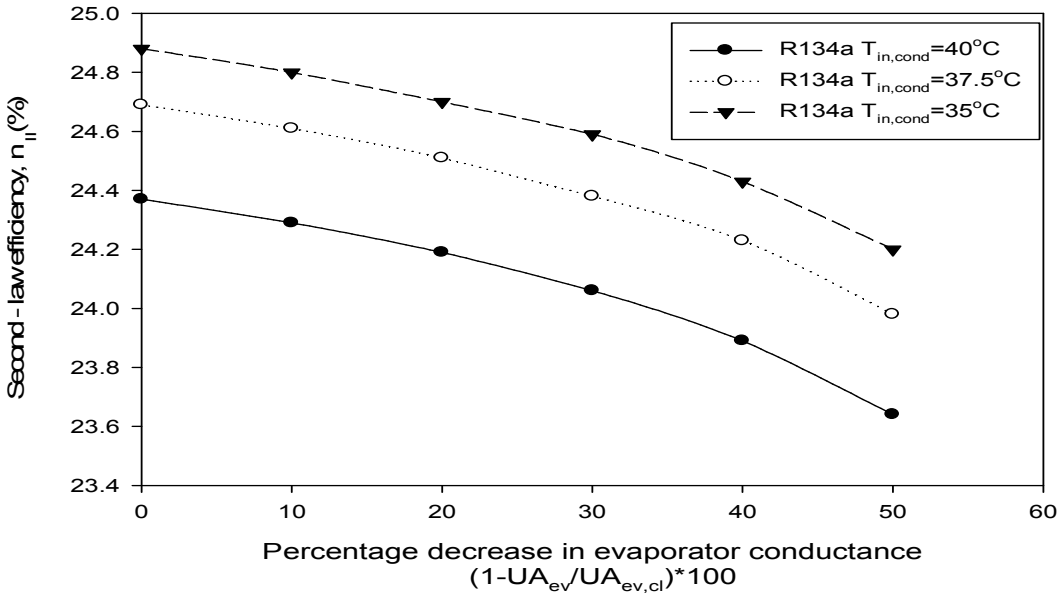

Figure 4.67 Second-law efficiency (%) vs. Percentage decrease in evaporator conductance for R134a.

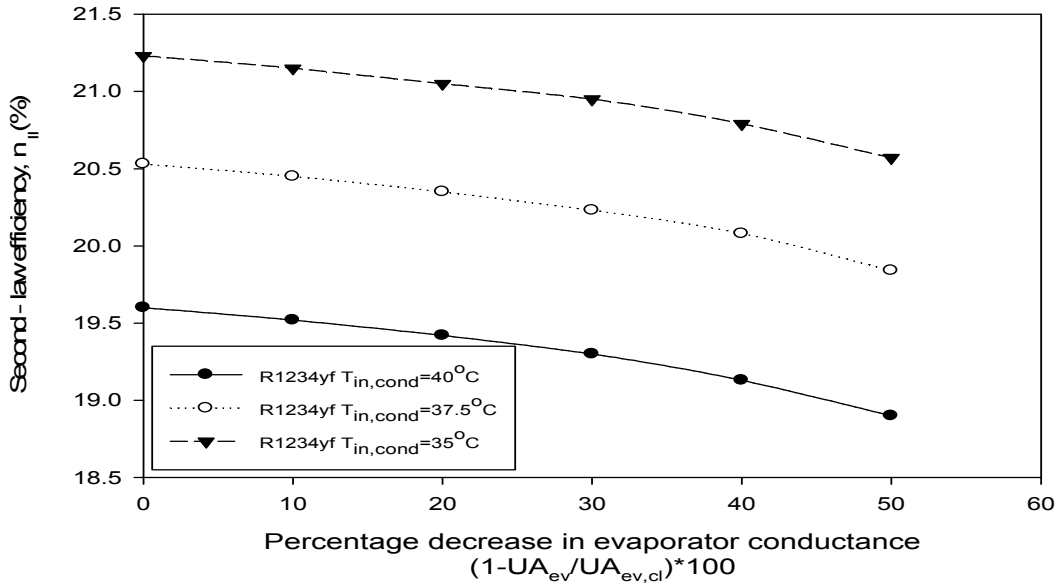

Figure 4.68 Second-law efficiency (%) vs. Percentage decrease in evaporator conductance for R1234yf.

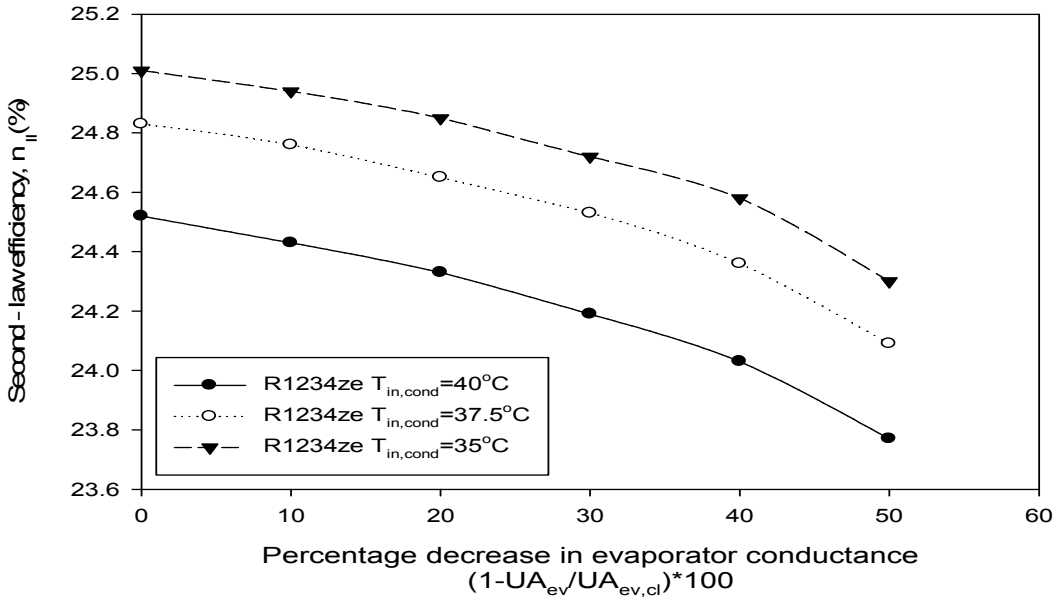

Figure 4.69 Second-law efficiency (%) vs. Percentage decrease in evaporator conductance for R1234ze.

On comparing results of R1234yf, R1234ze with R134a in evaporator fouling at $T_{in,cond}$ = 40°C, 37.5 °C, 35 °C (50% fouling), the following results are observed as shown in tables 4.15.

Table 4.15 Comparison of second- law efficiency for Refrigerants R1234yf, R1234ze with R134a.

Refrigerant	**UA_{evap}%**	**η_{II} ($T_{in,cond}$=40°C)**	**η_{II} ($T_{in,cond}$=37.5°C)**	**η_{II} ($T_{in,cond}$=35°C)**
R1234ze	50	23.77 %	24.11 %	24.33 %
R1234yf	50	18.90 %	19.84 %	20.57 %
R134a	50	23.64 %	23.98 %	24.20 %

From the above tables it is clear that, the second-law efficiency decreases on comparing R1234yf with R134a, while its value increases on comparing R1234ze with R134a.

Figures 4.70-4.72 shows the variation of second-law efficiency (η_{II}) %, with condenser and evaporator fouling from 0% to 50%, at $T_{in,cond}$ = 40°C, 37.5 °C, 35 °C, for refrigerants R134a, R1234yf and R1234ze.

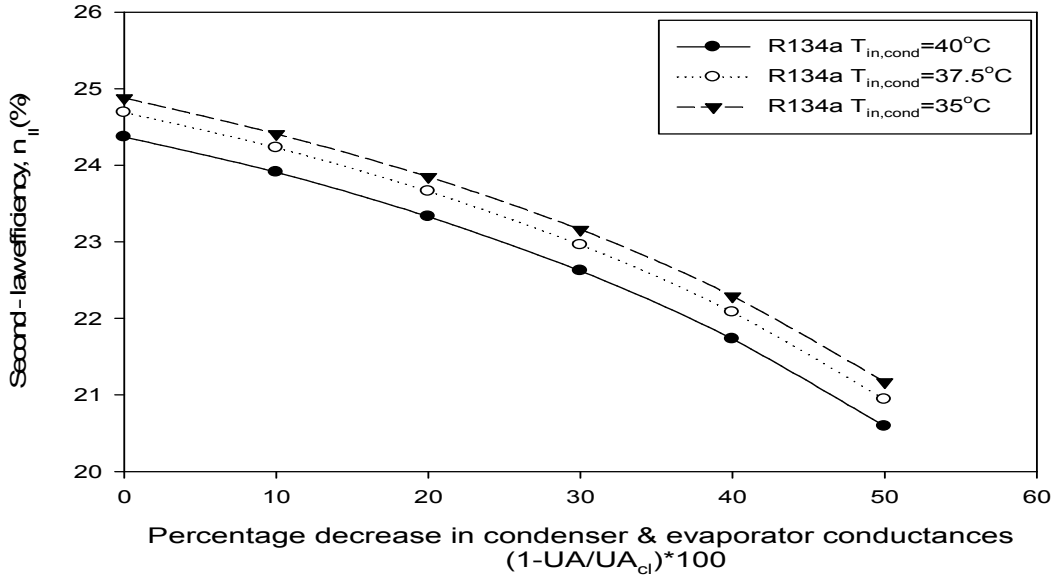

Figure 4.70 Second-law efficiency (%) vs. Percentage decrease in condenser & evaporator conductances for R134a.

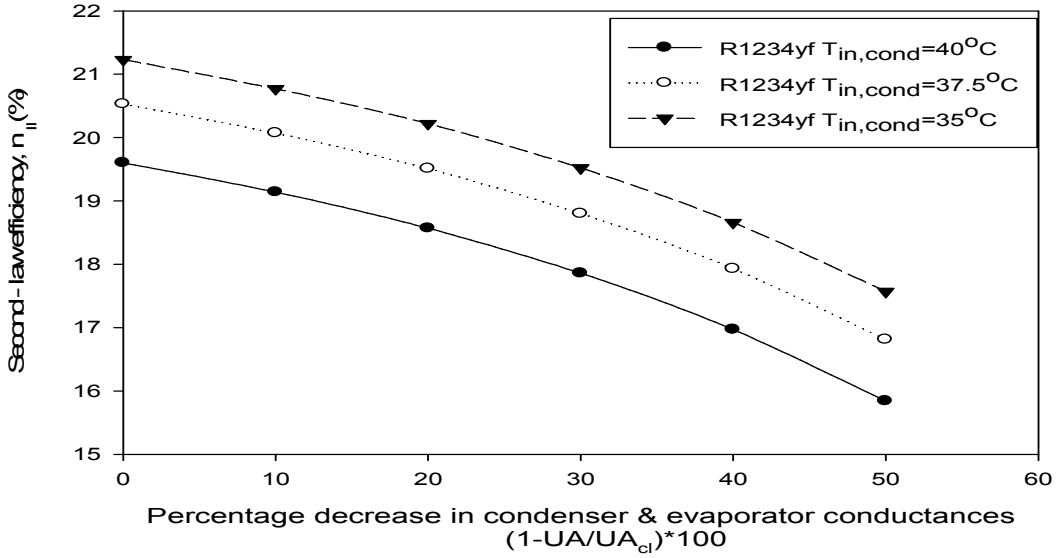

Figure 4.71 Second-law efficiency (%) vs. Percentage decrease in condenser & evaporator conductances for R1234yf.

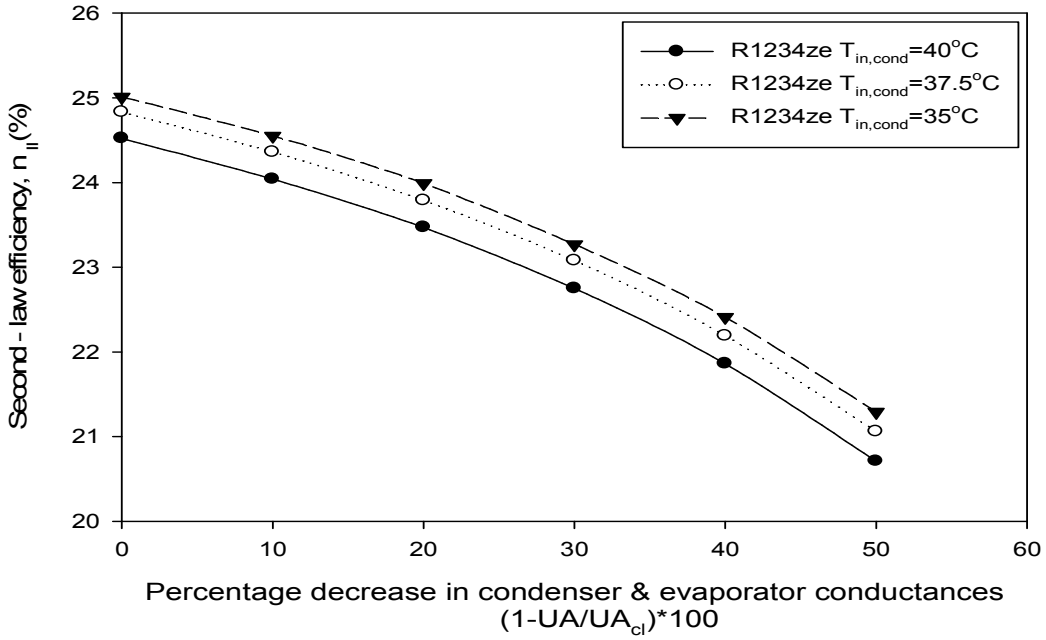

Figure 4.72 Second-law efficiency (%) vs. Percentage decrease in condenser & evaporator conductances for R1234ze.

On comparing results of R1234yf, R1234ze with R134a in condenser and evaporator fouling at $T_{in,cond}$ = 40°C, 37.5 °C, 35 °C (50% fouling), the following results are observed as shown in tables 4.16.

Table 4.16 Comparison of second-law efficiency for Refrigerants R1234yf, R1234ze with R134a.

Refrigerant	**$UA_{cond,evap}$%**	**η_{II} ($T_{in,cond}$=40°C)**	**η_{II} ($T_{in,cond}$=37.5°C)**	**η_{II} ($T_{in,cond}$=35°C)**
R1234ze	50	20.71 %	21.06 %	21.29 %
R1234yf	50	15.84 %	16.81 %	17.57 %
R134a	50	20.59 %	20.94 %	21.17 %

From the above tables it is clear that, the second-law efficiency decreases on comparing R1234yf with R134a, while its value increases on comparing R1234ze with R134a.

CHAPTER 5

CONCLUSIONS AND SCOPE FOR FUTURE WORK

5.1. Conclusions

On the basis of results obtained from thermodynamic model, following conclusions are drawn-

Effect of fouling on the performance of a simple vapour compression cycle has been evaluated by varying condenser coolant inlet temperature $T_{in,cond}$ (i.e. 35^{o}C, 37.5 ^{o}C and 40 ^{o}C), and also by varying condenser and evaporator conductances (i.e. 0% - 50%), for the refrigerant R134a, R1234yf and R1234ze.

In condenser fouling it has been observed that:-

a) The value of W_{cp}% increases up to 9.12 for R1234yf, and 7.41 for R1234ze, where as in R134a its value increases up to 7.38 at $T_{in,cond}$ = 35^{o}C. i.e. W_{cp}% (R134a) < W_{cp}% (R1234ze) < W_{cp}% (R1234yf).

b) The value of Qevap% decreases up to 13.25 for R1234yf and 8.62 for R1234ze, where as for R134a its value decreases up to 8.76 at $T_{in,cond}$ = 40^{o}C. i.e. Qevap% (R1234yf) < Qevap% (R134a) < Qevap% (R1234ze).

c) The value of COP% decreases up to 19.29 for R1234yf and 14.47 for R1234ze where as in R134a its value decreases up to 14.49 at $T_{in,cond}$ = 40^{o}C. i.e. COP% (R1234yf) < COP% (R134a) < COP% (R1234ze).

In evaporator fouling it has been observed that:-

a) The value of W_{cp}% decreases up to 8.31 for R1234yf and 9.66 for R1234ze, where as in R134a its value decreases up to 9.63 at $T_{in,cond}$ = 35^{o}C. i.e. W_{cp}% (R1234ze) < W_{cp}% (R134a) < W_{cp}% (R1234yf).

b) The value of Qevap% decreases up to 11.19 for R1234yf and 12.13 for R1234ze, where as for R134a its value decreases up to 12.08 at $T_{in,cond}$ = 35^{o}C.i.e. Qevap% (R1234ze) < Qevap% (R134a) < Qevap% (R1234yf).

c) The value of COP% decreases up to 3.59 for R1234yf and 3.04 for R1234ze, where as in R134a its value decreases up to 2.99 at $T_{in,cond}$ = 40^{o}C.i.e. COP% (R1234yf) < COP% (R1234ze) < COP% (R134a).

In condenser and evaporator fouling it has been observed that:-

a) The value of W_{cp}% decreases up to 2.55 for R1234yf and 2.91 for R1234ze, where as in R134a its value decreases up to 2.95 at $T_{in,cond}$ = 35^{o}C.i.e. W_{cp}% (R134a) < W_{cp}% (R1234ze) < W_{cp}% (R1234yf).

b) The value of Qevap% decreases up to 20.87 for R1234yf and 17.67 for R1234ze, where as for R134a its value decreases up to 17.69 at $T_{in,cond}$ = 40^{o}C.i.e. Qevap% (R1234yf) < Qevap% (R134a) < Qevap% (R1234ze).

c) The value of COP% decreases up to 19.21 for R1234yf and 15.55 for R1234ze where as in R134a its value decreases up to 15.54 at $T_{in,cond}$ = 40^{o}C.i.e. COP% (R1234yf) < COP% (R1234ze) < COP% (R134a).

The maximum decrease in effectiveness of the fouled heat exchanger is observed up to 31% by the time its UA% value is halved (i.e. 50%), and the effectiveness of the fouled heat exchanger decreases equally with the same percentage for all the refrigerants.

The second-law efficiency obtained for R1234ze is the highest among the refrigerants considered both under fouled & unfouled condition. At $T_{in,cond}$ = 40^{o}C, on the basis of the second law efficiency under 50% fouled conditions, the refrigerants can be arranged as R1234yf (15.84%) < R134a (20.59%) < R1234ze (20.71%).

5.2. Scope for future work

1) The present model can be applied for performance evaluation of other refrigerants being used in VCRS for different application.
2) The effect of pressure & heat losses has been neglected in present study and hence the same can be considered for further study of VCRS under fouled conditions.

REFERENCES

1. Selbas, R., Kızılkan, O., Şencan, A., 2006. Thermoeconomic optimization of subcooled and superheated vapor compression refrigeration cycle. Energy 31, 2108–2128.

2. Wang, X., Hwang, Y., Radermacher, R., 2008. Investigation of potential benefits of compressor cooling. Applied Thermal Engineering 28, 1791–1797.

3. Arora, A., Kaushik, S.C., 2008. Theoretical analysis of a vapour compression refrigeration system with R502, R404A and R507A. International Journal of Refrigeration 1 – 8.

4. Khan, J., Zubair, S.M., 1999. Design and performance evaluation of reciprocating refrigeration system. International Journal of Refrigeration 22, 235-243.

5. Winkler, J., Aute, V., Radermacher, R., 2008.Comprehensive investigation of numerical methods in simulating a steady-state vapor compression system. International Journal of Refrigeration 31, 930-942.

6. Cabello, R., Navarro, J., Torrella, E., 2005. Simplified steady-state modelling of a single stage vapour compression plant Model development and validation. Applied Thermal Engineering 25, 1740–1752.

7. Aprea, C., Greco, C., 2003. Performance evaluation of R22 and R407C in a vapour compression plant with reciprocating compressor. Applied Thermal Engineering 23, 215-227.

8. Ding, G., 2007. Recent development in simulation techniques for vapour-compression refrigeration systems. International Journal of Refrigeration 1-15.

9. Monte, F., 2002. Calculation of thermodynamic properties of R407C and R410A by the Martin–Hou equation of state — part II: technical interpretation. International Journal of Refrigeration 25, 314–329.

10. Monte, F., 2002. Calculation of thermodynamic properties of R407C and R410A by the Martin–Hou equation of state — part I: theoretical development. International Journal of Refrigeration 25, 306–313.

11. Küçüksille, E., Selbas, R., Sencan, A., 2008. Data mining techniques for thermophysical properties of refrigerants. Energy Conversion and Management. Energy Conversion and Management.

12. Ahamed, J.U., Saidur, R., Masjuki, H.H., 2010. A review on exergy analysis of vapor compression refrigeration system. Renewable and Sustainable Energy Reviews 15, 1593-1600.

13. Lee, T.S., Liu, C.H., Chen, T.W., 2006. Thermodynamic analysis of optimal condensing temperature of cascade-condenser in CO_2/NH_3 cascade refrigeration systems. International Journal of Refrigeration 29, 1100-1108.

14. Calm, J., 2008. The next generation of refrigerants – Historical review, considerations, and outlook. International Journal of Refrigeration 31, 1123-1133.

15. McLinden, M. O., Monika, T., Lemmon E. W., 2010. Thermodynamic Properties of *trans*-1,3,3,3-tetrafluoropropene [R1234ze(E)]: Measurements of Density and Vapor Pressure and a Comprehensive Equation of State. International Refrigeration and Air Conditioning Conference at Purdue, July 12-15, 2010.

16. Reasor, P., Aute, V., Radermacher, R., 2010.Refrigerant R1234yf Performance Comparison Investigation. International Refrigeration and Air Conditioning Conference at Purdue, Paper 1085.

17. Pearson, A., 2005. Carbon Dioxide---new uses for an old refrigerant. International Journal of Refrigeration 28, 1140-1148.

18. Herbert, R., M., Mohan, L., D., 2009. On the performance of R22 and a HFC/HC refrigerant mixture over a range of charge quantity in a window air conditioner. Acreconf.

19. Qureshi, B.A., Zubair, S.M., 2011.Performance degradation of vapor compression refrigeration system under fouled conditions. International Journal of Refrigeration 34, 1016-1027.

20. Qureshi, B.A., Zubair, S.M., 2012.The impact of fouling on performance of a vapor compression refrigeration system with integrated mechanical sub-cooling system. Applied Energy 92, 750-762.

21. Arora, C.P., “Refrigeration and Air-conditioning, 2002, second edition, New Delhi: Tata McGraw Hill.

22. Stoecker, W.F., Jones, J.W., 1982. Refrigeration and Air Conditioning. McGraw-Hill, New York, USA.

23. Incropera, F.P., DeWitt, D.P., Bergman, T., Lavine, A., 2006. Fundamentals of Heat and Mass Transfer, sixth ed. John Wiley & Sons, Inc..